

TECHNISCHE UNIVERSITÄT MÜNCHEN

Lehrstuhl für Proteomik und Bioanalytik

**Studies on the functional domains in oncogenic JAK2 and identification of drug
resistant mutations in FIP1L1-PDGFR**

Sivahari Prasad Gorantla

Vollständiger Abdruck der von der Fakultät Wissenschaftszentrum Weihenstephan für
Ernährung, Landnutzung und Umwelt
der Technischen Universität München
zur Erlangung des akademischen Grades eines

Doktors der Naturwissenschaften
genehmigten Dissertation.

Vorsitzender: Univ.- Prof. Dr. M. Klingenspor
Prüfer der Dissertation: 1. Univ.- Prof. Dr. B. Küster
2. Univ.- Prof. Dr. J. G. Duyster

Die Dissertation wurde am 28.10.2010 bei der Technischen Universität München eingereicht
und durch die Fakultät für Wissenschaftszentrum Weihenstephan für Ernährung, Landnutzung
und Umwelt am 15.02.2011 angenommen.

Abbreviations

α	Alpha
AB	Antibody
AP	Alkaline phosphatase
APC	Antigen presenting cell
APS	Ammonium per sulfate
AA	Aminoacid
AML	Acute myeloid leukemia
β	Beta
bp	Basepair
BM	<i>Bonemarrow</i>
BSA	Bovine serum albumin
BFU-E	Burst forming units-Erythrocytes
C	Celsius
CD	Cluster of Differentiation
cDNA	Complementary DNA
CFU-E	Colony forming units-Erythrocytes
CFU-preB	Colony forming unit-pre B cell
CFU-GM	Colony forming unit Granulocytes-Monocytes
CFU-M	Colony forming units-Monocytes
CIAP	Calf intestinal alkaline phosphatase
cpm	Counts per minute
Co-IP	Co-Immunoprecipitation
c-Ski	Sloan-Kettering virus nuclear oncoprotein
Da	Dalton
DAPI	4',6 Diamidino-2-phenylindol
DEPC	Diethylpyrocarbonate
DMEM	Dulbecco's Modified Eagle Medium
DMSO	Dimethylsulfoxide
DNA	Desoxyribonucleic acid

dNTP	2'-desoxynucleoside-5'-triphosphate
DTT	Dithiothreitol
E	Extinction
E.coli	Escherichia coli
EDTA	Ethylendiamine-N,N,N',N'-tetra acetic acid
Epo	Erythropoietin
EpoR	Erythropoietin receptor
ERK	Extracellular signal regulated kinase
ES	Embryonic stemcell
ET	Essential Thrombocythemia
Et al.	Et aliter
F	Fahrenheit
FACS	Fluorescence activated cell sortor
FERM	Band 4.1 ezrin, radixin and moesin
FIP1L1	FIP1-like 1
FCS	Fetal calf serum
FITC	Fluoresceinisothiocyanate
For	Forward
FP	FIP1L1-PDGFR α
FS	Forward scatter
G	Gravitational Force(9,81 m/s)
GFP/eGFP	Enhanced green fluorescent protein
GST	Glutathione S-Transferase
h	Hour
H&E	Heamatoxyline and Eosin
HES	Hyper Eosinophilic Syndrome
HRP	Horseradish peroxydase
Ig	Immunoglobulin
IL	Interleukin

IMF	Idiopathic myelofibrosis
IPTG	Isopropyl- β -D-Thiogalactopyranoside
IRES	Internal ribosomal entry site
JAKs	Janus Kinase (Just another Kinase)
JH	Jak homology domain
kb	Kolbase(n),1000 Basepair
kDa	Kilodalton
LB	Luria-Bertani
LIF	Leucemic inhibitory factor
M	Marker/ Mol pro Liter, molar
m	Milli (10^{-3})
mA	Milliampere
Mef	Mouse embryonic fibroblast
min	Minute(n)
miRNA	microRNA
mM(mmol/l)	10^{-3} Mol/Liter
mRNA	Messenger RNA
MPNs	Myeloproliferative neoplasms
N	nano
NaCl	Sodium chloride
Neo	Neomycin
ng	10^{-9} Gramm, Nanogram
nM(nmol/l)	10^{-9} Mol/l
nm	10^{-9} Meter, Nanometer
OD	Optical Density
PAGE	Polyacrylamide Gelelectrophoresis
PBS	Phosphate buffered saline
PBST	PBS with 0.1% Tween 20
PCR	polymerase chain reaction

PDGF-AA	PDGFR alpha ligand AA
PDGFRA	Platelet derived Growth Factor Receptor Alpha
PE	Phycoerythrin
PFA	Paraformaldehyde
pH	Potential for Hydrogen
PI	Propidiumiodide
PMSF	Phenylmetansulfonylfluoride
PTC	Premature termination codons
PTK	Protein tyrosine kinase
PTP	Protein tyrosine Phosphatase
PVI.	Polycythemia Vera
PVDF	Polyvinylidifluoride
rev	reverse
RNA	Ribonucleic acid
RT	Room temprature
RT-PCR	Reverse Transcription Polymerase chain reaction
RTQ-PCR	Real-Time-quantitative-PCR
s.cervisiae	Saccharomyces cerevisiae
SCF	Stem cell factor
SDS	Sodium dodecyl sulfat
SH2	Src homology domian
siRNA	Small interfering RNA
SM	Systemic mastocytosis
SRC	Sarcoma virus
STATs	Signal transducer and activator of transcription
TEMED	N,N,N',N'-Tetramethylethylendiamin
Tris	Tris(hydroxymethyl)aminomethan
U	Unit
UV	Ultraviolet

V	Volt
v/v	Volume/Volume
WT	Wild type
w/v	Weight/volume
μCi	10^{-6} Curie
μg	10^{-6} gram
μM	10^{-6} Mol/Liter
WB	Western blot

Table of contents

1	Introduction	
1.1	JAK2 mediated myeloproliferative diseases	2
1.1.1	JAK2.....	4
1.1.2	Structure of JAK2.....	5
1.1.3	JAK2 mediated cytokine signaling cascade	7
1.1.4	Models of JAK2V617F	9
1.1.5	Inhibitors against JAK2V617F	14
1.2	HES/CEL.....	16
1.2.1	Identification and generation of FIP1L1-PDGFR A	16
1.2.2	Molecular mechanism of FIP1L1-PDGFR A activation.....	17
1.2.3	Treatment and drug resistance to FIP1L1-PDGFR A positive HES/CEL	18
1.3	Objectives.....	20
2	Materials and method	
2.1	MATERIALS	21
2.1.1	Reagents	21
2.1.2	Medium and supplements for cell culture	23
2.1.3	Enzymes	23
2.1.4	Hormones.....	24
2.1.5	Radioactive substances.....	24
2.1.6	Membranes	24
2.1.7	Antibodies	24
2.1.8	Cell lines.....	25

2.1.9	Vectors and DNA constructs	24
2.1.10	Bacterial Strains	24
2.1.11	Oligonucleotides for PCR (5'→3')	26
2.1.12	Oligonucleotides for site directed mutagenesis (5'→3').....	27
2.1.13	Oligonucleotides for sequencing (5'→3').....	31
2.1.14	Molecular markers for nucleic acids and proteins	31
2.1.15	Mouse Strains	31
2.1.16	Materials and kits for molecular biology	31
2.1.17	Instruments.....	32
2.1.18	Buffers.....	33
2.2	METHODS	36
2.2.1	Methods involving nucleic acids.....	36
2.2.1.1	Isolation, purification and measurement of DNA.....	36
2.2.1.2	Agarose gel electrophoresis.....	37
2.2.1.3	Restriction digestion, ligation and cloning of DNA.....	36
2.2.1.4	Site directed mutagenesis and DNA sequence analysis.....	37
2.2.2	Inhibitors	38
2.2.3	Cell Lines and Cell Culture	38
2.2.4	cDNA constructs and generation of stable cell lines.....	39
2.2.5	Immunoblotting and Immunoprecipitations (IPs).....	40
2.2.6	Membrane preparation from Ba/F3 cells	40
2.2.7	Retrovirus preparation and viral titer measurement	41
2.2.8	Bone marrow transduction and transplantation model.....	41

2.2.9	Analysis of transplanted mice	41
2.2.10	Resistance screen and mutation identification	42
2.2.11	Proliferation and apoptosis assay.....	43
2.2.12	Real time RT-PCR.....	43
2.2.13	Pulse-chase experiments	43
2.2.14	Invitro kinase assay.....	44
2.2.15	GST purification and GST binding studies	44
2.2.16	EpoR surface staining.....	44
2.2.17	Structure analysis	44
3	RESULTS.....	45
3.1	JAK2V617F-mediated IL3-independent growth of Ba/F3 cells requires an intact FERM and SH2 domain	45
3.1.1	JAK2V617F-mediated constitutive activation of JAK2 requires expression of cytokine receptor in Gamma 2a cell line.....	47
3.1.2	Mutation of SH2 domain decreased the activation of the cytokine (IL-3) induced signal transduction in Gamma2A cell lines	48
3.1.3	High levels of EpoR can compensate for the loss of SH2 function in JAK2V617F.....	49
3.1.4	Mutation of SH2 domain does not effect the protein turn over and intrinsic kinase activity of V617FJAK2	53
3.1.5	Mutation of the SH2 domain does not affect the membrane distribution of JAK2	53
3.1.6	Protein-protein interaction and transphosphorylation of JAK2V617F is dependent on an intact SH2 domain.....	57
3.1.7	JAK2V617F-mediated myeloproliferative disease in mice requires a functional SH2 domain.....	62

3.2 The concentration of imatinib determines the frequency and type of FP resistance mutations.....	68
3.2.1 With nilotinib, the profile of resistance mutations narrows to FP/D842V at clinically achievable concentrations.....	70
3.2.2 Sorafenib produces resistant FP cell clones at very low frequency.....	73
3.2.3 Limited cross resistance of identified FP exchanges favours nilotinib and sorafenib over imatinib.....	74
3.2.4 FP G610R which was identified with imatinib and sorafenib lacks kinase activity and failed to transform Ba/F3 cells.....	86
3.2.5 Structure analysis and discussion.....	87
3.2.5.1 Position D842V (E,G,H): DFGLARDI.....	90
3.2.5.2 Position F604S and combination mutants	93
3.2.5.3 Position T674I: the gate keeper and double mutants.....	94
3.2.5.4 Mutants in the α C- β 4 loop (N656Y, V658G, N659Y).....	95
3.2.5.5 Position Y849	96
4 DISCUSSION.....	97
4.1 FERM domain is absolutely required for JAK2V617F mediated transformation	97
4.2 JAK2V617F-mediated myeloproliferative disease in mice requires intact SH2 domain.....	98
4.3 In vitro resistance screening identifies nilotinib and sorafenib as candidates to overcome imatinib resistance in myeloproliferation with FIP1L1-PDGFR.....	100
4.4 CONCLUSIONS	106
5 Summery/Zusammenfassung.....	107
6 Literature	111

7	Publications/Presentations	125
8	Lebenslauf	128
8	Acknowledgements	



1. Introduction

Myeloproliferative neoplasms (MPNs) are clonal hematological malignancies that result in the overproduction of mature myeloid cells. Typical features of MPNs include splenomegaly, thrombosis, bone marrow fibrosis, extramedullary hematopoiesis and finally leukemic transformation in the bone marrow. MPNs are basically divided into two main groups. The First group of MPNs includes chronic myeloid leukemia (CML). CML is identified by the presence of both mature and immature myelogenous cells in the blood and bone marrow. Cytogenetically CML can be characterized by the presence of the Philadelphia (Ph) translocation, which leads to the expression of the Bcr-Abl fusion gene. The Second group of MPNs include polycythemia vera (PV), essential thrombocythemia (ET), and idiopathic myelofibrosis (IMF) ¹. PV can be distinguished from other chronic MPNs by the remarkable increase of red blood cell mass and total blood volume. An increased erythrocyte cell count, packed cell volume and hemoglobin with normal erythrocytic indices are the characteristic features of PV. ET is characterized by significant increased in circulating platelets, usually in excess of $1000 \times 10^9/L$. IMF is a chronic MPD of unknown cause, characterized by bone marrow fibrosis and extramedullary hematopoiesis. Patients with IMF usually exhibit progressive anemia and marrow fibrosis. In addition to these two groups less common disorders like chronic neutrophilic leukemia and chronic eosinophilic leukemia (CEL)/hypereosinophilic syndrome (HES) are grouped as atypical MPNs by the World Health Organization (WHO) ².

Clinical features of CML, PV, ET, and IMF have significant overlaps that they were thought to be related diseases before 1960. However, in 1960 Nowell et al. identified the Ph chromosome due to a translocation $t(9:22)$ in CML patients ³. Identification of the Ph chromosome led to classification of MPNs into Ph chromosome “positive” MPNs and ph chromosome “negative” MPNs. Later multiple groups extensively analyzed the bone marrow samples from PV, ET, and IMF patients since these diseases do not show any cytogenetic abnormalities. Interestingly bone marrow samples from PV patients showed cytokine hypersensitivity to erythropoietin and also growth of erythroid progenitors in the absence of exogenous cytokines ⁴. Similar cytokine independent growth of progenitor

cells were also identified in other disorders like acute myeloid leukemia (AML), PV, ET and IMF. This observation suggested a common molecular mechanism of transformation among these disorders. X chromosome inactivation studies in PV, ET and IMF patients samples revealed that these diseases were clonal stem cell disorders^{5,6}.

Recently several independent groups described the somatic mutation in janus kinase (JAK2) by using different experimental strategies⁷⁻⁹. First James et al. observed that siRNA mediated inhibition of JAK2 in PV hematopoietic progenitors abrogated endogenous erythroid colonies (EEC) formation which led them to further screen for JAK2 mutations⁷. Green and coworkers used gene sequencing followed by allele specific PCR to identify mutation of JAK2 in PV, ET and IMF⁹. Josef Prchal first observed that acquired uniparental disomy (UPD) of the chromosome 9p24 is common in PV patients¹⁰. Based on this observation, Kralovics et al. sequenced the genes in the minimal region of UPD to identify mutations in the JAK2 allele¹¹. Finally, Levine et al. performed a systemic survey of the kinome in PV patients using high through put DNA sequencing which finally led them to identify mutations in JAK2⁸. All these groups identified a high incidence of JAK2 point mutation at codon 617 named as JAK2V617F in different MPNs.

1.1 JAK2 mediated myeloproliferative diseases

The V617F mutation within the pseudokinase domain of JAK2 has frequently been identified in patients with myeloproliferative neoplasms (MPNs). In polycythaemia vera it has been identified as 95% patients are JAK2V617F positive. JAK2V617F mutation has also been identified in 20-40% in ET and 50% in idiopathic myelofibrosis patients^{7-9,11} (Table1). In addition to MPD, JAK2V617F has also been observed at lower frequencies in chronic myelomonocytic leukemia (3-8%), myelodysplastic syndrome (4%), and rarely in systemic mastocytosis^{12,13}. A subset of JAK2V617F-negative PV patients showed gain of function mutations affecting exon 12 of JAK2. Scott et al. identified four different exchanges in exon 12 of JAK2¹⁴ (Figure 1). In addition to exon 12 mutations, one activation mutation affecting the kinase domain (T875N) in JAK2 was also identified with low frequency¹⁵. Recently, Malinge et al. identified a novel JAK2

activation mutation (Δ IREED) in a patient with a down syndrome and B cell precursor acute lymphoblastic leukemia ¹⁶.

Table1: Frequency of the JAK2V617F mutation in myeloproliferative neoplasms (MPNs)

Disease	JAK2 V617F	JAK2exon12	MPL515
PV	81-99%	5%	-
ET	41-72%	-	1%
IMF	39-57%	-	5%
CMML	3-9%		-
AML	5%		-

JAK2 also has been identified as fusion partner in multiple translocations. TEL-JAK2 fusion protein is generated from the t(9;12) (p24;p13) translocation and has been described in both T and pre-B acute lymphoid leukemia ¹⁷ (Figure.1). Another translocation involving JAK2 is PCM1-JAK2 generated from the t (8:9) (p21:p24) in patients with a myeloproliferative/myelodysplastic disorder and a CML-like disease ^{18,19}. In addition to these two fusions JAK2 was also shown as the fusion partner to BCR in atypical CML ²⁰. Campbell et al. findings suggested that 40% to 50% of ET patients are truly JAK2 mutation negative ²¹. These results suggest that there might be additional, novel mutations in other genes in this subset of patients. The Majority of JAK2V617F negative ET and IMF patients have clonal granulopoiesis. Impaired expression of thrombopoietin receptor (MPL) has been observed in platelets from patients with MPD ²². Given that the expression of homodimeric type I cytokine receptor is required for the JAK2V617F mediated transformation ²³, Pickman et al. analyzed for mutations in the EpoR, TpoR, and GCSFR in JAK2V617F negative PV, ET and IMF patients. Their study

identified a tryptophan to leucine substitution at the transmembrane (TM) - juxtramembrane (JM) junction of MPL (MPLW515L)²⁴. The MPLW515L allele occurs in approximately 10% of patients with JAK2V617F negative IMF and a small portion of ET patients²⁵. Expression of MPLW515L resulted in factor independent growth and activation of the JAK-STAT signaling pathway in cell lines. Retroviral expression of MPLW515L in recipient mice resulted in myeloproliferative disease similar to human IMF including reticulin fibrosis, megakaryocytic hyperplasia, splenomegaly and extramedullary hematopoiesis²⁵.

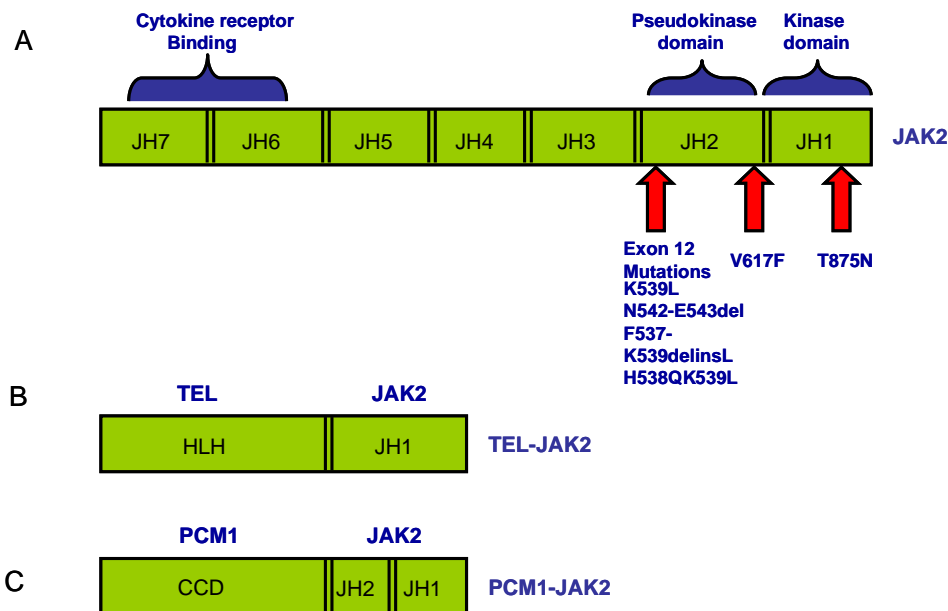


Figure 1: Location of JAK2 activating mutations and structure of JAK2 fusion proteins: (A) The V617F mutation is located within the JH2 (pseudokinase domain). The exon 12 mutations are located proximal of the JH2 domain. The T875N mutation is located in the JH1 (kinase domain) domain of JAK2. (B) The helix loop helix domain of TEL is fused to the JH1 domain of JAK2. TEL-JAK2 is involved in both T- and pre B-acute lymphoid leukemia. (C) The Coiled coil domain of pericentreolar material 1(PCM1) is fused to the JH1 and part of the JH2 domain of JAK2. PCM1-JAK2 fusion protein is found in atypical CML.

1.1.1 JAK2

Cytokines and interferons play main roles in the regulation of a wide variety of cellular functions ranging from proliferation, differentiation, survival to specialized functions like host resistance to pathogens. Cytokine receptors are basically classified as type I and

typeII cytokine receptor super family depending on the conserved sequence motif. Type I cytokines includes short chain cytokine like IL-2, IL-3, IL-4, IL-5, GM-CSF, IL-7, IL-9, IL-13, IL-15 and long chain cytokines like IL-6, IL-11, OSM, CNTF, CT-1, growth hormone, prolactin, erythropoietin and thrombopoietin. Interferons INF α , INF β and INF γ were included in the typeII cytokines²⁶. The Cytokine receptor super family do not have intrinsic tyrosine kinase activity and depend on the JAK family kinases to activate the STAT signaling pathway^{27 28-30}.

Four JAKs have been discovered using two different approaches. Tyk2 was first identified by low-stringent hybridization screening of a T cell cDNA library with the c-fms catalytic domain³¹. Whereas JAK1, JAK2, and JAK3 were identified with PCR based strategy using primers corresponding to a conserved motif within the catalytic domain of tyrosine kinases^{32 33 34 35 36}.

JAKs are cytoplasmic tyrosine kinases consist of 1150 aminoacids with an apparent molecular weight of 120-130 kDa. The mRNA transcript length ranges from 4.5 to 5.5 kb. Different splice variants of the JAKs have been identified. JAK2 has two spliced transcripts where as JAK3 has even multiple spliced forms³⁴. JAK1, JAK2, and Tyk2 are ubiquitously expressed where as JAK3 expression is restricted to the hematopoietic system³⁶.

In humans the JAK1 gene resides on chromosome 1p31.3 and JAK2 at 9p24. JAK3 and Tyk2 are located on chromosome 19³¹. The murine JAKs genes are located on chromosome 4 (JAK1), 19 (JAK2), 8(JAK3) and 9 (Tyk2)³⁷.

1.1.2 Structure of JAK2

The hall mark of JAK family kinases is the existence of tandem kinase and pseudokinase domains. The tandem manner by which these two domains are assembled was reminiscent of Janus, a Roman God of gates and doorways (two opposing faces). In addition to kinase and pseudokinase domains several other segments of homology were recognized among JAKs and designated as JAK homology (JH) domains. Seven JH domains were (JH1-JH7) described (Figure 1.2). At the carboxy terminal JH1 and JH2 domains are located. JH1 domain contains classical tyrosine kinase domain which is required for the catalytic activity of JAK2. Similar to other tyrosine kinases, mutation of a lysine residue in the subdomain II which binds to ATP abrogates kinase activity^{38,39}.

Multiple autophosphorylation sites have been identified in the activation loop of JAK2. Mutation of Tyr 1007 to Phe in JAK2 abrogates kinase activity and cytokine mediated signals⁴⁰. Additionally, Tyr 1007 in JAK2 interacts with JAK binding protein (JAB) also known as suppressor of cytokine signaling 1 (SOCS1)⁴¹.

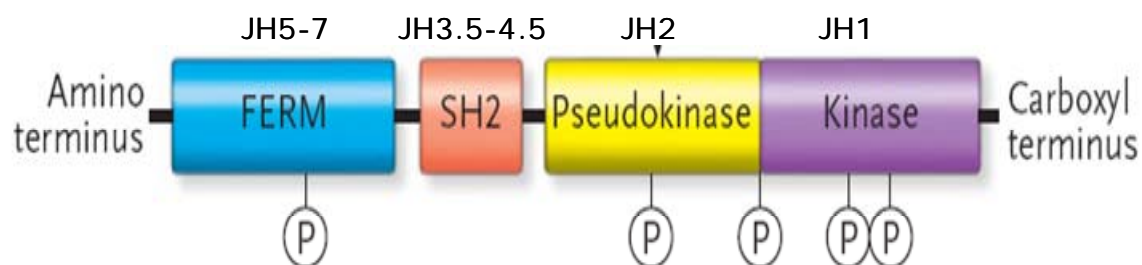


Figure 1.2: Structure of JAK2: A unique feature of JAKs is a tandem kinase and the pseudokinase domains. Regions of the homology shared by JAKs have been termed as JAK homology (JH) domains. The JH1 domain is the kinase domain and the JH2 domain is the pseudokinase domain play a major role in the regulation of catalytic activity of JAKs. The middle SH2-like domain occupies the region between JH3.5-JH4.5. The N terminal FERM domain is important for the association with cytokine receptor subunits.

JH2 is a so called pseudokinase domain which plays a major role in the regulation of the kinase activity of JH1 domain. The Pseudokinase domain is similar in structure to classical kinase but lacks the kinase activity. The JH2 domain lacks the third Gly of the conserved GXGXXG motif in the kinase subdomain I. Both tyrosine and serine kinases contain aspartic acid residue required for the proton acceptor in the phosphotransfer reaction. Interestingly, the pseudokinase domain lacks this aspartic acid residue. The pseudokinase domain also lacks the conserved Phe residue in the Asp-Phe-Glu motif in the subdomain VII, which is important for binding the adenine ring in ATP. Lack of these key residues suggested that the pseudokinase domain would not have kinase activity and this has been confirmed^{32 42}. Several reports have been demonstrated that a deletion of the JH2 domain leads to hyperactivation of JAK2 kinase domain. In growth hormone mediated cell signaling, deletion of the pseudokinase domain led to more robust signaling, and these results provided a strong evidence that the JH2 domain play a role in negative regulation of the kinase activity of JAK2⁴³. Saharinen et al. showed that the JH2 domain of JAK2 interacts with the JH1 domain and suppress the activity of JAK2. Homology based molecular modeling of JH2 showed three inhibitory regions (IR1-3),

which mediate intermolecular interaction with the JH1 domain and regulate JAK2 kinase activity⁴⁴. The proximity of the recently discovered V617F mutation to the IR1 of the JH2 domain may explain the constitutive activity of JAK2V617F. However, there is no conclusive explanation for the inhibitory function of the JH1 domain, since the complete three-dimensional structure of any JAK member has not been reported yet.

The amino terminal region of JAK2 contains the JH3 through JH7 domains. This region is required for the interaction with the receptor and may be responsible for the interaction between JAK2 and other regulatory molecules. By using structure prediction tools Kampa et al presented a three dimensional view of a putative SH2 domain located in JH3-JH4. In JAK2 the SH2 like segment has a conserved Arg residue corresponding to the classical phosphotyrosine binding pocket of the SH2 domain. However, the JAK2 SH2 domain does not seem to bind phospho tyrosine residues and the actual function of the SH2 domain in JAK family kinases has not been clearly understood^{33 45}. A mutation of the highly conserved arginine at position 426 within the SH2 domain of JAK2 did not have an impact on interferon- γ signaling⁴⁶. Radtke et al. were able to show that the SH2 domain of JAK1 does not exert the function of a classical SH2 domain, but might mediate receptor binding and receptor surface expression⁴⁷.

Adjacent to the SH2 like domain of JAK2 is the FERM domain which occupies the region between JH5 to JH7. The name FERM domain stands for the proteins which this domain was originally described (Band 4.1 (F), Ezrin (E), Radixin (R), and Moesin (M)). The N terminal domain of JAK2 interacts with the relatively conserved membrane proximal domain of cytokine receptor (proline rich box1 motif) and this binding is essential for signal transduction. Deletion of the N-terminal region in JAK2 especially the JH6 and JH7 region eliminates cytokine receptor binding^{46 48}. In addition to receptor interaction the FERM domain of JAK2 also carries special functions like processing and surface expression of EpoR⁴⁹.

1.1.3 JAK2 mediated cytokine signaling cascade

Numerous cytokine type I receptors including receptors for erythropoietin (Epo), thrombopoietin (Tpo), granulocyte-colony stimulating factor (G-CSF), granulocyte

macrophage-colony stimulating factor (GM-CSF), interleukin-3 (IL-3), and interleukin-5 (IL-5) do not have an intrinsic tyrosine kinase domain and require JAK2 for signal transduction⁵⁰. In Epo receptor (EpoR)-expressing cells, it has been proposed that ligand binding leads to a conformational change of the receptor, which promotes JAK2 activation through reciprocal interaction and phosphorylation of two juxtapositioned JAK2 molecules⁵¹. Subsequently, activated JAK2 phosphorylates tyrosine residues within the cytoplasmic tail of the cytokine receptor, which then serve as docking sites for signal transducers and activators of transcription (STATs). Seven STAT proteins have been discovered and are denoted STAT1, STAT2, STAT3, STAT4, STAT5a, STAT5b, and STAT6. Most of the STATs are approximately 700 to 800 amino acids in length. The STATs exist as clusters on chromosomes.

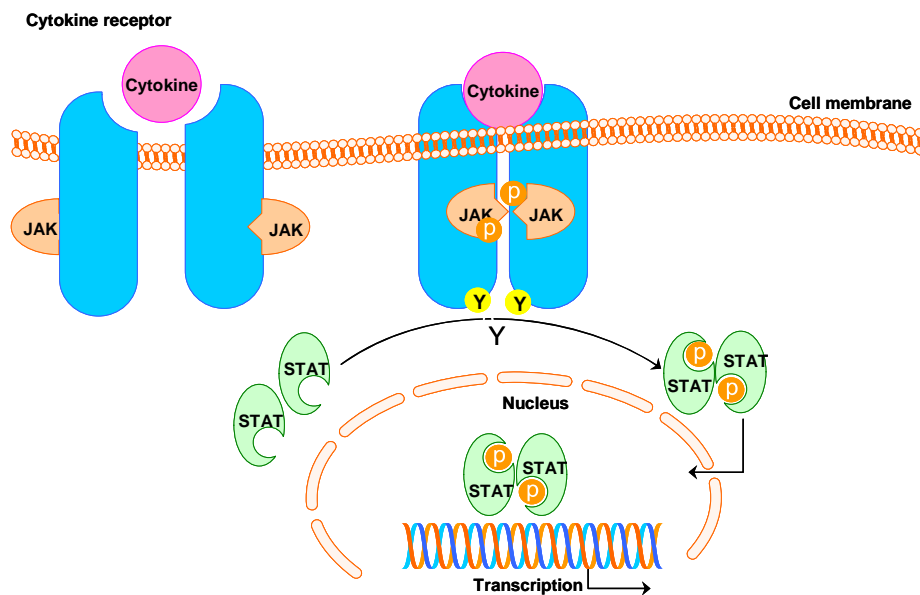


Figure 1.3: Schematic representation of cytokine mediated JAK-STAT signal transduction. In this model of the homodimeric receptor Epo and GH (growth hormone) there are two receptor subunits. JAKs constitutively associated with the two receptor subunits. Upon ligand binding to the extracellular domain of the receptor JAKs are activated. The activated JAKs in turn phosphorylate a tyrosine motif on the intracellular domain of the receptor subunit. STATs then bind to the receptor via the SH2 domain and are phosphorylated by JAKs. Then form homo –or hetero dimers, and translocate the nucleus, where they bind to the crucial DNA target sequences.

STATs themselves are phosphorylated and released from the receptor and form dimers. The dimeric form can then translocate into the nucleus and modulate expression of target genes. STATs have several essential functions they are 1) able to bind phosphorylated

tyrosines 2) able to dimerize 3) able to translocate into the nucleus 4) able to bind DNA and able to up regulate gene expression. Numerous type 1 cytokine receptors which require JAK2 for signal transduction particularly activates STAT5⁵²⁻⁵⁴. JAK2 deficiency results in an absence of erythropoiesis. JAK2^{-/-} mice results suggest that JAK2 is the predominant JAK kinase involved in myeloid cell differentiation and proliferation^{55,56}. The basic scheme of JAK-STAT signaling pathway is summarized in Figure 1.3.

1.1.4 Models of JAK2V617F

The JAK2V617F mutation has been identified in more than 90% of PV patients and in about 50% of patients with ET and IMF. It was thus an intriguing question how a unique mutation can cause a three different diseases. James et al. proposed a “four hypothesis model” to explain different diseases mediated by the JAK2V617F⁵⁷ mutation.

Hypothesis 1: The phenotype depends on the cell targeted by JAK2V617F

X-linked chromosome analysis have demonstrated that PV, ET and IMF are clonal diseases^{5,6}. Clinical features of MPNs are increased and clustered megakaryocytes in ET and PV, increased granulopoiesis in PV and IMF and increased erythropoiesis only in PV⁵⁸. It was assumed that the cells derived from multipotent hematopoietic stem cell (HSC) targeted by molecular events might be responsible for these different diseases. It can be hypothesized that the phenotype of a particular disease is determined by the character of the cells in which JAK2V617F mutation first occurred. For example, if the mutation occurred in self renewing cells with high capacity to produce platelets this would lead to thrombocytosis. Accordingly occurrence of the mutation in a stem cell with ability to produce erythrocytes lineages would result in PV like phenotype. To support this hypothesis various studies have shown that PV and IMF patients have JAK2V617F mutation in granulocytes, erythrocytes, megakaryocytes and lymphoid lineages^{59,60}. It was also suspected that occurrence of JAK2V617F mutation in HSC modulates the transcription programme which leads to different differentiation properties. Supporting this recently Dawson et al. showed that JAK2V617F is constitutively translocated to the nucleus in HEL (JAK2V617F positive) cells and modulates the transcription of several genes⁶¹. James and coworkers also showed differences in the transcriptional programme

of HSC compartment between PV and IMF patients⁶². Ishi and coworkers further more showed that the HSC of IMF patients is predominantly JAK2V617F positive where as the majority of HSC in PV express JAK2–wild type⁶³.

Hypothesis 2: JAK2V617F is the sole event responsible for the MPN and the phenotype depends on the genetic back ground of the patients

It is assumed that same recurrent JAK2V617F mutation occurs in a HSC in all MPN patients but the phenotype difference is due to the genetic background of a given patient. Pardanani and coworkers analyzed the single nucleotide polymorphisms (SNP) in the genes encoding the JAK2, EpoR, MPL, G-CSFR in PV, ET, and IMF patients and showed JAK2 and EpoR SNPs were preferentially associated with certain MPN phenotypes⁶⁴. Retroviral transplant mouse models provided a valuable evidence for the hypothesis that genetic back ground can modulate the phenotype⁶⁵⁻⁶⁷. Retroviral transplantation of JAK2V617F bone marrow to the lethally irradiated C57B1/6 mice leads to a PV-like disease characterized by a marrow trilineage hyperplasia, splenomegaly and strong polycythemia associated with the presence of EEC^{65,66}. Interestingly when Balb/C mice were transplanted with JAK2V617F, the first phase of the disease was not only a polycythemia but also a leukocytosis^{65,67,68}. The second phase of the disease in these mice is more pronounced myelofibrosis. However, a part from these reports no strong evidence could be accumulate that the phenotype of the disease depends on the genetic background of the patients.

Hypothesis 3: Phenotype depends on the level of JAK2V617F activity

In most of the MPN patients the status of JAK2V617F is either homozygous or heterozygous. Homozygous JAK2V617F in MPN patients is mediated by mitotic recombination^{10,11}. The presence of the different copy numbers of the JAK2V617F allele led to the dosage hypothesis for the phenotype diversity (Figure.1.4). Sequencing data from the MPN patients also showed JAK2V617F is homozygous status in many PV and IMF patients where as JAK2V617F is in heterozygous status in ET patients⁶⁹. According to this model, a low level of JAK2V617F kinase activity would favor an ET phenotype and high level for PV phenotype. Depending on the level and duration of exposure,

sustained JAK2V617F activity would ultimately lead to IMF phenotype⁷⁰. Tefferi et al. also showed the PV patients with high JAK2V617F burden display higher hemoglobin levels and higher rate of fibrotic transformation compared to heterozygous PV patients⁶⁹. Collectively transgenic mouse models also provided strong evidence that the expression level of JAK2V617F protein determine the MPN phenotype. High level of JAK2V617F leads to a PV like disease and equal levels to wild type leads to ET phenotype levels⁷¹. Another report supporting the dosage hypothesis is the analysis of erythroid progenitors at single cell level which showed striking differences between ET and PV. JAK2V167F allele status was homozygous in erythroid colonies from PV patients and heterozygous JAK2V617F in patients with ET^{72,73}.

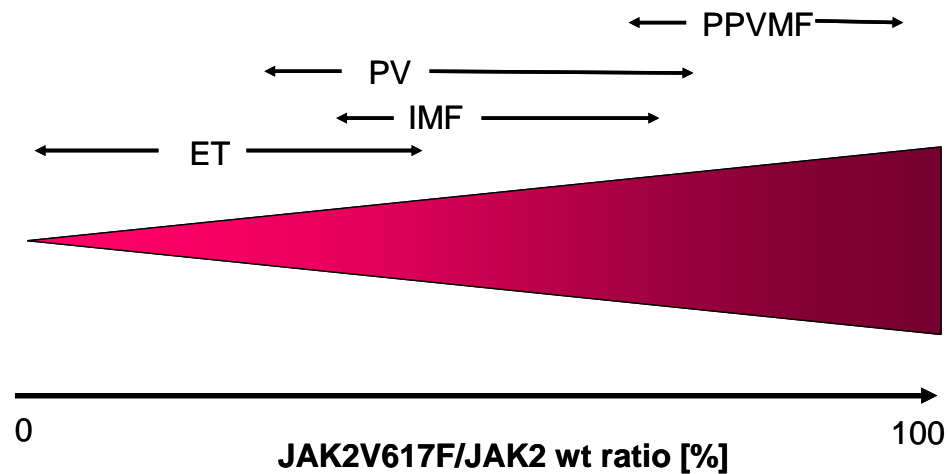


Figure 1.4: Gene dosage effect of JAK2V617F in comparison to wild-type: The ratio between the JAK2V617F and the wild-type determines the phenotype of the disease. High level of JAK2V617F leads to PV and IMF phenotype where as low level leads to ET like phenotype. Progression from PV to post-PV MF (PPVMF) is associated with an increase in the JAK2V617F allele burden due to mitotic recombination or trisomy 8.

Another way to modulate the JAK2V617F activity is by proteins which negatively regulating the JAK2 activity. Suppressors of cytokine signaling SOCS3, SOCS1, and SHP1 are the candidate proteins involved in the suppression of JAK2 signaling pathway. A recent study showed epigenetic inactivation of SOCS3, SOCS1, and SHP1 in MPDs but no correlation was made with the presence of JAK2V617F^{74,75}. Receptor interaction also plays a major role in lineage restriction. JAK2 is a crucial tyrosine kinase required

for many type I receptors including erythropoietin receptor, thrombopoietin receptor, and also for cytokines like IL-3, and GM-CSF receptors. These receptors are expressed specifically during myeloid to erythroid differentiation. MPL is expressed at high levels in megakaryocyte precursors, suggesting that a small amount of JAK2V617F is enough to induce ET whereas EpoR is expressed at low levels on erythroid progenitors, suggesting that high activity of JAK2V617F is required for PV. It has been demonstrated that JAK2V617F-mediated transformation of Ba/F3 cells is facilitated by the expression of homodimeric type I cytokine receptor such as the EpoR²³. Recently Lu and et al. showed that dimerization of the EpoR is necessary for the constitutive activation of JAK2V617F⁷⁶. However, parental Ba/F3 cells expressing JAK2V617F but lacking the EpoR are also able to proliferate IL-3-independently^{7,77}. These results indicate that the interaction between cytokine receptors and JAK2V617F may be crucial for oncogenic transformation, even though the exact mechanism and receptor requirements remain largely unclear. Funakoshi et al. showed that level of interaction between the receptor and JAK2V617F may influence the phenotype⁷⁸. These results further demonstrate that cell specific receptor expression and the stronger interaction with JAK2V617F leads to different phenotypes.

Hypothesis 4: JAK2V617F is an event secondary to an unknown pre-JAK2 event determining the phenotype

Another way to explain JAK2V617F mediated different phenotypes is to assume that JAK2 mutation is not the sole event responsible for the pathogenesis of the disease but another molecular event would occur before the JAK2V617F mutation. This event would be responsible for the different phenotypes. Supporting this hypothesis Kralovics et al. data showed that MPN patients had JAK2V617F/JAK2 allelic ratios below 25%.⁷⁹ X chromosome inactivation studies in the MPN patients showed strong correlation between clonality and JAK2V617F mutation in only PV patients but not in ET and IMF patients^{80,81}. These studies suggest that the first hit would be responsible for a clonal expansion and that the JAK2V617F mutation would occur as a second hit. Cambell et al. analyzed the leukemic transformation of JAK2V617F positive MPN patients. Most of the patients developed a JAK2V617F negative acute myeloid leukemia (AML). Based on their observation they proposed three models to explain the transformation of JAK2V617F negative AML. One possibility is that leukemic transformation may have occurred in a

JAK2V617F cell that subsequently becomes JAK2V617F negative. Another possibility is that the leukemia could have developed from a normal stem cell, not part of the original clone. Third model to explain the development of JAK2V617F negative AML is that in these patients, initial pre JAK2 event which resulted from an unidentified mutation⁸². Recently, many groups also described several patients with additional molecular abnormality associated with the JAK2V617F, such as BCR-ABL⁸³, MPL mutations²⁵ or other JAK2 mutations⁸⁴.

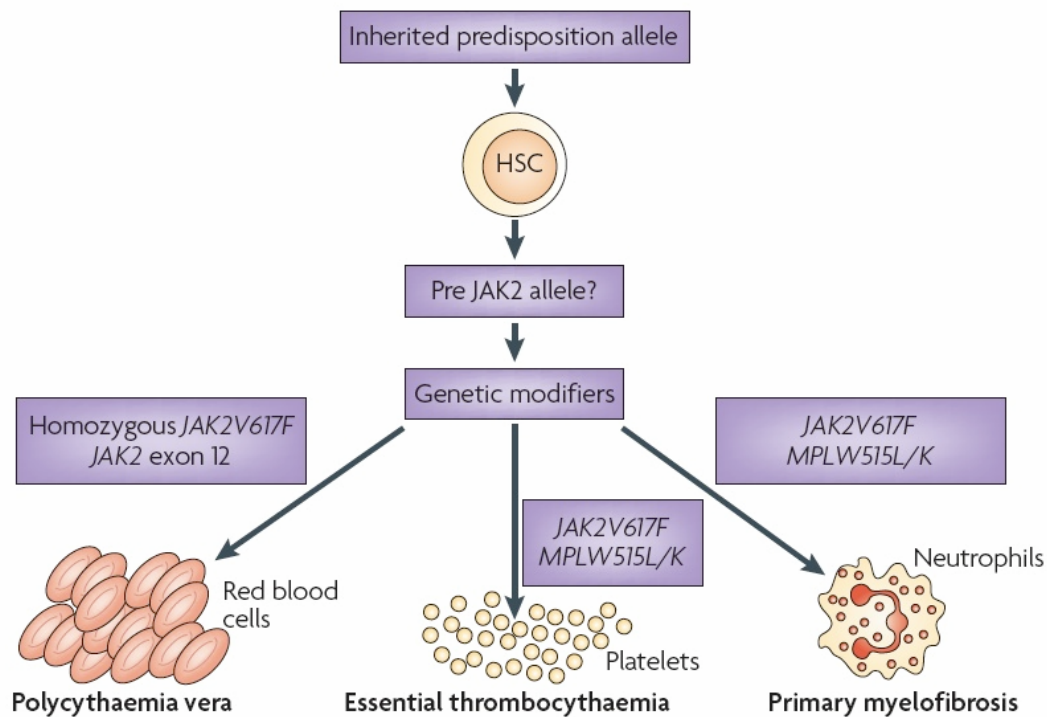


Figure 1.5: A proposed model of MPNs pathogenesis (Levine et al. Nature reviews cancer 2007). Occurrence of the JAK2V617F mutation leads to PV, ET and IMF. James et al. proposed four hypotheses to explain the different phenotypes mediated by the JAK2V617F mutation. The phenotype depends on the cell targeted by the molecular event, status of the JAK2V617F allele and additional mutations, genetic background of the host and finally inherited predisposition allele which all together determine the phenotype of MPNs.

Another evidence for the presence of pre JAK2 event is the observation of wild-type EEC together with JAK2V617F positive EEC in JAK2V617F positive PV patients⁸⁵. These results suggest that unknown pre JAK2 event would not only responsible for the disease but also promote erythropoietin independent differentiation. Another important observation which supports the hypothesis of the pre JAK2 event is the analysis of

familial cases of MPNs^{86,87}. This analysis showed occurrence of different MPNs within the same families, such as JAK2V617F-positive ET, JAK2V617F-positive IMF, JAK2 wild type mastocytosis and BCR-ABL CML. This indicates that in these families a germ line pre JAK2 mutation that predisposes family members to different MPNs. Linkage analysis is a powerful tool for the identification of unknown pre JAK2 event responsible for the development of MPNs in these families and accordingly investigation is on going. Recently, three independent groups identified a genetic haplotype that predisposes to the subsequent development of JAK2V617F⁸⁸⁻⁹⁰. Their results provide the first strong evidence that the JAK2V617F mutation is not the sole abnormality causing MPNs. Figure 1.5 summarizes the four hypothesis model of JAK2V617F mediated MPNs.

1.1.5 Inhibitors against JAK2V617F

Great advances have been made in recent years in the developing powerful kinase inhibitors and this development was clearly boosted by the great clinical success with BCR-ABL kinase inhibitor imatinib. Most of the drug discovery efforts were focused on the identification of kinase inhibitors which are ATP-mimetic small molecular inhibitors. The identification of JAK2V617F mutation in MPNs resulted in great deal of excitement and optimism in the development of small molecular inhibitors against JAK2. The JAK family consists of four members and all share very similar structural features. JAK1 plays a major role in lymphoid development and the JAK1 knock out mice showed a perinatal lethal phenotype. JAK2 is absolutely required for erythropoietin signaling and JAK2 knock out mice showed embryonic lethal due to lack of erythropoiesis. JAK3 deficient mice have severe combined immunodeficiency (SCID) phenotype. This indicates that JAK family kinases have non redundant important functions. That's why using JAK inhibitors may cause severe side effects. It is also very important to keep in mind that V617F mutation is located in a region out side of the kinase domain and ATP competitive inhibitors of JAK2 are not likely to discriminate between wild- type and mutant JAK2. Several JAK2 inhibitors are already in clinical studies among them INCB018424, TG101348, XL019, and CEP701. These compounds are entered phase III studies.

INCB018424 is a potent and selective inhibitor of JAK1 and JAK2 with IC₅₀ of 3.3 and 2.8nm respectively⁹¹. In murine models of JAK2V617F driven disease, treatment of

mice with INCB018424 showed a significant reduction of spleen size and also an increased over all survival compared to vehicle treated mice. INCB018424 also showed inhibition of CD34+ cells isolated from PV patients and also showed significant suppression of pro-inflammatory cytokines such as IL-1, TNF- α , IL-6, VEGF, and bFGF⁹¹. Patients treated with INCB018424 showed reduction in spleen size, alleviation of constitutional symptoms and reduction of plasma concentration of proinflammatory and angiogenic cytokines. Despite the clinical improvements INCB018424 treated MPN patients data showed JAK2V617F allele burden was reduced very modest level^{92,93}.

TG101348 is a selective and potent JAK2 inhibitor. It has a 35-and 334- fold selectivity for JAK2 as compared with JAK1 and JAK3 respectively⁹⁴⁻⁹⁶. Extensive investigation of TG101348 was conducted using multiple *invitro* and *invivo* systems. TG101348 treatment resulted in the apoptosis of JAK2V617F Ba/F3 and HEL cell lines. In murine model of JAK2V617F induced PV, mice treated with TG101348 showed decrease in hematocrit, spleen size and overall survival compared to vehicle treated mice⁹⁴. Treatment of the IMF patients with TG101348 showed 50% reduction in spleen size, marked reduction in WBC count and 50% of reduction in granulocyte mutant allele burden⁹⁶.

CEP-701 is a derivative of indolocarbazole K252. It showed strong inhibitory activity of JAK2 (IC₅₀=1nM). CEP-701 showed inhibition of Ba/F3 cells expressing JAK2V617F, HEL cells and primary cells from MPD patients. Preliminary clinical observation in myelofibrosis studies showed decreased spleen size, improvement in blood cell count, myelosuppression⁹⁷.

XL019 is a potent JAK2 inhibitor (IC₅₀=2nM) and it was demonstrated that high degree of selectivity against other JAK family members. XL019 showed strong inhibition of HEL cell lines and also primary cell lines from PV and IMF patients. In *in vivo* studies using HEL xenograft models XL019 treatment showed strong suppression of STAT5 activity.

So far all these compounds inhibit both mutated and unmutated JAK2. Therefore it would be very important to identify the JAK2V617F specific small molecular inhibitor.

1.2 HES/CEL

Idiopathic hypereosinophilic syndrome (HES) and chronic eosinophilic leukemia (CEL) are characterized by an unexplained persistent eosinophilia exceeding 1.5×10^9 eosinophils per liter for more than 6 months and finally leads to tissue infiltration and organ damage ⁹⁸. The word hyper eosinophilic syndrome was coined by Hardy and Anderson to describe patients with prolonged eosinophilia of unknown reason. Hyper eosinophil syndrome (HES) or chronic eosinophilic leukemia (CEL) are diagnosed after the exclusion of reactive causes of eosinophilia. However CEL has been differentiated from HES by presence of increased peripheral blood (more than 2%) or marrow (5%-19%) blasts or the identification of clonal cytogenetic abnormality in the myeloid lineage ⁹⁹. Recent discovery of dysregulated tyrosine kinases in the myeloproliferative diseases led to the revision the WHO classification and a semi molecular classification scheme with myeloid and lymphoid neoplasms with eosinophilia and abnormalities of PDGFRA, PDGFRB or FGFR1 was introduced ¹⁰⁰.

1.2.1 Identification and generation of FIP1L1-PDGFR

Imatinib treatment of HES patients was reported in 2001. Patients who were resistant to corticosteroids, hydroxy urea and IFN- α had undergone imatinib therapy at a concentration of 100mg per day. After 35 days of imatinib therapy the patients showed complete disappearance of peripheral eosinophils. The rational reason for the use of imatinib was completely unclear that time. Later another report also showed complete hematological remission of four HES patients who were treated with imatinib ¹⁰¹. A third report with imatinib therapy was a 54 –year old HES patient with splenomegaly and WBC count range from $9700/\text{mm}^3$ with 68% eosinophilia. After imatinib treatment at the concentration of 100mg per day, the patient showed complete hematological remission with decreased WBC count and 0% eosinophils ¹⁰².

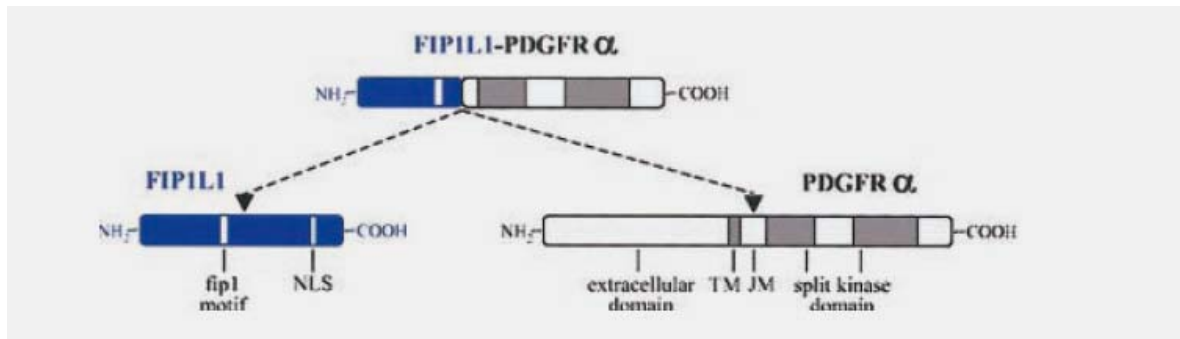


Figure 1.6: Generation of FIP1L1-PDGFR α (Gotlib et.al: 2004). FIP1L1-PDGFR α is generated by a fusion of 5' part of FIP1L1 to 3' part of PDGFR α gene by deletion of 800kb on chromosome number 4q12. NLS indicates the nuclear localization signal, TM is transmembrane region; and JM stands for juxtramembrane region.

Finally in 2003, a constitutively activated tyrosine kinase could be identified in a subset of patients with primary eosinophilia. The most common molecular feature is FIP1L1-PDGFR α (FP)^{103,104}, generated by a small interstitial deletion at chromosome 4q12¹⁰³ (Figure 1.6). Cools et al first described the FIP1L1-PDGFR α fusion in 9 of 16 patients (56%). Later several groups independently identified FIP1L1-PDGFR α fusion in HES patients with different frequencies¹⁰⁴⁻¹⁰⁶. Overall data showed that 10-20% of patients with Idiopathic hypereosinophilic syndrome are FIP1L1-PDGFR α positive¹⁰⁰.

1.2.2 Molecular mechanism of FIP1L1-PDGFR α activation

The FIP1L1-PDGFR α fusion gene is generated by deletion of 800kb region on chromosome number 4q12¹⁰³. HES patients positive for FIP1L1-PDGFR α appeared as normal karyotype because the 800 kb deletion is not visible in conventional chromosomal banding. The deletion takes place between 5' FIP1L1 to 3' PDGFR α ¹⁰³ (Figure 1.6). The break point varies from patient to patient but the FIP1L1-PDGFR α fusion is always in frame. The break points in the FIP1L1 part is scattered over the 40 kb region where as in PDGFR α it is restricted to exon 12¹⁰³. FIP1L1 encodes a protein of 520 aminoacids playing a major role in polyadenylation in yeast^{107,108}. FIP1L1 homologous were also identified in plants, worms, flies, rats and mice but the actual function of FIP1L1 in humans and mice is not determined so far. All these organisms share a 42 aminoacids common fip1 motiff (pfam domin no. PF05182; [http:// pfam.wustl.edu/cgi-bin /get desc?](http://pfam.wustl.edu/cgi-bin/get_desc?)

acc=pf05182) . Data base analysis derived from different tissues and cell types predicted that FIP1L1 is under the control of a ubiquitous promoter.

FIP1L1-PDGFR α activates several signaling molecules e.g. phosphoinositol 3-kinase, ERK1/2 or STAT5^{103 109}. Retroviral expression of FIP1L1-PDGFR α in mice bone marrow induce myeloproliferative disease¹¹⁰. Later Yamaka et.al showed that the expression of FIP1L1-PDGFR α together with overexpression of IL-5 leads to a phenotype with typical features of HES¹¹¹. Unlike to the other reported fusion kinases such as ETV6-PDGFR β , ZNF198-FGFR1 or BCR-ABL proteins, FIP1L1-PDGFR α does not have a dimerization motif. Recently Stover et al. showed that deletion of the juxtramembrane domain of PDGFR α is sufficient for kinase activation where as FIP1L1 part is dispensable¹¹². Consistent with this findings patients data also reported that break points within the FIP1L1 are variable but break points within the PDGFR α are tightly clustered¹⁰⁰. The production of the fusion construct is still under the control of the FIP1L1 promoter which might be a functional important.

1.2.3 Treatment and drug resistance to FIP1L1-PDGFR α positive HES/CEL

The Abl, Kit and PDGFR small molecule kinase inhibitor imatinib mesylate (Gleevec) constitutes the current standard treatment for Bcr-Abl positive CML and is active in gastrointestinal stromal tumor (GIST), were it suppresses constitutively activating mutations of c-kit or PDGFR α . Both, in CML¹¹³⁻¹¹⁹ as well in GIST¹²⁰⁻¹²⁴, acquired resistance to imatinib is associated with the emergence of secondary kinase domain mutations that interfere with drug binding to the target kinase. Alternative kinase inhibitors are emerging as the most promising strategy to overcome drug resistance induced by kinase domain mutations. In CML, novel Abl kinase inhibitors display only partially overlapping profile of resistance mutations with imatinib¹²⁵⁻¹²⁷. Sequential treatment with imatinib and the approved, second-generation Abl kinase inhibitors nilotinib (Tasigna) and dasatinib (Sprycel) has already become reality¹²⁸. The selection of the appropriate inhibitor is based on the presence of specific Bcr-Abl resistance mutations. Imatinib has demonstrated clinical activity and induced complete remissions in the majority of cases with myeloproliferation positive for PDGFR-A abnormalities including FP^{103,104,129-131}, and BCR-PDGFR α ¹³², but also in PDGFR-B abnormalities, including ETV6-PDGFR β ^{133,134}, TEL-PDGFR β ¹³³, and others¹³⁵⁻¹⁴³.

The Abl, Kit and PDGFR small molecule kinase inhibitor imatinib mesylate (Gleevec) was reported to induce remissions in cases of idiopathic hypereosinophilic syndrome¹⁰¹. In CML and Ph+ ALL, resistance to imatinib is associated with the emergence of point mutations within the Abl kinase domain that obviate binding to the drug target. The first exchange reported was Bcr-Abl/T315I¹¹³, which is known to give rise to imatinib (Gleevec), nilotinib (Tasigna) and dasatinib (Sprycel) resistance^{113,144,145}. In the meantime more than 40 different exchanges have been described to confer imatinib resistance in patients with CML and Ph+ ALL¹¹³⁻¹¹⁹. So far, four cases of FIPL1-PDGFR α positive myeloproliferation with acquired imatinib resistance due to a point mutation in the PDGFR α kinase domain have been reported^{103,146-148}. Strikingly in all four cases, a PDGFR α /T674I exchange was identified, which corresponds to (T315I) in Abl. Thus, it can be foreseen that like in CML, an array of different PDGFR-A and -B mutations might emerge as more patients with myeloproliferation positive for PDGFR or fusions are treated with imatinib.

1.3 Objectives

The oncogenic JAK2V617F mutation is found in the majority of myeloproliferative diseases like polycythemia Vera (PV), essential thrombocythemia (ET) and primary myelofibrosis (PMF). However, the molecular mechanism leading to constitutive kinase activity is largely unclear. JAK2 contains seven conserved domains, which are designated as JAK homology (JH) domains JH1-JH7. JH1 is a functional tyrosine kinase domain that becomes activated following cytokine stimulation. The pseudokinase domain (JH2) is adjacent to the kinase domain (JH1) and is thought to play a role in auto-inhibition of the kinase activity of JAK2. The N-terminal FERM domain mediates binding of JAK2 to membrane proximal regions of cytokine receptors. The presence of a SH2 or SH2-like domain located between the FERM and the pseudokinase domain has been identified using structure prediction tools, but the function of the JAK2 SH2 domain has not been determined yet. Since the SH2 domain is adjacent to the pseudokinase domain containing the V617F mutation, we hypothesized a possible role of the SH2 domain for the constitutive phosphorylation of JAK2V617F. Our goal was to determine the role of the SH2 domain and FERM domain in JAK2V617F-mediated transformation and myeloproliferation.

FIP1L1-PDGFR alpha (FP) is a constitutively activated protein kinase which was reported in chronic eosinophilic leukemia (CEL) and in cases of hypereosinophilic syndrome and mastocytosis with eosinophilia. Imatinib is clinically active against FIP1L1-PDGFR positive disease. However, clinical resistance to imatinib has been observed in FIP1L1-PDGFR positive leukemia and was shown to occur due to a secondary mutation (T674I) in the PDGFR alpha kinase domain. So other part of the work was focused on the identification of drug resistance mutations in FIP1L1-PDGFR against PDGFR inhibitors imatinib, nilotinib and sorafenib. We therefore aimed to generate specific resistance profiles for available PDGFR kinase inhibitors.

2. MATERIALS AND METHODS

2.1 MATERIALS

2.1.1 Reagents

2-Mercaptoethanol	Sigma-Aldrich, Taufkirchen
3-[N-Morpholino]-Propanesulfonicacid (MOPS)	Sigma-Aldrich, Taufkirchen
Acrylamide/Bisacrylamide Gel 30	Carl Roth, Karlsruhe
Agarose	Carl Roth, Karlsruhe
Aluminumhydroxide Gel	Sigma-Aldrich, Taufkirchen
Ammoniumchloride	Fluka, Taufkirchen
Ammoniumhydrogencarbonate	Sigma-Aldrich, Taufkirchen
Ammoniumpersulfate (APS)	Sigma-Aldrich, Taufkirchen
Ampicillin	Sigma-Aldrich, Taufkirchen
Aqua ad injectabilia, steril	Braun, Melsungen
Bacto™Agar	BD Biosciences, Heidelberg
Bacto™Tryptone	BD Biosciences, Heidelberg
Bromophenolblue	Sigma-Aldrich, Taufkirchen
BSA, Fraktion V	Carl Roth, Karlsruhe
Calcimchloride	Merck, Darmstadt
Calciumhydrogencarbonate	Sigma-Aldrich, Taufkirchen
Chloroform	Sigma-Aldrich, Taufkirchen
Complete™Protease Inhibitor Cocktail	Roche Diagnostics, Penzberg
Coomassie Brilliant Blue	Sigma-Aldrich, Taufkirchen
Diethylenpyrocarbonate(DEPC)	Fluka, Taufkirchen
Dimethylsulfoxide (DMSO)	Sigma-Aldrich, Taufkirchen
Dinatriumhydrogenphosphate	Merck, Darmstadt
Dithiothreitol (DTT)	Promega, Heidelberg
dNTP-Mix, 10mM	Fermentas, St. Leon-Rot
Glacial acetic acid	Carl Roth, Karlsruhe
Ethanol	Riedel-de Haën, Taufkirchen
Ethidiumbromide	Carl Roth, Karlsruhe
Ethylendiamine-N,N,N',N'-tetraacetic acid (EDTA)	Fluka, Taufkirchen

MATERIALS AND METHODS

Formaldehyde, 37%-ig	Sigma-Aldrich, Taufkirchen
Glucose	Carl Roth, Karlsruhe
Glutaraldehyde 2,5%	Fluka, Taufkirchen
Glutathione-Sepharose	Pharmacia Biotech, Freiburg
Glycerol	Fluka, Taufkirchen
Glycerol-2-phosphate	Sigma-Aldrich, Taufkirchen
Glycine	Merck, Darmstadt
HEPES	Fluka, Taufkirchen
Isopropanol	Merck, Darmstadt
Isopropyl- β -D-Thiogalactosid (IPTG)	Sigma-Aldrich, Taufkirchen
Calcimchloride	Merck, Darmstadt
Calciumhydrogencarbonate	Sigma-Aldrich, Taufkirchen
Lipopolysaccharide (LPS)	Sigma-Aldrich, Taufkirchen
Magnesiumchloride	Carl Roth, Karlsruhe
Methanol	Merck, Darmstadt
N,N-Dimethylformamide	Merck, Darmstadt
Sodium Acetate	Fluka, Taufkirchen
Sodium Azid	Sigma-Aldrich, Taufkirchen
Sodium Chloride	Carl Roth, Karlsruhe
Sodium Citrate	Fluka, Taufkirchen
Sodium Dihydrogen Phosphate	Merck, Darmstadt
Sodium Dodecyl Sulfate (SDS)	Carl Roth, Karlsruhe
Sodium Fluoride	Fluka, Taufkirchen
Sodium Hydroxide	Merck, Darmstadt
Sodium Ortho Vanadate	Sigma-Aldrich, Taufkirchen
Sodium pyrophosphate	Fluka, Taufkirchen
Permeabilization Buffer (10x)	eBioscience, an Diego, USA
Phosphat buffered saline (PBS), 10X	Biochrom AG, Berlin
PMSF	Roche, Penzberg
Polybrene	Sigma-Aldrich, Taufkirchen
Propidiumiodid	Sigma-Aldrich, Taufkirchen
Tetramethylethylendiamine (TEMED)	Fluka, Taufkirchen

Tris (hydroxymethyl) aminomethane (TRIS)	Carl Roth, Karlsruhe
Triton X-100	Sigma-Aldrich, Taufkirchen
Milk powder	Fluka, Taufkirchen
Tween 20	Fluka, Taufkirchen
Xylolcyanolblue	Sigma-Aldrich, Taufkirchen

2.1.2 Medium and supplements for cell culture

β -Mercaptoethanol, 50mM	Gibco/Invitrogen, Karlsruhe
DMEM, cell culture medium	PAA, Pasching, Austria
FCS Gold	PAA, Pasching, Austria
G418 (Neomycin)	Calbiochem, Darmstadt
Pencilin and streptomycin 100x	PAA, Pasching, Austria
HANK`s BSS	PAA, Pasching, Austria
L-Glutamine, 100x	Gibco/Invitrogen, Karlsruhe
IL-3	R and D, Karlsruhe
Hygromycin	Calbiochem, Darmstadt
Diphtheria Toxin (DT)	Calbiochem, , Darmstadt
Lipofectamin™2000, Transfection reagent	Invitrogen,Karlsruhe
MethoCult®	StemCellTechnologies, Canada
Opti-Mem®	Gibco/Invitrogen, Karlsruhe
PBS, 10X, sterile	PAA, Pasching, Austria
RPMI 1640 (high Glucose, Glutamine)	PAA, Pasching, Austria
Trypsin-EDTA- 10X	PAA, Pasching, Austria

2.1.3 Enzymes

2.1.3.1 Restriction enzymes

EcoR1 (100U/ μ l)	Fermentas, St. Leon-white
HindIII(10U/ μ l)	Fermentas, St. Leon-red
NcoI (10U/ μ l)	Fermentas, St. Leon-red

Not1 (10U/ μ l)	Fermentas, St. Leon-red
Sall (10U/ μ l)	Fermentas, St. Leon-red
DpnI (10U/ μ l)	Fermentas, St. Leon-yellow
BamHI (100U/ μ l)	Fermentas, St. Leon-white
Xho1 (100U/ μ l)	Fermentas, St. Leon-red

2.1.3.2 DNA polymerases

High Fidelity PCR Enzyme Mix	Fermentas, St. Leon-Red
Pfu-DNA Polymerase	Fermentas, St. Leon-Red
Taq-DNA Polymerase	Fermentas, St. Leon-Red

2.1.3.3 Other enzymes

<i>CIAP</i> 20-30U/ μ l (Alkaline Phosphatase)	Invitrogen, Karlsruhe
Proteinase K	Sigma-Aldrich, Taufkirchen
SuperScript TM II Reverse Transcriptase	Invitrogen, Karlsruhe
T4-DNA Ligase	Fermentas, St. Leon-Red

2.1.4 Hormones

Epo (Erythropoietin)	Stock solution 5U/200 μ l
----------------------	-------------------------------

2.1.5 Radioactive substances

³² P- γ -ATP	Hartmann Analytica, Freiburg
³⁵ S Methionine	Hartmann Analytica, Freiburg

2.1.6 Membranes

PVDF Membran (Immobilon P)	Millipore, Schwalbach/Ts
----------------------------	--------------------------

2.1.7 Antibodies

Antibodies were used against phospho-JAK2 (21870-R), HA (Y-11), STAT5 (G-2), EpoR (M-20), IL3R alpha (V-18), and beta chain (T-20) were obtained from Santa Cruz Biotechnology (Heidelberg, Germany). Antibodies to phosphotyrosine (PY20), flag, myc,

JAK2, PDGFRA were purchased from Upstate Biotechnology (Biozol, Eching, Germany). PDGFRA antibodies were obtained from Upstate Biotechnology (06-495, Millipore, Schwalbach, Germany). Antibodies to phosphotyrosine were purchased from Upstate Biotechnology (4G10, Millipore, Schwalbach, Germany) and BD Transduction (PY20, BD Biosciences, Heidelberg, Germany). Monoclonal antibody against phospho-STAT5 was kindly provided by Thomas T. Wheeler and Henry B. Sadowski (Hamilton, New Zealand)¹¹⁴. anti-actin from Sigma (A5316, Sigma-Aldrich, Taufkirchen, Germany). Antibodies against to AKT (9272), p.AKT (9271), Erk1/2 (9102), p.ERK1/2 (9101), Src (2108), p.Src tyr 416 (2101s) were purchased from cell signaling technology.

2.1.8 Cell lines

HeLa	Human cervical carcinoma cell line, DSMZ
NIH3T3	Murine embryonic fibroblast cell line, DSMZ
ΦNX-Eco	Retroviral ecotropic virus packaging cell line
Gamma2A (γ2A)	Human fibrosarcoma cell line provided from Harvey Lodish
Ba/F3	Murine pro B cell line, DSMZ
COS-1	Monkey kidney cell line, DSMZ
EOL-1	Human Hyper Eosinophilic Syndrome patient cell line, DSMZ
HEL	Human Erythroid Leukemia, DSMZ

2.1.9 Vectors and DNA constructs

2.1.9.1. Vectors

MSCV MigR1	J.Miller/ W. Pear, Philadelphia,USA
pcDNA 3.1/Zeo(-)	Invitrogen, Karlsruhe
pCMV-Tag	Invitrogen, Karlsruhe
PGEX-4T-2 1	Amersham Biosciences, Freiburg

2.1.10 Bacterial Strains

<i>E.Coli</i> DH5α™	Invitrogen, Karlsruhe
---------------------	-----------------------

Epicurian Coli™ XL-1Blue Supercompetent Cells Stratagene, Heidelberg

OneShot® BL21 Star™ Chemically Competent *E.coli* Invitrogen, Karlsruhe

2.1.11 Oligonucleotides for PCR (5'→3')

GST_ JAK2 SH2 Domain

For: GATCGATCGAATTCACGTCAGGCCGGGTCCAGCACTG

Rev: GATCGATCCTCGAGTCAACCACTCAAAGAGCTCCTCCACCC

Flag tag JAK2

For:

CTGAAAAAGACTTCGCATGGATTACAAGGATGACGACGATAAGGAATGGCCT
GCCTTAC

Rev:

GTAAGGCAGGCCATTCCCTTATCGTCGTCATCCTTGTAATCCATGCAGAGTCT
TTTTCAG

Myc tag JAK2

For: CCCCCGGGCTGCAGGAGTTCGGAATTGCCTGCC

Rev: GGCAGGCCATCCCGAACTCCTGCAGCCCCGGGGG

GST-FP

For: GATCGAATTCTGTCCGGCCGGCGAGGTCGAG

Rev: GATCCTCGAGTAATTACAGGAAGCTGTCTTC

GST_ SHP2 SH2 domain (N ter)

For: GATCGAATTCTGACATCGCGGAGATGGTTTCAC

Rev: GATCCTCGAGTAACACCTTTCAGAGGTAGGATCTG

GST_ SHP2 phosphatase domain

For: GATCGAATTCTGTGGGAAGAATTTGAGACACTA

Rev: GATCTTCGAGTAAATAATGCTGGACGGCCATATAG

GST-SHP2

For: GATCGAATTCTGACATCGCGGAGATGGTTTCAC

Rev: GATCCTCGAGTAATCTGAACTTTTCTGCTG

 Δ FIP1L1-W (INS) PDGFRA

For: GATCGATCGAATTCATGATTCGCTGGAGGGTCATTGAATC

Rev: GATCGATCGAATTCTAATCCACCAGGTCTGAAGAGTCT

 Δ FIP1L1- PDGFRA

For: GATCGATCGAATTCATGCTGCCTTATGACTCAAGATGG

Rev: GATCGATCGAATTCTAATCCACCAGGTCTGAAGAGTCT

2.1.12 Oligonucleotides for site directed mutagenesis (5'→3')

V617F JAK2

For: GGAGTATGTTTCTGTGGAGACGAGAATATTC

Rev: GAATATTCTCGTCTCCACAGAAACAACATACT

R426K JAK2

For: GGACTGTATGTACTTAAATGCAGTCCTAAGGAC

Rev: GTCCTTAGGACTGCATTTAAGTACATACAGTCC

L40A/Y41A JAK2

For: GTTCTTCAGGTGTATGCTGCTCATTCCCTTGGGAAATC

Rev: GATTTCCCAAGGGAATGAGCAGCAGCATAACCTGAA

F604S FP

MATERIALS AND METHODS

For: GGGGTCTGGAGCGTCTGGGAAGGTGGTTGAAG

Rev: CTTCAACCACCTTCCCAGACGCTCCAGACCCC

G610R FP

For: GAAGGTGGTTGAACGGACAGCCTATGGATTAAG

Rev: CTTAATCCATAGGCTGTTCGTTCAACCACCTTC

P618S FP

For: CTATGGATTAAGCCGGCCCCAACCTGTCATG

Rev: CATGACAGGTTGGGGCCGGCTTAATCCATAG

V658A FP

For: CCACATTTGAACATTGCGAACTTGCTGGGAGCC

rev: GGCTCCCAGCAAGTTCGCAATGTTCAAATGTGG

V658G FP

For: CCACATTTGAACATTGGAACTTGCTGGGAGCC

Rev: GGCTCCCAGCAAGTTTCCAATGTTCAAATGTGG

L694V FP

For: GAATAGGGATAGCTTCGTGAGCCACCACCCAG

Rev: CTGGGTGGTGGCTCACGAAGCTATCCCTATTC

S772Y FP

For: CTCATATAAGAAGAAATATATGTTAGACTC

Rev: GAGTCTAACATATATTTCTTCTTATATGAG

M862I FP

For: CCCGTGAAGTGGATTGCTCCTGAGAGC

Rev: GCTCTCAGGAGCAATCCACTTCACGGG

T674I FP

For: GGCCCCATTTACATCATCATAGAGTATTGCTTC
Rev: GAAGCAATACTCTATGATGATGTAAATGGGGCC

D842E FP

For: GACTTTGGCCTGGCCAGACAGATCATGCATGATTCG
Rev: CGAATCATGCATGATCTGTCTGGCCAGGCCAAAGTC

D842G FP

For: GACTTTGGCCTGGCCAGAGGGATCATGCATGATTCG
Rev: CGAATCATGCATGGATCCCTCTGGCCAGGCCAAAGTC

D842H FP

For: GACTTTGGCCTGGCCAGACAGATCATGCATGATTCG
Rev: CGAATCATGCATGATCTGTCAGGCCAGGCCAAAGTC

D842V FP

For: CTTTGGCCTGGCCAGAGTCATCATGCATGATTCG
Rev: CGAATCATGCATGATGACTCTGGCCAGGCCAAAG

Y849L FP

For: GAGATCATGCATGATTCGAACCTTGTGCTGAAAGGC
Rev: GCCTTTCAGCACAAGGTTTGAATCATGCATGATCTC

T874I FP

For: GACAACCTCTACACCATACTGAGTGACGTCTGG
Rev: CCAGACGTCACTCAGTATGGTGTAGAGGTTGTC

R841G FP

For: GACTTTGGCCTGGCCGGAGACATCATGCATGATTCG
Rev: CGAATCATGCATGATGTCTCCGGCCAGGCCAAAGTC

V850G FP

For: CATGATTGAACTATGCGTCGAAAGGCAGTACC

Rev: GGTACTGCCTTTTCGACGCATAGTTCGAATCATG

P864S FP

For: GTGAAGTGGATGGCTTCTGAGAGCATCTTTG

Rev: CAAAGATGCTCTCAGAAGCCATCCACTTCAC

N659D FP

For: CATTGAAACATTGTAGACTTGCTGGGAGCCTGC

Rev: GCAGGCTCCCAGCAAGTCTACAATGTTCAAATG

N656Y FP

For: CTGGGGCCACATTTGTACATTGTAAACTTGCTG

Rev: CAGCAAGTTTACAATGTACAAATGTGCCCCAG

S903C FP

For: GGCATGATGGTGGATTGTACTTTCTACAATAAG

Rev: CTTATTGTAGAAAGTACAATCCACCATCATGCC

A640G FP

For: CAGTGAAAAACAAGGTCTCATGTCTGAACTG

Rev: CAGTTCAGACATGAGACCTTGTTTTTCACTG

K688R FP

For: GTCAACTATTTGCATCGGAATAGGGATAGC

Rev: GCTATCCCTATTCCGATGCAAATAGTTGAC

T799P FP

For: GATTTGTTGAGCTTCCCCTATCAAGTTGCCCGAGG

Rev: CCTCGGGCAAGTTGATAGGGGAAGCTCAACAAATC

2.1.13 Oligonucleotides for sequencing (5'→3')

FIP1L1:

For: ATCAAGACAGGGGGAAGAG

rev: CAGGCAGAGGAATGATGTAGCCAC.

PDGFRA TK1 and KI:

For: CCATGGCGT AAACCTGGTGC

Rev: CAGGCAGAGGAATGATGTAGCCAC

PDGFRA TK2:

For: GGGCCACATTTGAACATTGTAAAC

Rev: GCATT GTCTGAGTCCACACG

2.1.14 Molecular markers for nucleic acids and proteins

GeneRuler™1kb DNA Ladder	Fermentas, St. Leon-Red
GeneRuler™ High Range RNA Ladder	Fermentas, St. Leon-Red
PageRuler™Prestained Protein Ladder	Fermentas, St. Leon-Red

2.1.15 Mouse Strains

Balb/c	HarlanWinkelmannGmbH,Borchen
--------	------------------------------

2.1.16 Materials and kits for molecular biology

Bio-Rad Protein assay	Bio-Rad, München
DNeasy® Blood & Tissue Kit	Qiagen, Hilden
Microvette® 300Z	Sarstedt, Nümbrecht
Platinum® SYBR® Green qPCR SuperMix-UDG	Invitrogen, Karlsruhe
QIAGEN® Plasmid Maxi Kit	Qiagen, Hilden
QIAprep® Spin Miniprep Kit	Qiagen, Hilden

QIAquick [®] Gel Extraction Kit	Qiagen, Hilden
QIAquick [®] Spin Purification Kit	Qiagen, Hilden
Rapid DNA Ligation Kit	Roche Diagnostics, Penzberg
RevertAid [™] H minus First Strand cDNA Synthesis Kit	Fermentas, St. Leon-Rot
RNeasy [®] Plus Mini Kit	Qiagen, Hilden
SuperSignal [®] Chemoluminescence Substrate	Pierce, Rockford, USA
Trizol [®] Reagent	Sigma-Aldrich, Taufkirchen

2.1.17 Instruments

ABI PRISM [®] 7700	Applied Biosystems, USA
Agarose gel Electrophoresis chamber	Biometra, Göttingen
CO ₂ -Incubator SW J 500 TV BB	Nunc, Wiesbaden
Digital watch LC 1200 S	Satorius, Göttingen
Durchflusszytometer (EPICS [®] XL)	Beckman-Coulter, Krefeld
ELISA Reader sunrise	Tecan, Crailsheim
Optimax	Protec, Oberstenfeld
Fluorescence microscope	Olympus Optical Co., Hamburg
Thermo heater 5436	Eppendorf, Hamburg
Incubator-Shaker Innova 4000	New Brunswick Scientific, USA
Cold centrifuge J2-HS, Rotor JA-14	Beckman, Fullerton, USA
Cold centrifuge 5417R, 5810R	Eppendorf, Hamburg
Light microscope Axiovert 25	Zeiss, Jena
LKB Ultraspec III, Spectrophotometer	Pharmacia, Uppsala, Schweden
Magnetic stirrer IKAMG RH	Janke & Kunkel, Staufen
Micro96 Harvester	Skatron Instruments, Norwegen
Microscope V 200	Hund, Wetzlar
Multi-Gel Long Electrophoresis chamber	Biometra, Göttingen
PCR-Thermocycler Primus 96	Peqlab, Erlangen
pH-Meter Φ32	Beckman, Fullerton, USA
Refrigerated Incubator-Shaker Innova	New Brunswick Scientific, USA
Sterile work bench, HeraSafe	Thermo Scientific, Karlsruhe
Scintillation counter (LS65000)	Beckman, Fullerton, USA

Stromgenerator, Powerpack P25	Biometra, Göttingen
Table centrifuge 5417R	Eppendorf, Hamburg
Transfer Electrophoresis Unit	Hofer, San Francisco, USA
Trio-Thermoblock	Biometra, Göttingen
Ultra-Turrax T8	IKA®-Werke, Staufen
Ultracentrifuge, Rotor VTI 80	Beckman, Fullerton, USA
UV crosslinker 2400	Stratagene, La Jolla, USA
UV-Lamp TI 2	Biometra, Göttingen
Vortex Genie2	Scientific Industries, USA
Water bath 1083	GFL, Burgwedel

2.1.18 Buffers

Amidoblack –staining	0.2% Naphtol Blue Black 25% Isopropanol 10% glacial acetic acid
Amidoblack destaining buffer	25% Isopropanol 10% glacial acetic acid
Coomassie-staining	0.25% Coomassie-blue 45% Methanol 10% glacial acetic acid
Coomassie-destaining	45% Methanol 10% glacial acetic acid
DEPC-H ₂ O:	0.1% DEPC in A.d. O.N after autoclave
DNA-Loading buffer (6X):	30% Glycerol (v/v) 0.25% Bromphenolblue (w/v)

	0.25% Xylolocyanol 50mM EDTA in A.d.
FACS-buffer:	0.1% BSA in PBS
Luria-Bertani (LB) Medium	1% Bacto-Tryptone 0.5% Bacto-beef extract 1% NaCl in A.d. With 1 M NaOH (pH7.0)
Lysis-buffer:	10 mM Tris/HCl (pH7.5) 130 mM NaCl 5 mM EDTA 0.5% Triton X-100 20 mM Na ₂ HPO ₄ /NaH ₂ PO ₄ (pH7.5) 10 mM Sodiumpyrophosphate (pH7) 1mM Sodiumorthovanadate 20 mM NaF 1mM Glycerol-2-Phosphate 1Protease-Inhibitor Cocktail tablet Ad 10ml A.d.
Lysis-buffer P50:	10mM Tris/HCl (pH7.5) 1mM Calciumacetate 1.5mM Magnesiumacetate 2 mM DTT 1Protease-Inhibitor Cocktail tablet Add for 10ml A.d.
MOPS-buffer:	20mM MOPS 50mM Sodiumcitrate 10mM EDTA with1 M NaOH (pH7.0)

NETN-buffer:	0.5% (v/v) NP40 20mM Tris/HCl (pH8) 100mM NaCl 1 mM EDTA 1 mM PMSF 1 mM Benzamidine 1 Protease-Inhibitor Cocktail tablet ad 10ml A.d.
RBC (<i>Red Blood Cell</i>)-Lysis buffer:	150 mM NH ₄ Cl 1 mM KHCO ₃ 0.1 mM Na ₂ EDTA, pH7.3 in A.d.
RNA-Loading buffer (5X):	0.2% Bromphenolblue 4mM EDTA 7.2% Formaldehyde (37%) 20% Glycerol 3% Formamide 40% RNA-Loading buffer
Separating buffer for SDS-PAGE (4X):	0.5 M Tris (pH6.8) 0.4% SDS in A.d.
SDS-Electrophoresis buffer:	25 mM Tris 192 mM Glycine 0.1% SDS in A.d.
SDS-loading buffer (2X):	1 M Tris/HCl (pH6.8) 200mM DTT 4% SDS 0.2% Bromophenolblue

	20% Glycine in A.d.
SSC-buffer (20X): (<i>Standard Saline Citrate</i>)	0.3 M Sodium citrate HCl (pH7.0) 3M NaCl
TAE-buffer (10X):	0.4M Tris 1.1% Acetic acid 2% 0.5M EDTA (pH8) in A.d.
TNE-buffer:	10mM Tris (pH8) 100mM NaCl 1mM EDTA
Transfer buffer:	25mM Tris 192mM Glycine 0.1% SDS in A.d. 20% Methanol in A.d.
Stocking gel buffer SDS-PAGE (4X):	1.5M Tris (pH8.8) 0.4% SDS in A.d.

2.2 METHODS

2.2.1 Methods involving nucleic acids

2.2.1.1 Isolation, purification and measurement of DNA

DNA was isolated and purified by using “QIAprep spin Miniprep Kit” for minipreps (5 ml of bacterial culture). For maxiprep “Machery-Nagel affinity column chromatography” was used. DNA was extracted and purified from agarose gels using “QI prep quick gel extraction kit”. Purity of the DNA was measured by using “Nanodrop”.

2.2.1.2 Agarose gel electrophoresis

TAE-Buffer : 0.4M Tris, 1.1% Glacial Acetic Acid, 2% 0.5 M EDTA

DNA-Loading buffer: 50% (M/V) Glycerine, 0.5% (M/V) Bromophenol blue, 0.5M EDTA

DNA is separated by using agarose gel electrophoresis. Separation of DNA molecules is dependent on the size of the particles. High percentage agarose gels (1.5%-2%) are used to separate small DNA fragments (<500 bp). Low percentage agarose gels (0.5%-1%) are used to separate high molecular DNA fragments (>1000 bp). Agarose was melted in microwave and poured on a sealed horizontal gel apparatus to a depth of 4 - 8 mm. DNA samples were mixed with gel loading buffer and loaded onto the gel. Ethidium bromide is used to stain DNA for visualization. DNA bands were visualized using a UV transilluminator. Visualized DNA bands were cut with a scalpel and the DNA from the gel piece was isolated by using gel extraction protocol as described (2.2.1.1).

2.2.1.3 Restriction digestion, ligation and cloning of DNA

All restriction enzymes were purchased from either New England Biolabs or Fermentas and used according to manufacturer's protocol. In brief, 2µg of plasmid DNA, 2µl of 10 X enzyme buffer, 1µl of restriction enzyme and water to make final volume to 20µl. Incubated the Reaction mixture was incubated 37⁰ for one hour. to avoid relegation of vector DNA, alkaline phosphatase treatment was performed at 37⁰ for one hour. Digested DNA was then separated on agarose gel, isolated from the gel by using DNA gel extraction kit. Cloning of the JAK2, FIP1L1-PDGFR α and SHP2 fragment were described in cDNA constructs section.

2.2.1.4 Site directed mutagenesis and DNA sequence analysis

Point mutations in JAK2 and FIP1L1-PDGFR α were introduced using site-directed mutagenesis method (Fermentas) according to the manufactures instructions. Primers were designed such that the mutation is present at the desired nucleotide location and a PCR was performed for 18 cycles. The resulting PCR product contains the template DNA as well as the mutated product. To avoid the unmutated template from the PCR product, *DpnI* restriction digestion was performed. The nicks left in the PCR product are sealed upon transformation into appropriate bacterial strain. Bacterial colonies were then picked for the minipreps and the DNA product was sequenced before for the further analysis.

2.2.2 Inhibitors

Imatinib and nilotinib were a kind gift from Novartis Pharma AG, Basel, Switzerland. Sorafenib was purchased from American Chemicals Custom Corporation, San Diego, CA, USA. Nilotinib and sorafenib were dissolved in dimethyl sulfoxide (DMSO) to make stock solution of 10mM. Imatinib was dissolved in water to make stock solution of 10mM. PD166326 was dissolved in water and 10mM stock solution was prepared and stored at -20°C . MG 132, Leupeptin and cyclohexamide were purchased from sigma. 10mM Stock solutions were prepared and stored at -20°C . Cyclohexamide is prepared freshly by dissolving in dimethyl sulfoxide (DMSO) and used $40\mu\text{g/ml}$.

2.2.3. Cell Lines and Cell Culture

Murine Ba/F3 were obtained from the DSMZ (Braunschweig, Germany) and were grown in RPMI1640 medium containing 10% fetal calf serum, 200U/ml penicillin and 200ug/ml streptomycin (Gibco, Karlsruhe, Germany), in the presence of murine interleukin-3 (mIL-3) (R+D systems, Wiesbaden, Germany). 293T cells were maintained in Dulbecco modified eagle medium (Gibco) containing 10% fetal calf serum similarly NIH3T3 cell were grown in the DMEM containing 10% fetal calf serum and 200U/ml penicillin and streptomycin. γ 2A cells were kindly provided by Harvey Lodish. EpoR-Ba/F3 cells were maintained in the presence of human erythropoietin (Ortho Biotech, Neuss, Germany). The γ 2A human fibrosarcoma cell line was maintained in Dulbecco modified eagle medium containing 10% fetal calf serum with penicillin and streptomycin. Human EOL1 cell line was obtained from the DSMZ (Braunschweig, Germany) and was grown in RPMI1640 medium containing 10% fetal calf serum, 200U/ml penicillin and 200ug/ml streptomycin (Gibco, Karlsruhe, Germany).

2.2.4 cDNA constructs and generation of stable cell lines

Human WT JAK2 cDNA was purchased from RZPD (Berlin, Germany). EcoR1 site in the JAK2 was silenced by site directed mutagenesis method (Quickchange, Stratagene, Heidelberg, Germany). WT JAK2 was cloned into MSCV (Mig)-EGFP by using EcoR1 enzyme and Flag-tag was inserted into WT JAK2 by site directed mutagenesis method.

The V617F, R426K and Y40A/L41A mutations were inserted by site-directed mutagenesis and primers were described in the material section (Quickchange, Stratagene, Heidelberg, Germany). All the constructs were verified by DNA sequencing. Myc-tagged WT and mutant JAK2 were generated by cloning WT JAK2 into the EcoRI site of pCMV-Myc and subsequently subcloned into the retroviral MSCV-neo vector. JAK2 SH2 domain was generated by PCR and subcloned into pGEX4T.1 vector that expresses GST upstream of and in frame by using the EcoRI and XhoI enzymes. Human FP was isolated from EOL1-cells and cloned into MSCV (Mig)-EGFP. FP point mutations were introduced in MSCV-EGFP-FP using the QuickChange mutagenesis kit (Quickchange, Stratagene, Heidelberg, Germany). WT and F604S FP were cloned into pGEX4T.1 vector by using the EcoRI enzyme in frame with GST. Similarly various domains of SHP-2 were generated by PCR and subcloned into the pGEX4T.1 vector that express the GST by using the EcoRI and XhoI enzymes. All the constructs were verified by DNA sequencing and before establishing the stable cell lines all the constructs were checked for expression in NIH293T cells. WT JAK2 and mutant JAK2 constructs were stably expressed in Ba/F3 cells by retroviral infection method. High titer ecotropic retroviral supernatants were generated by transient transfection of the Φ NX-Eco packaging cell line with bicistronic vectors encoding Flag tag JAK2 in the MSCV (Mig)-IRES-EGFP vector and also with JAK2 mutants. Similarly viral supernatants were also generated from MSCV-IRES-EGFP-FP and other FP mutants. Viral supernatants collected from 48 hr and 72 hr after transfection were used to infect Ba/F3 cell lines. All the infections were performed in the presence of polybrene (4 μ g/mL). WT JAK2 and mutant JAK2 constructs were stably expressed in γ 2A cells by retroviral infection.

2.2.5 Immunoblotting and Immunoprecipitations (IPs)

Ba/F3 cells expressing the various JAK2 mutants were serum-starved 12h followed by cytokine stimulations. Cells were harvested with lysis buffer (20mM Tris[Ph 7.4], 150mM NaCl, 1% nonidet P-40, 2mM phenyl methyl sulfonyl fluoride, 2mM sodium orthovanadate) and cleared by centrifugation. Lysates used for direct immunoblotting were mixed with 1:1 with laemelli buffer and cooked at 95°C, 2 min and loaded on the SDS-PAGE gel. SDS-PAGE gels were transferred to nitrocellulose membrane (whatmann) in Towbin buffer containing 0.02% SDS and 20% methanol. Membranes

were blocked with milk or bovine serum albumin for 1 h at room temperature. Membranes were incubated with primary antibody in block buffer for 2 h at room temperature or over night at 4°C. Membranes were rinsed three times with wash buffer containing PBS and 0.05% Tween and then subsequently incubated with secondary antibody conjugated to horse reddish peroxidase (Santa Cruz). Bands were visualized using the enhanced chemoluminescence (ECL) system (Amersham, Braunschweig, Germany). Immunoprecipitations were carried on cell lysates by pre clearing the lysates with protein A agarose beads and followed by incubating with antibody of interest in cold room at 4°C, over night. Flag IPs were performed with agarose conjugated anti flag beads (Sigma) where as HA IPs were carried by using the anti HA conjugated agarose pink beads (Sigma). IL-3R β chain IPs were done with the anti IL-3R β (Santa Cruz C-20). Immunoprecipitates were washed with three times with lysis buffer before elution with Laemmli buffer.

2.2.6 Membrane preparation from Ba/F3 cells

Ba/F3 cells expressing various JAK2 mutants were washed three times with ice cold PBS and labeled with sulfo-NHS-biotin (Pierce, Rockford, IL) for 30 min on ice. Cells were washed with ice cold PBS and lysed with membrane lysis buffer followed by immunoprecipitation (IP) over night with streptavidin agarose (Karlsruhe, Germany). After repeated washing the unbound (cytosolic) and bound (membrane) fractions, the samples were collected and loaded.

2.2.7 Retrovirus preparation and viral titer measurement

Phoenix E helper-virus free ecotropic packaging cells (kind gift from G. Nolan, Stanford, USA) and NIH3T3 cells were maintained in DMEM (GIBCO-BRL) supplemented with 10% FCS. Phoenix E cells were transiently transfected using Lipofectamine 2000 (Invitrogen, Karlsruhe, Germany) and retroviral stocks were collected twice at 12-hour intervals beginning 24 hours after transfection. Retrovirus was tittered by transduction of 5×10^4 NIH3T3 cells with serial dilutions of retrovirus in the presence of 4 μ g/ml polybrene (Sigma). 48h post transduction percentage of infected cells was determined by

flow cytometric analysis of EGFP-expression. The titer (in Colony Forming units per ml [CFU/ml]) was calculated by multiplication of the total number of EGFP-positive cells with the dilution factor of the retroviral supernatant.

2.2.8 Bone marrow transduction and transplantation model

Murine bone marrow (BM) was harvested from male Balb/C donor mice 4 days after injection of 150 mg/kg 5-fluorouracil (Ribosepharm, Munich, Germany) and stimulated overnight in Iscove modified Dulbecco medium (Gibco) with 20% FCS supplemented with growth factors (10 ng/mL mIL-3, 10 ng/mL mIL-6, 50 ng/mL mSCF, R+D systems). Cells were infected by spin infection (1200g, 32°C, 90 minutes) using retroviral supernatant supplemented with growth factors and 4µg/mL polybrene (Sigma). Subsequently, cells were resuspended in Hanks balanced salt solution (Sigma) and injected into the tail vein of lethally irradiated (800 rad) female Balb/C recipient mice. Animals that received a transplant were monitored for signs of disease by serial measurement of peripheral blood (PB) counts. All animals were caged in a special caging system (Thoren Caging Systems, Hazleton, PA) with autoclaved food and acidified water. All procedures were reviewed and approved by the university's supervisory animal care committee.

2.2.9 Analysis of transplanted mice

Hemoglobin (Hb), hematocrit (HCT), platelets, and white blood cell counts (WBC) were determined using an automated counter (SCIL vet abc, Heska, Fort Collins, CO). Reticulocytes were stained with brilliant cresyl blue solution (1%) and quantified by light microscopy (per 1000 erythrocytes). Single cell suspension of spleen was prepared by using cell strainer and single cell suspension of BM was isolated by flushing the bones, followed by RBC lysis. Cells were frozen in 90% FBS and 10% DMSO. For histopathological examination, tissues were frozen in formalin solution and embedded in paraffin and stained with hematoxylin and eosin. For myelofibrosis spleen and BM were stained with silver for reticulin. For flow cytometry cells were washed in PBS+ 1% BSA (FACS buffer), blocked with FC block and stained with monoclonal antibodies in PBS+ 1% BSA for 30 minutes in dark. Antibodies used were PE- conjugated CD45, CD11b, Mac1, Gr-1. After washing with FACS buffer three times cells were resuspended in PI to

discriminate non viable cells. Flow cytometry was performed on a FACS cytometer. At least 10000 events were acquired, and data were analyzed using cell quest software (BD Biosciences). For western blots freshly isolated peripheral blood was subjected to RBC lysis and cell pellet was mixed with 2 x lamelli buffers.

2.2.10 Resistance screen and mutation identification

Screening for inhibitor-resistant colonies was performed by, Ba/F3 MSCV- EGFP- FP wild-type cells were pretreated with and with out the chemical mutagen N-ethyl-N-nitrosourea (ENU) twice for 12 hours at a concentration of 50 µg/mL^{115,116}. Thereafter, cells were cultured in 96-well plates at a density of 4 x 10⁵ cells per well and resistant cell clones were selected in the presence of imatinib, nilotinib and sorafenib at the indicated concentrations. Culture supernatants were replaced by fresh medium containing inhibitor after 48 hours. Visible cell colonies were picked, expanded, and analyzed. Resulting inhibitor-resistant sublines were cultured in the presence of inhibitor at a concentration corresponding to that used during the screen. Total RNA was extracted with TRIzol reagent (Invitrogen, Carlsbad, CA) from the resistant cell lines. For reverse-transcription-polymerase chain reaction (RT-PCR) of FP encompassing the fusion and the PDGFRA kinase domain, the following primers were used: FIP1L1 5'ATCAA GACAGGGGGAAGAG3' and PDGFRA 5'CAGGCAGAGGAATGATGTAGCCAC3'. Using this fragment as template, the following primers were used for nested PCR: FIP1L1 5'GTAGACCTTGATGCACCTGGAAGC3' and PDGFRA 5'GCATTG TCTGAGTCCACACG3'. For sequencing, the primers were 5'CCATGGCGT AAACCTGGTGC3' and 5'CAGGCAGAGGAATGATGTAGCCAC3' for PDGFRA TK1 and kinase insert, and 5'GGGCCACATTTGAACATTGTAAAC3' and 5'GCATT GTCTGAGTCCACACG3' for PDGFRA TK2. PCR products were sequenced by DNA sequencer (GATC, Constanz, Germany). Mutations were confirmed by ABI prisam and cloned into MSCV (Mig)-EGFP.

2.2.11 Proliferation and apoptosis assay

Proliferation was measured using an MTS (3-(4, 5 dimethylthiazol-2-yl)-5-(3-carboxymethoxyphenyl-2-(4-sulfophenyl)-2H-tetrazolium)-based method by absorption of formazan at 490 nm (CellTiter 96; Promega, Madison, WI). Measures were taken as

triplicates after 72 and 96 hours of culture without cytokines. Ba/F3 cells expressing the mutant FP were seeded into six well plates with indicated inhibitor concentrations. After 72 hr incubation, cells were washed twice with ice cold PBS, harvested with PBS supplemented with EDTA and stained with the Annexin-FITC apoptosis detection kit (BD Biosciences) according to the manufacturer's instructions. Percentage of apoptosis was determined by FACS analysis.

2.2.12 Real time RT-PCR

Total RNA was isolated from cell lines expressing WT and F604S FP by using trizol method. cDNA was synthesized from total RNA using first strand cDNA synthesis kit from Fermentas and oligonucleotides and random primers. Real time PCR was performed to amplify DNA fragments by using primers specific for FIP1L1-PDGFR α . GGCAATTGATATCGGTCAGA was used as forward primer and CAAGCACTAGTCCATCTCTTGG was used as reverse primer to quantify relative amount of FP mRNA. GAPDH and actin were used for control.

2.2.13 Pulse-chase experiments

WT and F604S FP were transiently expressed in 293T cells with turbofect (Fermentas). After 24hrs medium was changed with methionine free DMEM without serum for 0.5h which is the starvation period, later medium is supplemented with ^{35}S -Met and incubated for 1h which was the pulse period. Cells were then washed three times with phosphate buffer saline and incubated with medium supplemented with 1mM non-radioactive Met for 0, 15, 60, 120 minutes. Cells were collected at the indicated time points and FP was immunoprecipitated from cell lysates using agarose conjugated anti PDGFR α . The precipitated PDGFR α was subjected to SDS-PAGE and detected with autoradiograph.

2.2.14 In vitro kinase assay

Purified JAK2 kinase domain (KD) was obtained from Cell Signaling technology. Human V617F, V617FmSH2 JAK2s were immunoprecipitated from HEK293T cells were used in the kinase assay. In vitro kinase assay was performed in 50ul of kinase buffer containing 60mM HEPES pH 7.9, 5mM MgCl₂, 5mM MnCl₂, 3uM Na₃VO₄, 125mM DTT, 20uM ATP, ^{32}P - γ -ATP. Histone-3 (Roche) was used as a substrate for the JAK2

kinase assay. Similarly WT and F604S FP were purified from bacteria as GST bound proteins and invitro kinase assay was performed in the presence of kinase buffer containing 125mM Tris pH 7.9, 5mM Mgcl₂, 125mM DTT, 20uM ATP, ³²P-γ-ATP. SRC was used as substrate for the kinase assay.

2.2.15 GST purification and GST binding studies

Wild type FP, F604S FP and JAK2 SH2 domains were cloned into pGEX4T.1 vector to obtain a GST- fusion construct. Recombinant proteins were expressed in and purified from BL-21 strain (invitrogen) (as from instruction manual). GST fusion proteins were incubated for 3 h with glutathione-agarose beads in binding buffer (150 mM NaCl, 50mM Tris-HCl pH 8.0, and 5mM EDTA) at 4⁰ c. After being washed with three times in binding buffer, the beads were then incubated with their potential binding proteins for 3 h at room temperature. The beads were then washed with three times and after which bound proteins were eluted with Laemelli sample buffer.

2.2.16 EpoR surface staining

Surface expression of HA-EpoR was measured in stably transfected Ba/F3 cells and gamma2A cells expressing JAK2 mutant constructs. Cells were incubated for 30 minutes in cold phosphate buffer saline (PBS) containing 2% bovine serum albumin. Cells were then incubated for 1 hour with rabbit monoclonal anti-HA antibody (Santa cruz), washed three times with PBS containing 0.2% bovine serum albumin and incubated with R-phycoerythrin (PE) –conjugated anti rabbit IgG secondary antibody at 4⁰ C. Cells were washed with three times with PBS buffer containing 0.2% bovine serum albumin and were analysed by flow cytometry on a FACScan cytometer.

2.2.17 Structure analysis

Graphical inspection and structural superposition was done with PyMOL (DeLano, W.L. The PyMOL Molecular Graphics System (2002) on World Wide Web <http://www.pymol.org>). Individual features of inhibitor interactions and geometries were examined also using the electron density server ¹¹⁷ and 3D-Ligand Interaction analyser as linked in the PDB server pages ¹¹⁸.

3 Results

3.1. JAK2V617F-mediated IL3-independent growth of Ba/F3 cells requires an intact FERM and SH2 domain

It has been previously demonstrated that JAK2V617F is able to render Ba/F3 cells IL-3-independent⁷. However, the exact mechanism how the V617F mutation leads to activation of the JAK2 pathway remains largely unclear. The JAKs contain several conserved domains possibly involved in the constitutive activation of JAK2V617F. The C-terminal FERM domain has been shown to be required for receptor association of the JAKs and deletion of this domain leads to cytosolic localization and loss of JAK-mediated signaling^{49,154,155}. In addition, the SH2 domain is conserved in all JAKs and is adjacent to the pseudokinase domain containing the V617F mutation. However, little is known about the function of this domain in both WT- and oncogenic JAK activation. To investigate the role of these conserved domains in oncogenic JAK2 activation we generated a JAK2 FERM domain mutant (L40A/Y41A) and changed the highly conserved arginine at position 426 within the SH2 domain to a lysine (R426K). The corresponding mutations in JAK1 have been described earlier⁴⁷.

JAK2 constructs containing V617F, R426K or L40A/Y41A or combinations of these mutations were stably introduced into IL3-dependent Ba/F3 cells using retroviral gene transfer. As expected, JAK2 expression with or without mutations in the SH2 domain or FERM domain was not able to render Ba/F3 cells growth factor-independent, which was determined by both MTS assay and cell counting (Figure 3.1 a and b). In contrast, expression of JAK2V617F in Ba/F3 cells led to factor-independent growth as described previously⁷. JAK2V617F containing the FERM domain (JAK2 mFERM) mutation did not lead to this phenotype in Ba/F3 cells indicating that proper receptor scaffold is required for oncogenic JAK2-induced growth factor independence. Most strikingly, also cells expressing oncogenic JAK2V617F with the SH2 mutation (R426K) did not grow IL-3-independent (Figure 3.1 a and b). These findings strongly indicate a critical role of both the FERM and the SH2 domain for the transforming function of oncogenic JAK2V617F.

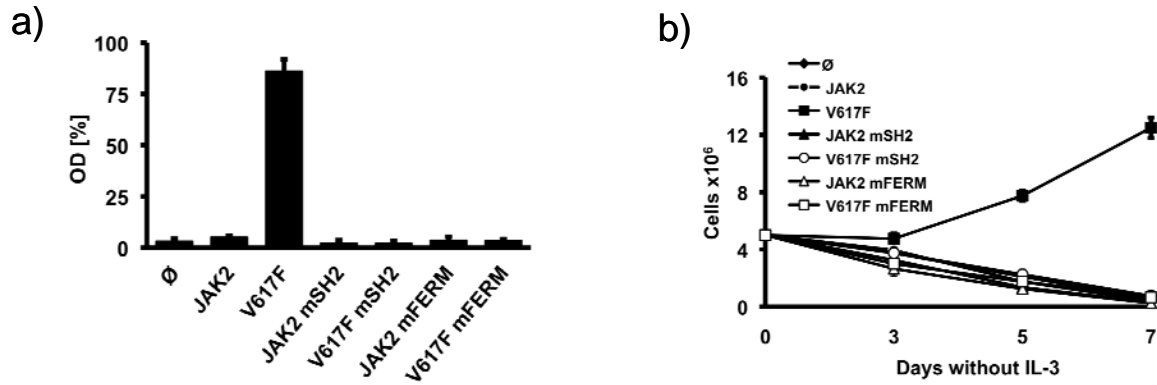


Figure 3.1: JAK2V617F requires an intact FERM and SH2 domain for transformation of Ba/F3 cell lines (a) Proliferation of parental Ba/F3 cells (\emptyset) and Ba/F3 cells expressing WT-JAK2 (JAK2) or JAK2 containing the V617F (V617F), R426K (JAK2 mSH2), L40A/Y41A (JAK2 mFERM) single mutations or the JAK2V617F+R426K (V617FmSH2) and JAK2V617F+L40A/Y41A (V617FmFERM) double mutations as indicated. Cell growth in the absence of IL-3 was quantified by the relative optical density (OD) after 96h using an MTS based assay. Absolute cell numbers over time were measured in the absence of IL-3 by trypan blue exclusion (b). The figures represent one out of three independent experiments. Values are expressed as mean of triplicates (\pm SEM).

JAK2V617F is constitutively phosphorylated in a ligand-independent manner resulting in cell growth in the absence of cytokines. We therefore determined the impact of the SH2 and FERM mutation on JAK2 and STAT5 phosphorylation (Figure 3.2 a). Consistent with cell proliferation data, WT-JAK2 expression did not reveal constitutive activation of JAK2-induced signaling in the absence of IL-3. In contrast, oncogenic JAK2V617F showed constitutive phosphorylation of JAK2 and STAT5. However, mutation of either the FERM or the SH2 domain abrogated growth factor-independent JAK2V617F signaling. Notably, IL-3 stimulation induced JAK2-dependent signaling in these cells (Figure 3.2 a). Since Ba/F3 cells express endogenous JAK2, we further delineated the phosphorylation status of overexpressed JAK2 harboring the R426K and L40A/Y41A mutation by flag-IP (Figure 3.2 b). Constitutive phosphorylation of JAK2V617F was detectable and further enhanced by IL-3 stimulation. In contrast, phosphorylation of JAK2V617F mSH2, JAK2 mSH2, and WT-JAK2 was completely dependent on IL-3 stimulation. FERM domain mutated JAK2 constructs were not phosphorylated even in the presence of IL-3. Thus, the FERM domain is absolutely required for oncogenic and cytokine-induced JAK phosphorylation, whereas the SH2 domain is required for the constitutive activation of oncogenic JAK2V617F only.

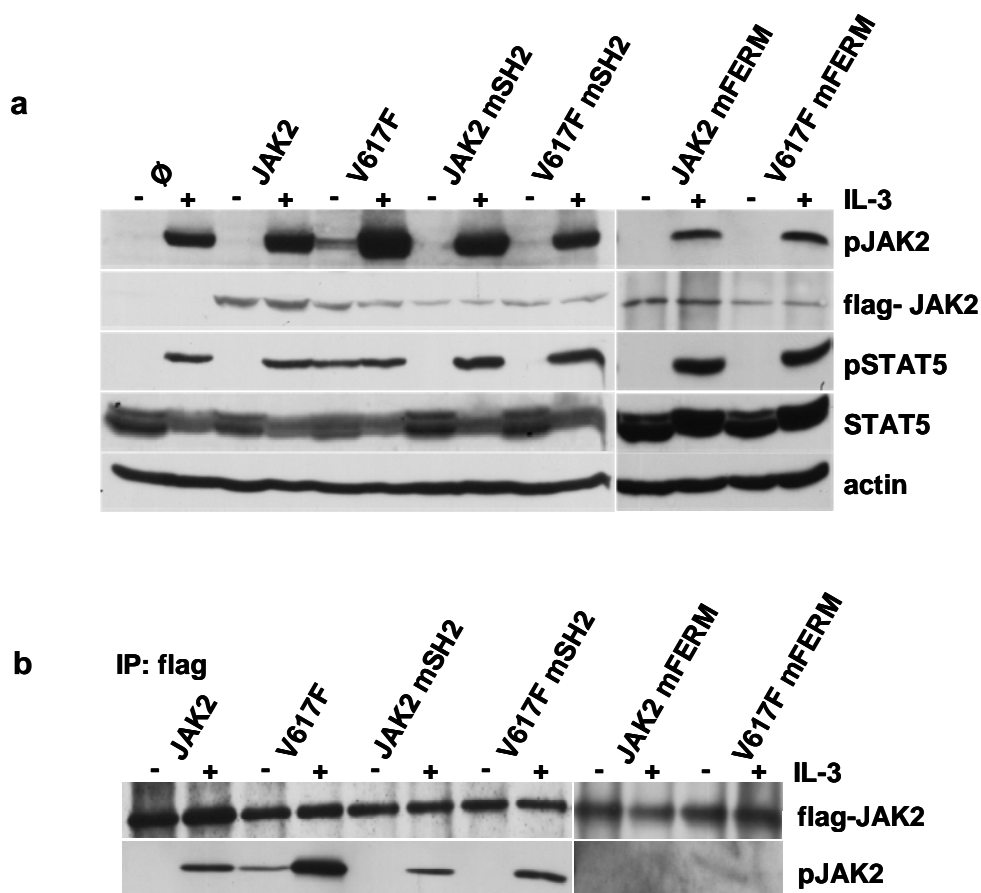


Figure 3.2: JAK2V617F requires an intact FERM and SH2 domain for constitutive ligand-independent activation. Parental Ba/F3 and Ba/F3 cells expressing WT and mutant JAK2 as indicated and described in figure 3.1 were serum-starved for 12h and stimulated with IL-3 or vehicle for 5 min. Lysates were subjected to western blotting with the indicated antibodies (a). Unstimulated and IL-3-stimulated cell lines expressing JAK2 constructs described in (a) were immunoprecipitated (IP) from whole-cell lysates using an anti-flag antibody and immunoblotted with the indicated antibodies (b).

3.1.1 JAK2V617F-mediated constitutive activation of JAK2 requires expression of Cytokine receptor in Gamma 2a cell line

Since JAK2V617F could further be activated by the addition of IL-3, we were interested to determine whether cytokine receptor expression is a prerequisite for the constitutive activation of this oncogene. We therefore stably reconstituted JAK2-deficient γ 2A cells, which do not express common cytokine receptors with WT JAK2 and JAK2V617F (Figure 3.3 a). As expected, even in the presence of IL-3 cells with WT-JAK2 expression did not show JAK2 or STAT5 activation. Strikingly, also oncogenic JAK2V617F did not display any activity in these cells, indicating a strict requirement of cytokine receptor

expression for its oncogenic activation. This notion was supported by the fact that additional expression of IL-3R alpha and beta chains was able to restore ligand-independent activation of JAK2V617F (Figure 3.3 b).

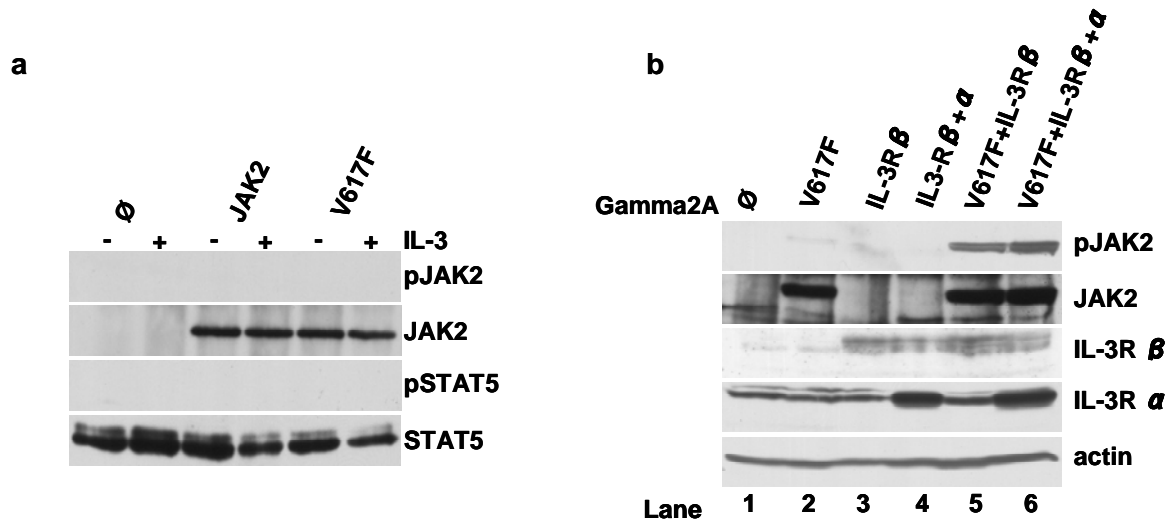


Figure 3.3: JAK2V617F mediated constitutive activation requires ectopic expression of cytokine receptor and β chain alone is sufficient to show constitutive activation of JAK2 in γ 2A cell lines: γ 2A cells stably expressing control vector (\emptyset), WT-JAK2 (JAK2) and V617F JAK2 (V617F) were serum starved 12hrs followed by cytokine (IL-3) stimulation (a). Cell lysates were prepared from the γ 2A cells stably expressing mock vector (\emptyset lane1) JAK2V617F alone (V617F lane2), IL-3R beta chain (IL-3R β lane 3) alone and together with JAK2V617F (V617F+IL-3R β lane 5) and IL-3R beta chain plus alpha chain (IL-3R β + α lane 4) alone and together with JAK2V617F (V617F+IL-3R β + α lane 6). Lysates were analysed for the activation of JAK2 followed by indicated antibodies (b).

3.1.2 Mutation of SH2 domain decreased the activation of the cytokine (IL-3) induced signal transduction in Gamma2A cell lines

Role of the SH2- like domain in JAK2 mediated signal transduction was not understood. In order to find the functional role of SH2 domain in cytokine mediated signal transduction, we created the gamma 2A ($JAK2^{-/-}$) cell line stably expressing IL-3R together with WT-JAK2 and JAK2 mSH2 (Figure 3.4 a). To this end the phosphorylation of WT-JAK2 and JAK2 mSH2 in γ 2A cells, ectopically expressing the human IL-3R with and without IL-3 stimulation was determined. JAK2 mSH2 showed a detectable but considerably decreased autophosphorylation and STAT5 phosphorylation compared to WT-JAK2 after IL-3 stimulation (Figure 3.4 b). Thus, the JAK2 SH2 domain seems to be required for both oncogenic and cytokine-induced JAK2 activation.

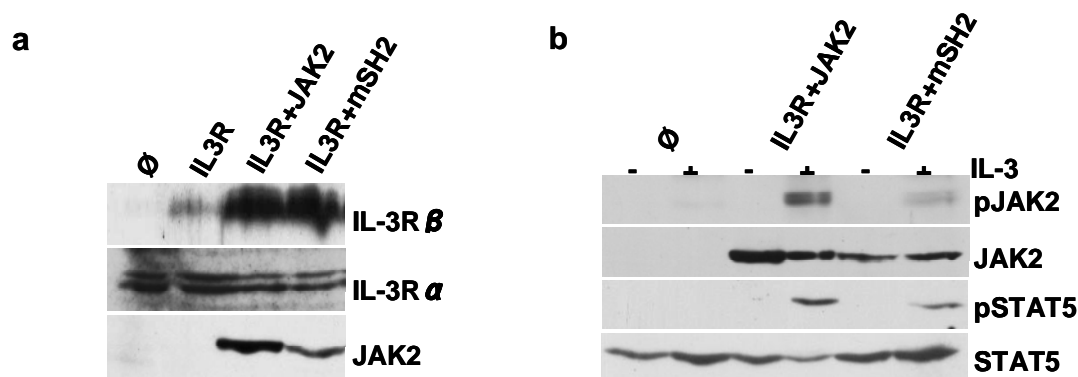


Figure 3.4: Mutation of SH2 domain impairs the maximal activation of JAK/STAT signal transduction in γ 2A cell lines : Cell lysates of γ 2A cell lines stably expressing control vector (\emptyset), WT JAK2 (JAK2) and JAK2R426K (JAK2 mSH2) along with IL-3R alpha and beta chains (IL-3R) were immunoblotted with the indicated antibodies (a). γ 2A cell lines stably expressing IL-3R, control vector (\emptyset), WT JAK2 (JAK2) and JAK2R426K (JAK2 mSH2) were serum-starved for 12h followed by stimulation with IL3 or vehicle. Cells were lysed and analyzed by immunoblotting with the indicated antibodies (b).

3.1.3 High levels of EpoR can compensate for the loss of SH2 function in JAK2V617F

It has been reported that co-expression of homodimeric type I cytokine receptor is a prerequisite for JAK2V617F-mediated transformation²³. We therefore determined the activation of JAK2 and STAT5 in parental and EpoR-transduced Ba/F3 cells (Figure 3.5). Interestingly, parental as well as EpoR-transduced Ba/F3 cells showed equal activation of JAK2V617F and STAT5 suggesting that endogenous IL-3R expression alone is sufficient for full JAK2V617F-mediated constitutive signaling.

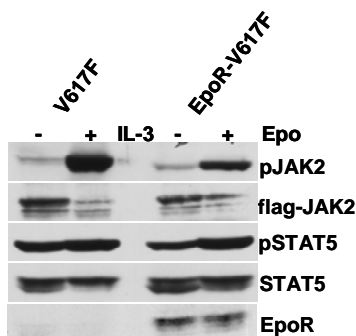


Figure 3.5: Endogenous IL-3R expression alone is sufficient for constitutive activation of JAK2V617F: (A) JAK2V617F-expressing Ba/F3 (V617F) and EpoR-Ba/F3 (EpoR) cells were serum-starved for 12h and stimulated with IL-3, Epo or vehicle. Cell lysates were subjected to immunoblotting using the indicated antibodies.

EpoR–Ba/F3 cells expressing JAK2V617F proliferated in the absence of Epo, whereas WT JAK2, JAK2 mSH2, and FERM domain-deleted JAK2 were unable to render the cells Epo-independent (Figure 3.6 a and b). In contrast to parental Ba/F3 cells, EpoR-expressing Ba/F3 cells could be transformed by JAK2V617F mSH2. These results as a start indicated that an intact SH2 domain might not be required for transformation of EpoR–Ba/F3 cells by JAK2V617F.

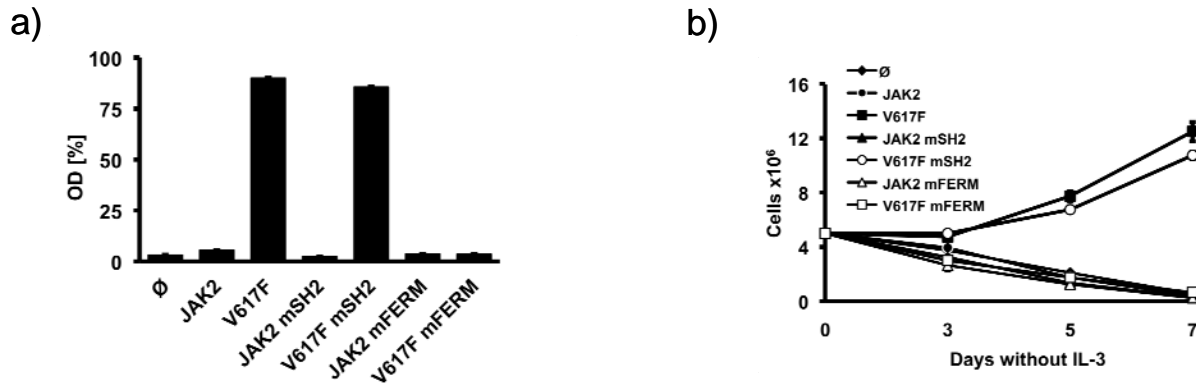


Figure 3.6: Over expression of EpoR rescues the SH2 domain mutated V617FJAK2: Proliferation of EpoR- Ba/F3 cells (∅) and EpoR–Ba/F3 cells expressing WT-JAK2 (JAK2) or JAK2 containing the V617F (V617F), R426K (JAK2 mSH2), L40A/Y41A (JAK2 mFERM) single mutations or the JAK2V617F+R426K (V617FmSH2) and JAK2V617F+L40A/Y41A (V617FmFERM) double mutations as indicated. Cell growth in the absence of IL-3 was quantified by the relative optical density (OD) after 96h using an MTS based assay (a). Absolute cell numbers over time were measured in the absence of IL-3 by trypan blue exclusion (b). The figures represent one out of three independent experiments. Values are expressed as mean of triplicates (±SEM).

Accordingly, we observed constitutive phosphorylation of JAK2 and the downstream signaling molecule STAT5 in EpoR–Ba/F3 cells expressing JAK2V617F or JAK2V617F mSH2 but not in WT JAK2, JAK2 mSH2, or FERM domain deleted JAK2 (Figure 3.7 a). To specifically determine the phosphorylation of the transduced JAK2 proteins, we performed flag IPs and found constitutive activation of JAK2V617F and JAK2V617F mSH2 in EpoR–Ba/F3 cells (Figure 3.7 b). In contrast, WT JAK2 and JAK2 mSH2 were only activated in the presence of Epo. Notably, FERM domain-mutant JAK2 proteins remained unphosphorylated even after Epo stimulation again indicating the requirement of receptor binding for both constitutive and Epo-induced JAK2 phosphorylation.

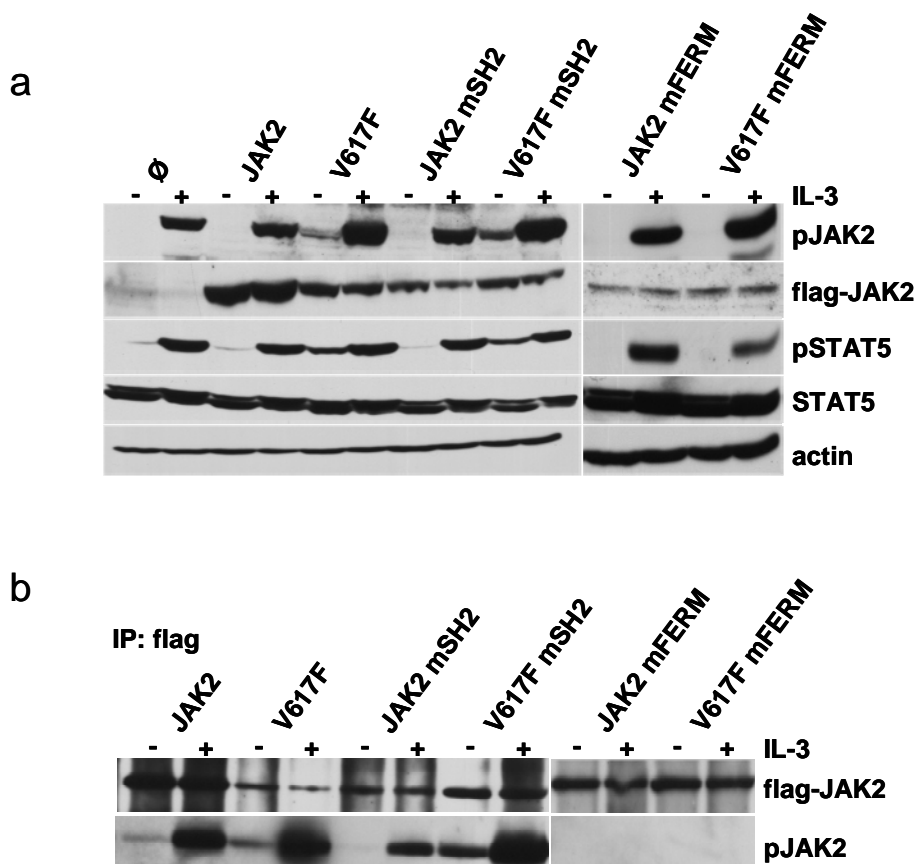


Figure 3.7: JAK2V617F requires an intact FERM but not SH2 domain for constitutive ligand-independent activation in EpoR-Ba/F3 cells. EpoR- Ba/F3 and EpoR-Ba/F3 cells expressing WT and mutant JAK2 as indicated and described in (Fig 3.6 a) were serum-starved for 12h and stimulated with IL-3 or vehicle for 5 min. Lysates were subjected to western blotting with the indicated antibodies (a). Unstimulated and IL-3-stimulated cell lines expressing JAK2 constructs described in (a) were immunoprecipitated (IP) from whole-cell lysates using an anti-flag antibody and immunoblotted with the indicated antibodies (b).

EpoR-Ba/F3 cells were selected by cytokine withdrawal, which might result in cells with very high EpoR expression levels. To determine whether the level of EpoR overexpression is crucial for the rescue of the SH2 mutated JAK2V617F we examined the level of EpoR expression before and after IL-3 withdrawal. As shown in figure 3.8 a JAK2V617F mSH2-positive cells expressing high EpoR levels are strongly selected. This result suggested that only high EpoR expression permits IL-3 independent growth induced by SH2-deficient JAK2V617F. Accordingly, constitutive activation of the JAK2-STAT5 axis could only be demonstrated in those JAK2V617F mSH2 cells, which were previously selected for high EpoR expression by IL-3 withdrawal and not in cells, which were permanently maintained in the presence of IL-3 (Figure 3.8 b). To confirm that only high density EpoR expression allows transformation by the JAK2V617F SH2 mutant, we

established single cell clones expressing JAK2V617F mSH2 together with high or low EpoR by limited dilution. Indeed, cell lines expressing low-level EpoR and SH2-mutated JAK2V617F did not reveal cytokine-independent growth (Figure 3.8 c and d). Thus, high-level EpoR expression is able to overcome the SH2 mutation of oncogenic JAK2. This might be due to the high abundance of the unstimulated receptor and the resulting high density of recruited JAK2 molecules at the membrane, facilitating the constitutive activation of SH2-mutated JAK2V617F.

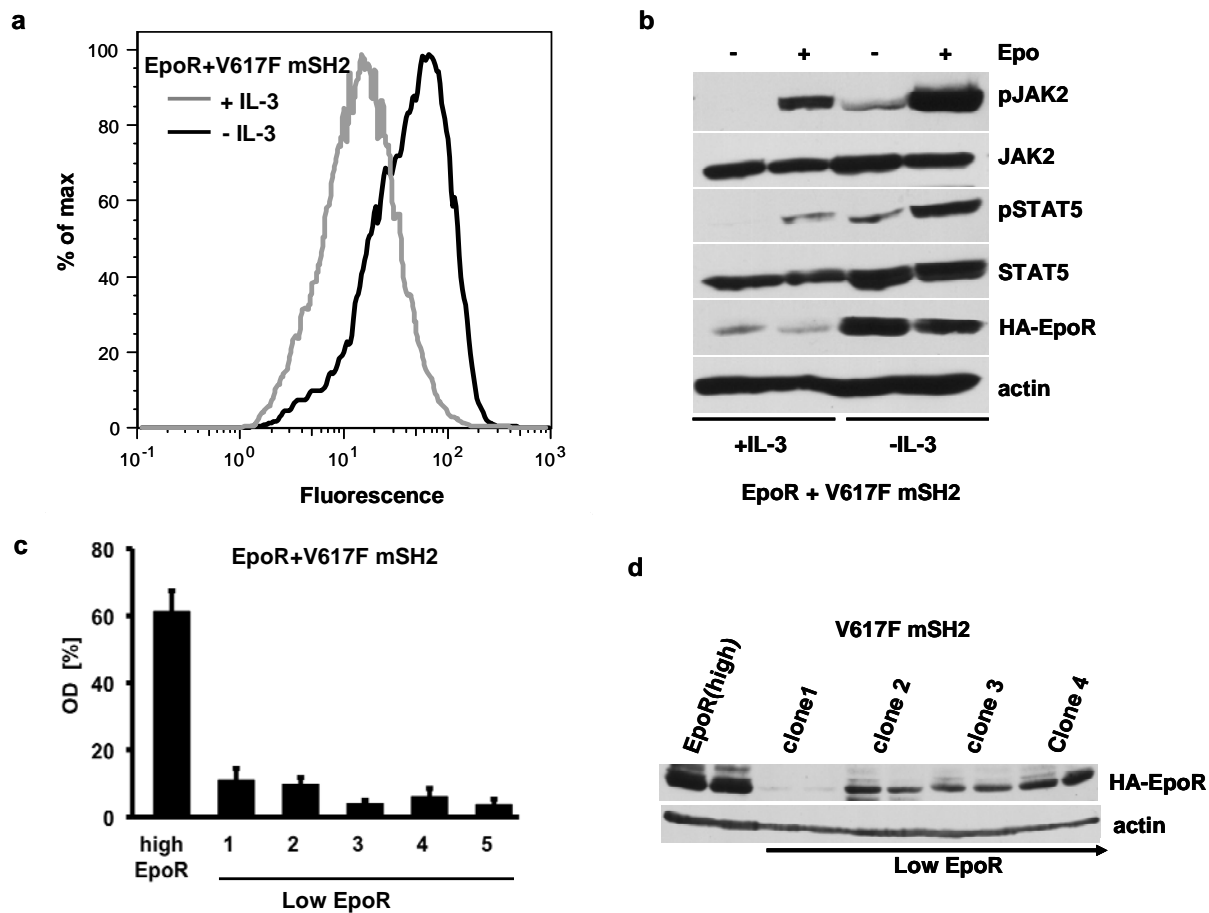


Figure 3.8: EpoR levels determine the transformation of JAK2V617F mSH2. Ba/F3 JAK2V617F mSH2 cells were transduced with MSCV-eGFP-EpoR (EpoR+V617F mSH2) and grown in the presence or absence of IL-3 over a period of three days. FACS analysis was used to determine surface expression levels of EpoR (a). Analysis of JAK2 and STAT5 activation in these two EpoR-expressing Ba/F3 cell populations in the absence and presence of Epo was determined by western blot (b). Proliferation of isolated SH2-mutated JAK2V617F (V617FmSH2) Ba/F3 single cell clones expressing high or low levels of EpoR as quantified by the relative optical density (OD) using MTS assay. The figure represents one out of two independent experiments. Values are expressed as mean of triplicates (\pm SEM) (c). Expression of EpoR levels in isolated clones were shown with indicated antibodies (d).

3.1.4 Mutation of SH2 domain does not effect the protein turn over and intrinsic kinase activity of V617FJAK2

In order to determine the role of SH2 domain in JAK2V617F mediated transformation we analyzed the protein turn over in both JAK2V617F and JAK2V617FmSH2 transfected Ba/F3 cells by cyclohexamide with indicated time points. Both JAK2V617F and JAK2V617FmSH2 showed equal protein turn over indicated that mutation of SH2 domain does not effect the protein turn over (Figure 3.9 a). Similarly the role of SH2 domain in JAK2V617F intrinsic kinase activity was measured by using the Histone-3 as a substrate⁶¹. Surprisingly mutation of SH2 domain does not affect the intrinsic kinase activity of JAK2V617F (Figure 3.9 b).



Figure 3.9: The SH2 domain mutation does not effect in protein turn over and intrinsic kinase activity of V617FJAK2. Ba/F3 cells expressing JAK2V617F (V617F), JAK2V617F+R426K (V617 mSH2) were treated with cyclohexamide with indicated time periods and lysates were checked for the flag JAK2. JAK2V617F (V617F), and JAK2V617F+R426K (V617 mSH2) showed equal protein turnover indicating that SH2 domain mutation did not change in protein stability (a). JAK2V617F (V617F) and JAK2V617F+R426K (V617FmSH2) were immunoprecipitated from HEK293 cells and checked for the kinase activity by using histone-H3 as substrate in the presence of radiolabelled γ^{32} ATP as described previously⁶¹. Purified recombinant JAK2 kinase domain (JAK2KD) was used as positive control. Equal substrate loading was shown in the coomassive staining and in the bottom panel cell lysates and equal Immunoprecipitation of JAK2 was shown (b).

3.1.5 Mutation of the SH2 domain does not affect the membrane distribution of JAK2

Since the assembly of cytokine receptors and JAK2 is important for JAK2 phosphorylation^{49,154,156} and JAK2V617F abundance at the cell membrane may be critical for constitutive activation, we studied the membrane localization of the FERM and SH2-mutated JAK2V617F protein (Figure 3.10 a and b). Biotinylated surface proteins of Ba/F3 cells were immunoprecipitated using streptavidin beads. Subsequently, JAK2 expression and activity was determined within the membrane and cytosolic fraction. WT JAK2, JAK2V617F and JAK2V617F mSH2 as well as receptor expression was detectable within the membrane fraction. In contrast, FERM domain-mutated JAK2V617F was absent in the membrane fraction (Figure 3.10 a). This indicates that the

FERM domain but not the SH2 domain mediates membrane localization. FERM domain-mutated JAK2V617F was also absent in the cytosolic fraction indicating that detachment from the cell membrane may lead to the degradation of the protein⁷⁸. In accordance with our previous results, JAK2V617F was constitutively activated whereas JAK2V617F mSH2 showed no autophosphorylation. Thus, these findings suggest that in contrast to FERM domain-mutated JAK2, the lack of constitutive activation of the SH2-mutated JAK2V617F cannot be ascribed to reduced membrane association. In addition, complex formation of WT and mutated JAK2 with the IL3R was determined by coimmunoprecipitation. In line with the fractionation experiment, the FERM domain but not the SH2 domain was required for complex formation of JAK2 and JAK2V617F with the IL-3R (Figure 3.10 b).

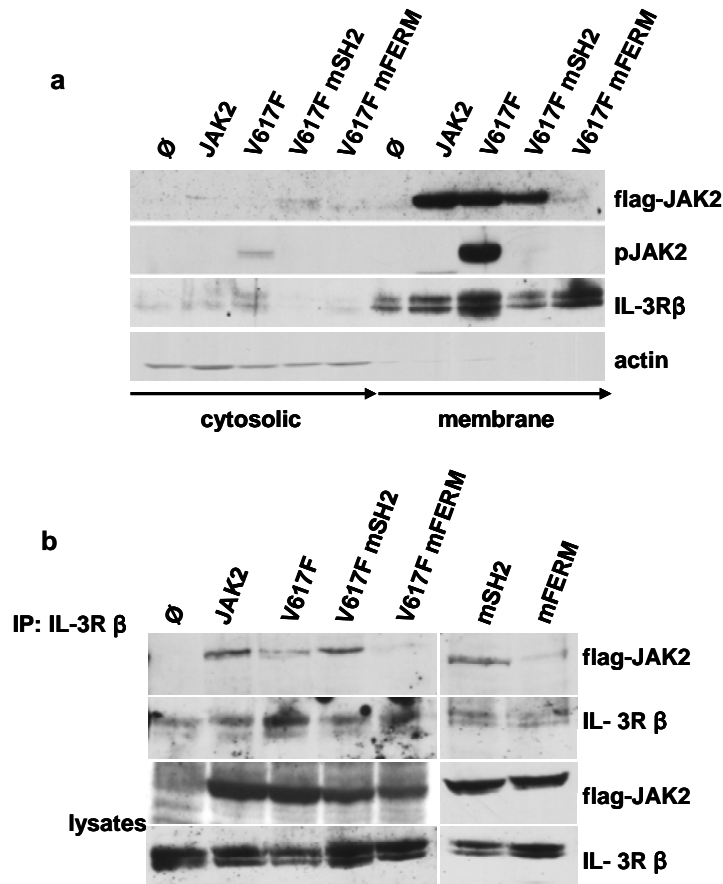


Figure 3.10: The SH2 domain mutation does not impair the membrane distribution of JAK2. Parental Ba/F3 (\emptyset) and Ba/F3 cells expressing WT JAK2 (JAK2), JAK2V617F (V617F), JAK2V617F+R426K (V617 mSH2) and JAK2V617F+L40A/Y41A (V617FmFERM) were surface biotinylated followed by streptavidin IP. The bound (membrane) and unbound (cytosolic) fractions were subjected to immunoblotting with antibodies to flag and phospho-JAK2. IL-3R β and actin were used as loading controls (a). IL-3 receptor beta chain (IL-3R β) was immunoprecipitated from parental Ba/F3 (\emptyset) and Ba/F3 cells expressing mutant JAK2 mentioned in (a) and checked for interaction of JAK2. In the bottom panel whole cell lysates were shown with indicated antibodies (b).

We also analyzed membrane distribution of JAK2 in EpoR-Ba/F3 cell lines by biotinylation. Similar to parental Ba/F3 cells, EpoR-Ba/F3 cells showed strong membrane recruitment of WT-JAK2, JAK2V617F and JAK2V617F mSH2, whereas FERM domain-mutated JAK2 abrogates membrane localization (Figure 3.11).

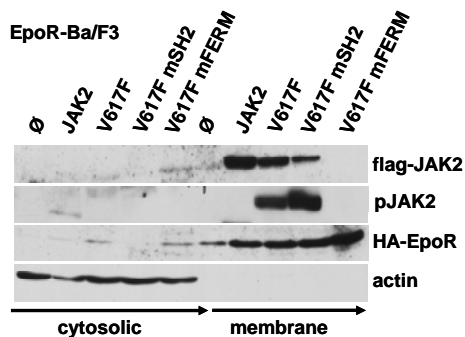


Figure 3.11: Mutation of the FERM domain but not the SH2 domain impairs membrane distribution of JAK2 in EpoR-Ba/F3 cells. EpoR-Ba/F3 cells expressing empty vector (\emptyset), WT-JAK2 (JAK2), JAK2V617F (V617F), JAK2V617F mSH2 (V617F mSH2) and JAK2V617F mFERM (V617F mFERM) were surface biotinylated followed by streptavidin immunoprecipitation. The bound (membrane) and unbound (cytosolic) fractions were subjected to immunoblotting with antibodies to flag, phospho-JAK2, EpoR. Actin was used as loading control.

In order to rule out that the SH2 domain plays a role in surface expression of the EpoR, we determined EpoR surface expression by FACS analysis in this cells. WT-JAK2, JAK2V617F, JAK2 mSH2 and JAK2V617F mSH2 showed equal levels of EpoR surface expression indicating that the SH2 domain is not required for EpoR membrane distribution (Figure 3.12). EpoR-Ba/F3 cells transfected with empty vector also showed comparable levels of EpoR surface expression suggesting that endogenous JAK2 protein levels are sufficient for proper EpoR maturation in Ba/F3 cells.

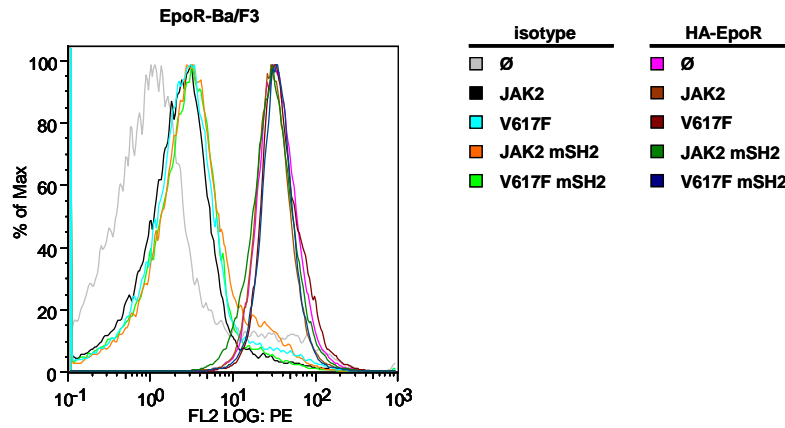


Figure 3.12: Mutation of the SH2 domain does not affect EpoR surface expression in Ba/F3 cells. EpoR surface expression of EpoR-Ba/F3 cells expressing empty vector (∅) WT-JAK2 (JAK2), JAK2V617F (V617F), JAK2 mSH2, JAK2V617F mSH2 (V617F mSH2) was measured by FACS analysis. Cells were stained with PE-conjugated antibodies to HA or the respective isotype control antibody.

Using JAK2-deficient γ 2A cells, Huang et.al showed that JAK2 is required for EpoR membrane expression and EpoR maturation through the interaction of the receptor and the FERM domain of JAK2⁴⁹. In accordance with these data, we demonstrated that EpoR maturation was impaired in the absence of JAK2 and restored after WT-JAK2 reconstitution by using FACS-based method. Similarly, JAK2 mSH2 was able to induce maturation of the EpoR, again confirming that the SH2 domain is dispensable for receptor maturation (Figure 3.13 a). Interestingly, also oncogenic JAK2V617F and JAK2V617F mSH2 induced EpoR maturation to the same extent than WT-JAK2 (Figure 3.13 b).

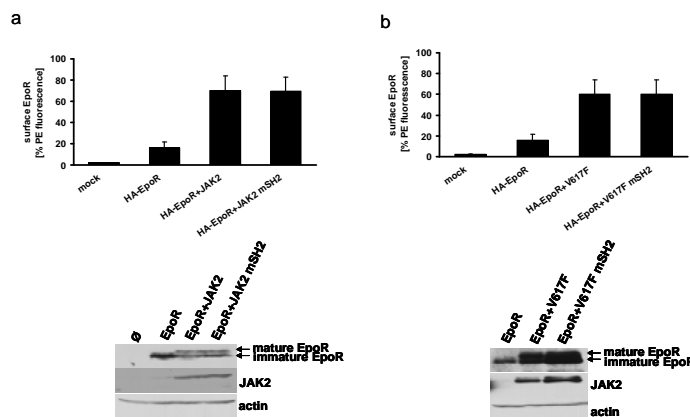


Figure 3.13: Mutation of the SH2 domain does not affect EpoR surface expression in γ 2A cells: Gamma 2A cells expressing the HA-EpoR alone or HA-EpoR together with WT-JAK2 (JAK2), JAK2 mSH2 were analyzed for EpoR expression by FACS-based method (top panel). In the bottom panel whole cell lysates were analyzed with the indicated antibodies. WT JAK2 and JAK2 mSH2 showed comparable EpoR maturation (a). Equal amounts of mature EpoR (upper band) were found in WT-JAK2 and JAK2 mSH2 (bottom panel). JAK2V617F (V617F), JAK2V617F mSH2 (V617F mSH2) also showed comparable EpoR maturation indicating that SH2 domain does not play a role in receptor maturation (b).

Maturation of EpoR in γ 2A cells was also further confirmed by treatment with Endo H. Consistent with the FACS-based method, mature EpoR (Endo H resistant form) was virtually undetectable in the absence of JAK2 expression. After JAK2 reconstitution both mature (Endo H-resistant) and immature EpoR forms (Endo H-sensitive) were observed. Interestingly, JAK2 mSH2, JAK2V617F and JAK2V617F mSH2 constructs also revealed similar levels of EpoR maturation, again indicating that SH2 is dispensable for EpoR maturation (Figure 3.14).

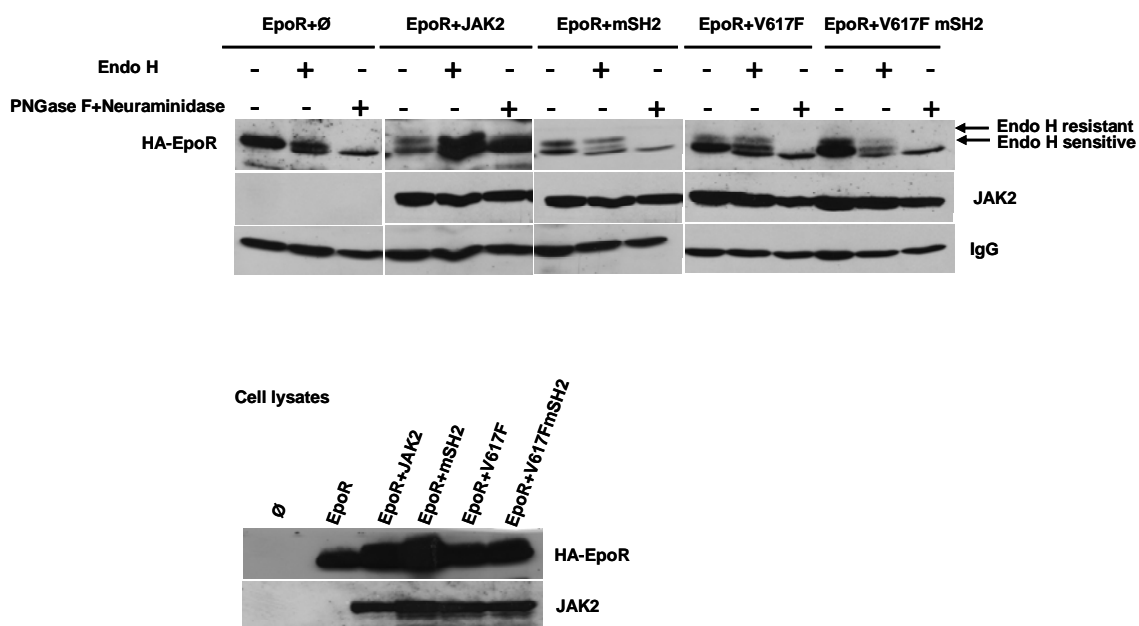


Figure 3.14: Mutation of the SH2 domain does not affect EpoR maturation in γ 2A cells: HA-EpoR was immunoprecipitated from the γ 2A cells, stably expressing HA-EpoR together with mock (\emptyset), JAK2, JAK2 mSH2, JAK2V617F, JAK2V617F mSH2 and treated with Endo H or with PNGase F and neuraminidase. After glycosidase treatment, the reaction products were subjected to western blot analysis with the indicated antibodies. Whole cell lysates were shown in the bottom panel.

3.1.6 Protein-protein interaction and transphosphorylation of JAK2V617F is dependent on an intact SH2 domain

The function of the SH2 domain in JAK proteins is largely unclear and the binding of the JAK SH2 domain to specific phosphorylated tyrosine residues could not be demonstrated so far⁴⁷. In order to study binding of tyrosine-phosphorylated proteins to the JAK2 SH2 domain, we performed GST pulldowns with the SH2 domain of JAK2 using Ba/F3 JAK2V617F cell lysates. Since the SH2 domain of c-Src resembles a typical SH2 domain, we used a GST expression construct containing the Src SH2 domain as a control.

Whereas GST-Src SH2 clearly precipitated a number of phosphorylated proteins, GST-JAK2 SH2 revealed no tyrosine-phosphorylated binding partners corroborating previous reports (Figure 3.15). However, GST-JAK2 SH2 was able to precipitate JAK2 itself as determined by a JAK2 immunoblot (Figure 3.15).

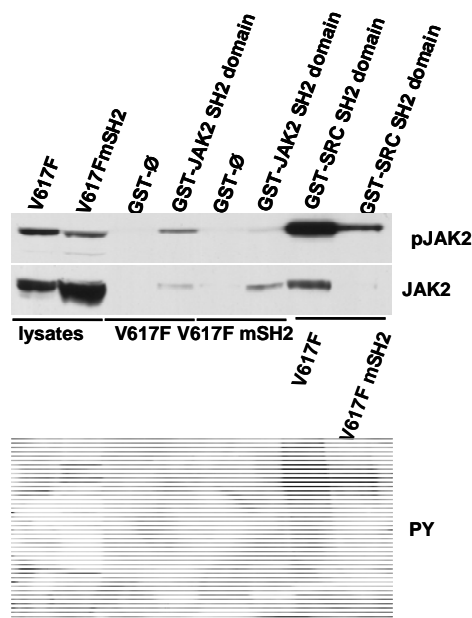


Figure 3.15: JAK2 SH2 domain does not fulfill classical SH2 domain function. The SH2 domain of JAK2 was expressed as GST-fusion protein and purified on glutathione beads. Cell lysates from V617FJAK2 (V617F) and V617F+R426KJAK2 (V617FmSH2) were incubated with purified JAK2 SH2 domain and analysed for phosphoproteins by using anti phosphotyrosine (PY) antibody. SRC-SH2 domain was used as a control for typical SH2 domain function. Similarly the bound proteins were also probed for JAK2 and pJAK2 antibodies.

Since the SH2 domain therefore might be crucial for JAK2 self-association and subsequent transphosphorylation, we investigated the interaction between JAK2 molecules by flag co-IP using both flag-tagged and myc-tagged JAK2 expression constructs. Both the constructs showed comparable pJAK2 signal, STAT5 signaling and transforming ability in Ba/F3 cells (Figure 3.16).

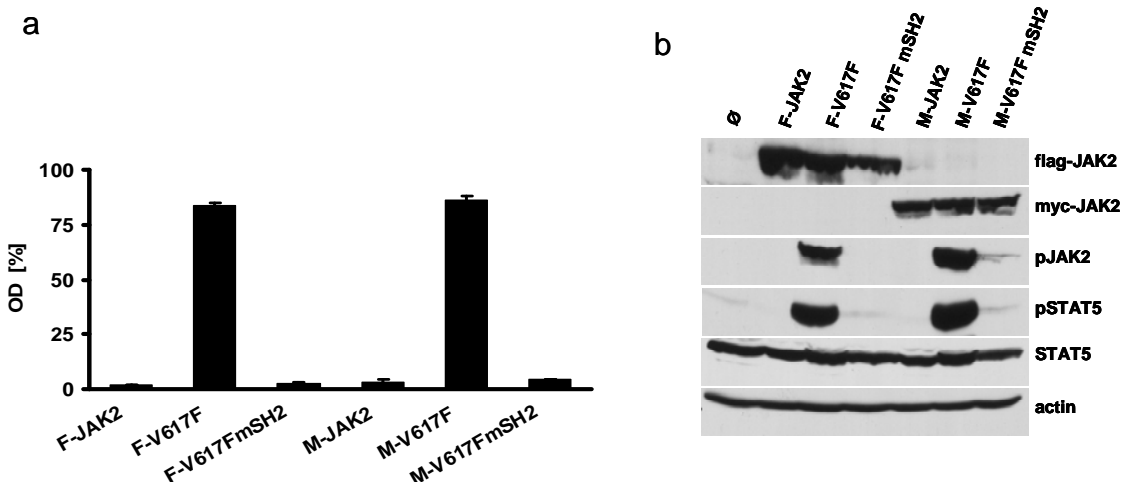


Figure 3.16: Flag-tagged and myc-tagged mutant JAK2 constructs showed similar transformation ability and signal transduction. Ba/F3 cells expressing flag-tagged WT-JAK2 (F-JAK2), JAK2V617F (F-V617F), JAK2V617F mSH2 (F-V617F mSH2) and myc-tagged WT-JAK2 (M-JAK2), JAK2V617F (M-V617F), JAK2V617F mSH2 (M-V617F mSH2) were grown in the absence of IL-3. Cell proliferation was measured by using MTS based method (a). Cells expressing the flag-tagged and myc-tagged JAK2 constructs mentioned in (a) were analyzed for the activation of JAK2 and STAT5 (b).

After confirming the flag-tagged and myc-tagged JAK2 construct signaling transduction in Ba/F3 cell lines, then we investigated the co interaction between the flag-tagged and myc-tagged JAK2 by flag co-IP. As shown in Figure 3.17 a, myc-tagged WT-JAK2 does not co-immunoprecipitate with flag-tagged WT-JAK2. In contrast, immunoprecipitation of flag-tagged JAK2V617F resulted in the co-IP of myc-tagged JAK2V617F. Constitutive phosphorylation of JAK2V617F could be observed in both the immunoprecipitated fraction and in the lysate. This result suggests that JAK2V617F but not WT-JAK2 binds to each other in the absence of ligand.

To determine the role of the SH2 domain for JAK2V617F self-association, we performed co-IP experiments using flag- and myc-tagged JAK2V617F mSH2 (Figure 3.17 b). Again, JAK2V617F revealed reciprocal interactions as well as high levels of constitutive phosphorylation. In contrast, overexpressed flag-tagged and myc-tagged JAK2V617F mSH2 could not be co-immunoprecipitated. This indicates that the SH2 domain seems to be crucial for the complex formation and subsequent transphosphorylation of JAK2V617F proteins.

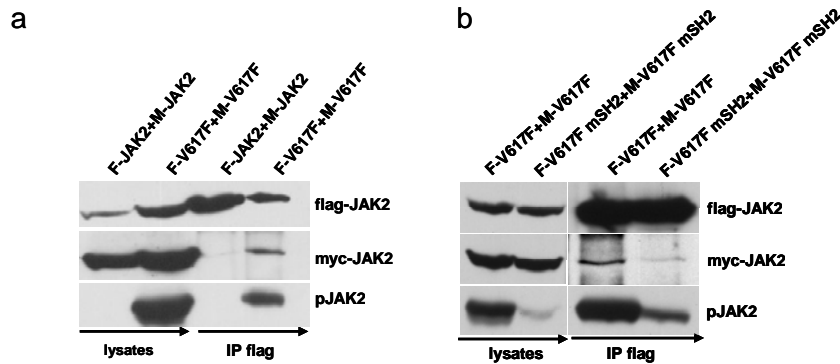


Figure 3.17: The SH2 domain is required for the transphosphorylation of JAK2V617F. (a) Two WT JAK2 or JAK2V617F constructs containing either a myc (M-JAK2, M-V617F) or flag tag (F-JAK2, F-V617F) were co-expressed in 293T cells. Flag-tagged JAK2 proteins were immunoprecipitated from cell lysates and analyzed for co-immunoprecipitation of myc-tagged JAK2 by anti-myc immunoblotting and phospho-JAK2. (b) 293T cells co-expressing either flag- and myc-tagged JAK2V617F (F-V617F, M-V617F) or flag- and myc-tagged JAK2V617F+R426K (F-V617F mSH2, M-V617F mSH2) were analyzed as described in (a).

To further confirm these results, we performed additional co-immunoprecipitation experiments using flag-tagged JAK2V617F and myc-tagged WT-JAK2 and vice versa (Figure 3.18). We could not detect co-immunoprecipitation of myc-tagged WT-JAK2 using flag-tagged JAK2V617F or vice versa indicating that constitutively activated JAK2 is only able to interact with each other. Similarly co-immunoprecipitations were carried out with the flag-tagged JAK2V617F mSH2 and myc-tagged WT-JAK2 and vice versa (Figure 3.18). As expected, flag-tagged JAK2V617F mSH2 could not co-immunoprecipitate myc-tagged WT-JAK2 and vice versa.

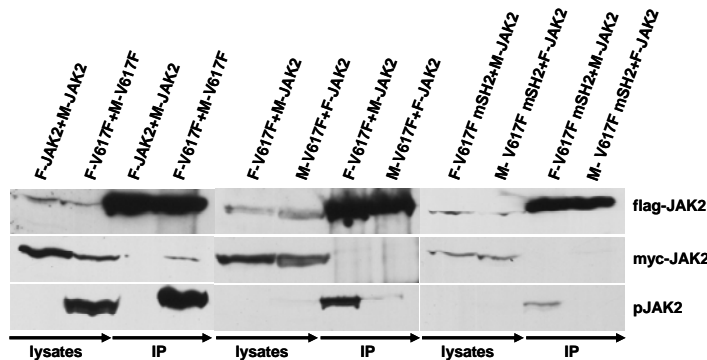


Figure 3.18: Flag-tagged JAK2V617F and JAK2V617F mSH2 are not able to co-immunoprecipitate myc-tagged WT-JAK2 and vice versa. WT-JAK2 or JAK2V617F constructs containing either a myc (M-JAK2, M-V617F) or a flag tag (F-JAK2, F-V617F) were co-expressed in 293T cells. Flag-tagged JAK2 proteins were immunoprecipitated from cell lysates and analyzed for co-immunoprecipitation of myc-tagged JAK2 by myc immunoblotting and phospho-JAK2 (left panel). Similarly, flag-tagged JAK2V617F (F-V617F) was co-expressed with myc-tagged WT-JAK2 and vice versa. Flag-tagged JAK2 proteins were immunoprecipitated from cell lysates and analyzed for co-immunoprecipitation of myc-tagged JAK2 by myc and phospho-JAK2 immunoblotting and vice versa (middle panel). In addition, experiments were also carried out with flag-tagged JAK2V617F mSH2 (F-V617F mSH2) and myc-tagged WT-JAK2 (M-JAK2) and vice versa (right panel).

We also performed Co-IP experiments in gamma2a cells lacking common cytokine receptors by stably expressing flag-tagged and myc-tagged JAK2 mutant constructs with and without EpoR (Figure 3.19). Here, co-immunoprecipitation of myc-tagged JAK2V617F with flag-tagged JAK2V617F could only be observed in EpoR-expressing γ 2A cells since JAK2V617F shows no activity in the absence of cytokine receptor expression. Therefore the results in gamma 2a cells support the notion that complex formation of JAK2V617F requires autophosphorylation. WT-JAK2 in accordance with the results in Figure 3.17 showed no complex formation even in the presence of cytokine receptor expression (Figure 3.19).

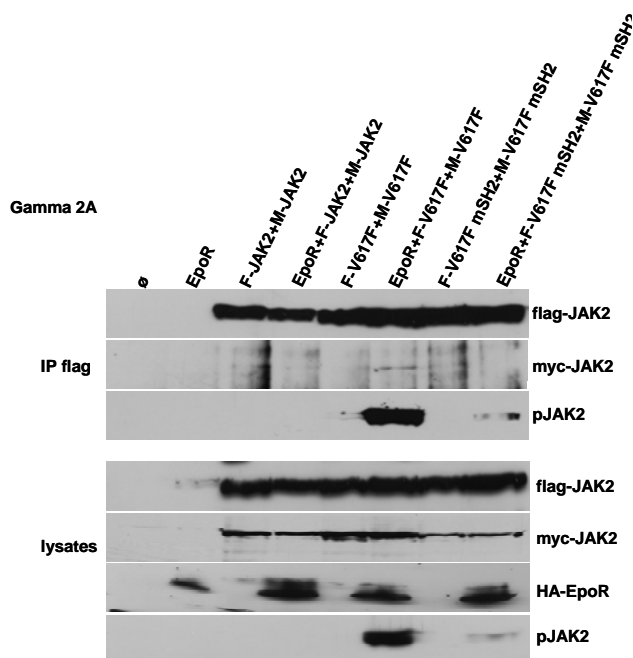


Figure 3.19: EpoR expression is required for JAK2V617F mediated transphosphorylation and constitutive activation in Gamma2A cells. Flag-tagged and myc-tagged JAK2 (F-JAK2 and M-JAK2), JAK2V617F (F-V617F and M-V617F) and JAK2V617F mSH2 (F-V617F mSH2 and M-V617F mSH2) were expressed with and without EpoR in γ 2A cells. Flag-tagged JAK2 proteins were immunoprecipitated from cell lysates and analyzed for co-immunoprecipitation of myc-tagged JAK2 by myc and phospho-JAK2 immunoblotting. In the bottom panel whole cell lysates were analyzed for expression of flag-tagged and myc-tagged JAK2, EpoR and phospho-JAK2.

To further investigate a potential requirement of the SH2 domain for constitutive JAK2V617F-dependent phosphorylation, we co-infected Ba/F3 cells with flag- and myc-tagged JAK2V617F constructs containing an intact SH2 (lane 2), mutated SH2 (lane 3),

and both (lane 4) and performed flag IPs (Figure 3.20). As expected, control cells expressing flag- and myc-tagged unmutated JAK2V617F showed high levels of constitutive flag-JAK2V617F phosphorylation. Consistent with our previous data, phosphorylation of JAK2V617F was almost completely abrogated when the SH2 domain was mutated in both constructs. Interestingly, flag-JAK2V617F mSH2 was partially phosphorylated when myc-JAK2V617F was co-expressed indicating that SH2-mutated JAK2V617F can be phosphorylated in the presence of JAK2V617F containing an intact SH2. According to these results, the SH2 domain might be involved in the transphosphorylation and constitutive activation of JAK2V617F. Taken together, constitutive phosphorylation of JAK2V617F seems to require reciprocal binding via the SH2 domain.

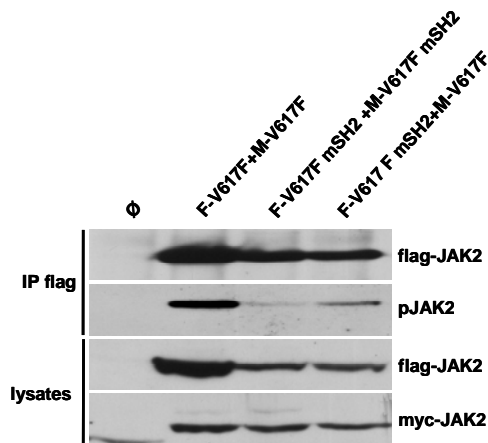


Figure 3.20: Expression of flag-tagged V617FJAK2 rescues the V617F mSH2 phosphorylation in Ba/F3 cell lines. Ba/F3 cells stably expressing flag- and myc-tagged JAK2V617F and JAK2V617F+R426K mutants as indicated were lysed analyzed by flag IP and subsequent phospho-JAK2 and flag immunoblot. Expression levels of the JAK2 constructs in the lysates were controlled by flag and myc western blot. The cell lines used in this experiment were mock-transduced Ba/F3 cells (Ø, lane 1), flag-JAK2V617F (F-V617F) with myc-JAK2V617F (M-V617F) (lane 2), flag-JAK2V617F+R426K (F-V617FmSH2) with myc-JAK2V617F+R426K (M-V617FmSH2) (lane 3), and flag-JAK2V617F+R426K (F-V617F mSH2) with myc-JAK2V617F (M-V617F) (lane 4).

3.1.7 JAK2V617F-mediated myeloproliferative disease in mice requires a functional SH2 domain.

Retroviral transduction of JAK2V617F in bone marrow cells leads to a MPN reminiscent of PV^{65,66}. To investigate the *in vivo* role of the SH2 domain in the molecular pathogenesis of a JAK2V617F-induced MPN using primary hematopoietic cells with physiological cytokine receptor density, we retrovirally introduced JAK2V617F, JAK2V617F mSH2, and empty vector in BM cells derived from Balb/c mice and

subsequently transplanted them into lethally irradiated recipient mice. Retroviral syngenic mouse model was shown in the Figure 3.21.

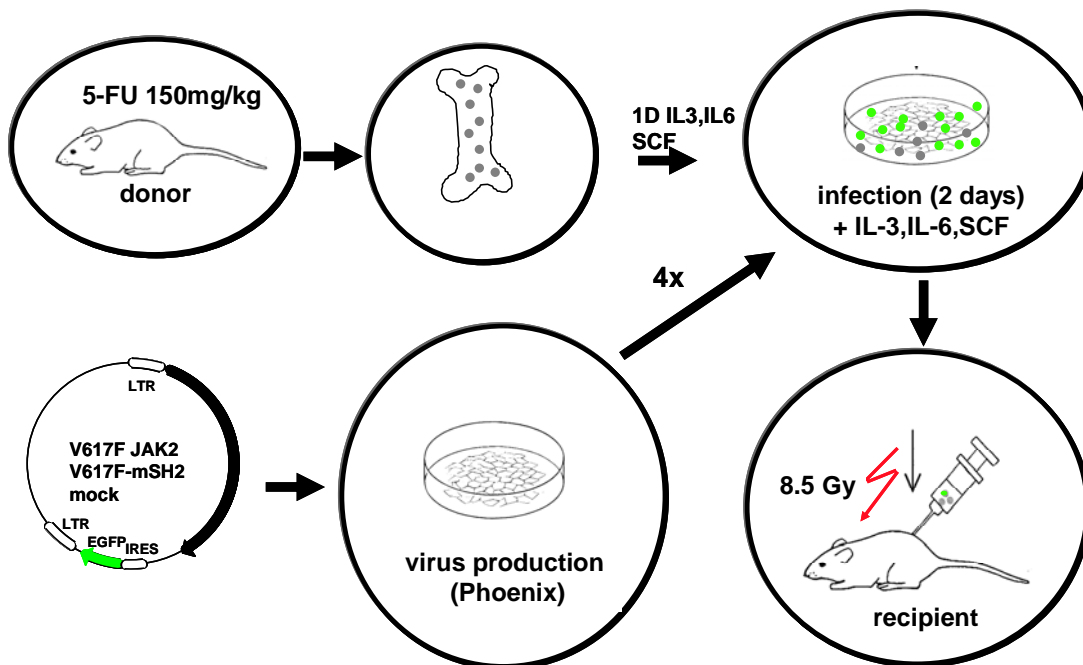
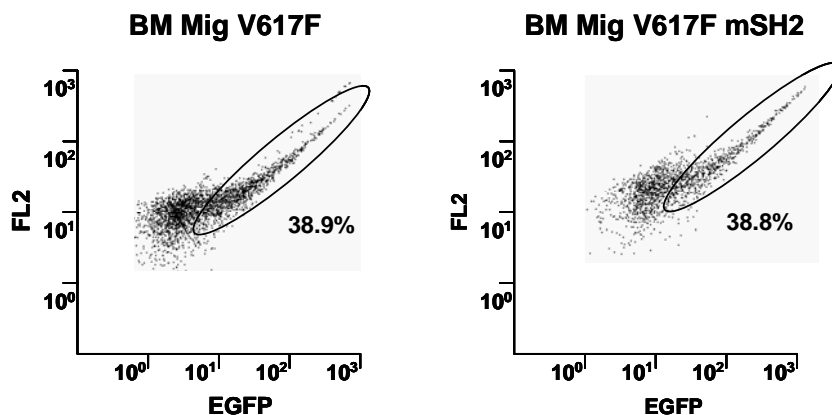


Figure 3.21: The schematic representation of retroviral mediated syngenic mouse model PV like disease. BM was isolated from the 5-FU (5-fluoro uracil) treated donor mice and cultured the isolated bone marrow in the presence of cytokines IL-3, IL-6 and SCF. V617FJAK2 and V617FmSH2JAK2 were cloned into MSCV-IRES-eGFP vector and transfected to HEK293 cells for the virus. Virus was collected from 36hrs and 48hrs time points after the transfection and collected virus was used to infect primary bone marrow as described in methods. After four rounds of infection, bone marrow was introduced into lethally irradiated recipient mice. Transplanted mice was analyzed for the disease outcome after two weeks.

V617FJAK2 and V617FmSH2JAK2 were equally transduced to primary bonemarrow isolated from Balb/c mice (Figure 3.22 a and b). Three independent transplantation experiments giving a total of 10 mice per construct were performed. Figure 3.15 shows the data from the first round of transplantation. Details on every transplantation performed can be seen in Table 3.1.

a)



b)

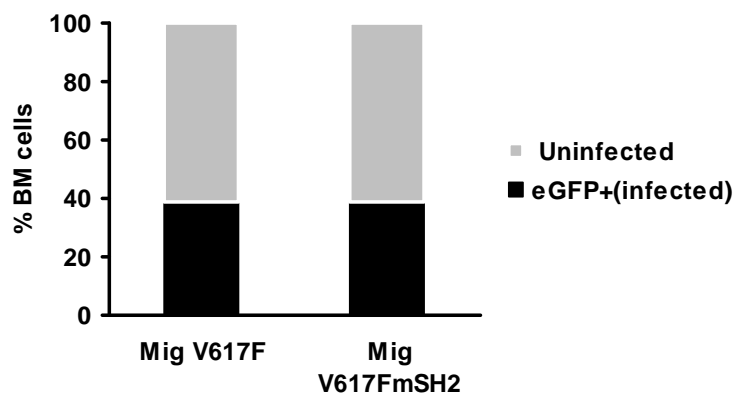


Figure 3.22: Transduction efficiency of primary bonemarrow: V617FJAK2 and V617FmSH2JAK2 were infected to the primary bone marrow and infection efficiency was measured with % of eGFP positive cells by FACS (a). Quantification of bonemarrow infected with V617FJAK2 and V617FmSH2JAK2 were shown in (b).

As previously reported, transplantation of JAK2V617F transduced BM leads to a marked leukocytosis, increased reticulocytes, blood hematocrit and hemoglobin levels in transplanted animals. The platelet counts did not exceed normal levels. This phenotype became evident three weeks after transplantation and sustained for months (Figure 3.23 a-e). Strikingly, Balb/c mice receiving bone marrow cells ectopically expressing JAK2V617F mSH2 did not develop signs of a MPD and revealed blood counts comparable to control mice. In addition to elevated blood counts, mice receiving JAK2V617F-infected BM developed a profound splenomegaly with a median spleen weight four times higher than that of control mice (Figure 3.23 f). Notably, BM transduced with JAK2V617F mSH2 did not give rise to a significant increase in spleen size and weight.

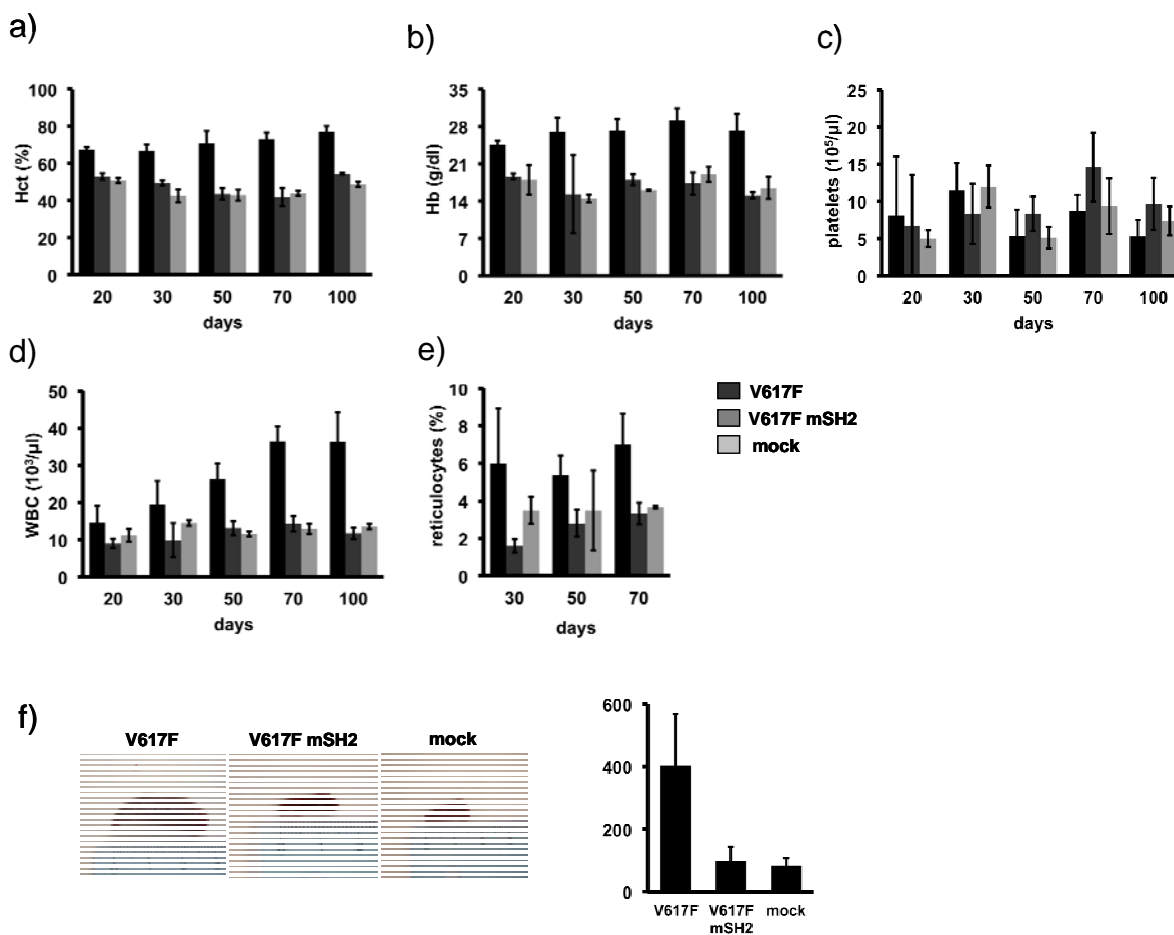


Figure 3.23. The SH2 domain is required for the induction of a JAK2^{V617F}-driven MPD in a murine BM transplantation model: Three independent transplantation experiments were performed. Data shown here are from one representative transplantation (1st) with at least three individuals transplanted in each group. In this experiment murine bone marrow was retrovirally infected with JAK2^{V617F} (V617F, n=4), JAK2^{V617F}+R426K (V617FmSH2, n=3) or empty vector (mock, n=2) and transplanted into lethally irradiated syngenic recipient mice. Hematocrit [%] (a), hemoglobin [g/dl](b), platelets [G/l] (c), WBC [G/l] (d), and reticulocytes [%] (e) of transplanted mice at the indicated time points after transplantation are shown. (f) Splens of representative transplanted animals are shown (left panel) and spleen size was quantified by weight [mg]. Values are expressed as mean (\pm SEM) of all animals transplanted. Detail on transplantation procedures are shown in Tabl.3.1

Table 3.1: Murine Bone Marrow Transplantation Experiments

Details on each individual transplantation. TX (Transplantation), CFU (Colony forming unit per ml), WBC (White Blood Cell Count), HCT (Hematocrit), Hb (Heamoglobin), Retic. (Reticulocytes), ND (not determined).

Tab 3.1

	Virus Titer [CFU/ml]	BM-Infection Efficacy [%]	n = mice	EGFP + cells transpl.	cells transpl.	d30 WBC [G/L]	d30 HCT [%]	d30 Hb [g/dl]	d30 Retic. [%]	d30 Platelets [G/L]	d60 WBC [G/L]	d60 HCT [%]	d60 Hb [g/dl]	d60 Retic. [%]	d60 Platelets [G/L]	Spleen weight [mg]
1st TX																
mock	5x10 ⁵	23	2	50,000	215,000	10 ±4	42 ±2	16 ±1.5	32 ±2	1208 ±270	13 ±1.2	44 ±2	19 ±2	37 ±2	938 ±370	83.5 ±23
V617F	4.3x10 ⁵	17	4	50,000	295,000	20 ±6	67 ±3	27 ±2.1	55 ±10	1148 ±366	38.5 ±4	74 ±2	32 ±2	67.5 ±10	871 ±200	600 ±40
V617F mSH2	4x10 ⁵	16.5	3	50,000	300,000	9.9 ±4	43 ±2	18 ±1.2	28 ±6	816 ±429	13 ±2	42 ±5	17.3 ±1	37.5 ±10	1438 ±507	98 ±45
2nd TX																
mock	1x10 ⁶	50	2	50,000	100,000	9.75±1.5	56.5 ±0.7	16.9±0.7	45 ±1.5	1068 ±85	12.3 ±3	59.2 ±7	16.8 ±2	35	780 ±133	187
V617F	8x10 ⁵	38,9	4	50,000	130,000	84.7 ±16	90.5±3.8	24 ±1.2	99 ±12.5	733 ±110	157.5 ±15	87.5 ±11	25.3 ±3.7	84.5 ±8.3	468 ±184	800 ±5
V617F mSH2	7,8x10 ⁵	38,8	3	50,000	130,000	10 ±0.5	60.3 ±0.5	18.3 ±0.8	38.6 ±3	806 ±339	14.9 ±1	63.3 ±1.5	18	39.6 ±3.2	994 ±45	201 ±10
3rd TX																
V617F	4x10 ⁵	19	4	50,000	270,000	24.8 ±2.5	89 ±2	22.3 ±1.4	ND	600 ±89	41.6 ±8	83.5 ±13	24.7 ±4	ND	604 ±155	ND
V617F mSH2	4,5x10 ⁵	18,3	4	50,000	270,000	9.6 ±2	56 ±1.5	16 ±1.3	ND	815 ±121	10.9 ±2.6	54 ±2.5	16 ±1.3	ND	1145 ±125	ND

Western blot analysis showed that both JAK2V617F and JAK2V617FmSH2 showed three times higher expression of exogenous JAK2 compared to mock transfected mice (Figure 3.24). Therefore, in murine hematopoietic cells with physiologic cytokine receptor expression, deficiency of SH2 function in JAK2V617F is associated with the loss of the oncogenic potential. Thus, a functional SH2 domain seems to be indispensable for JAK2V617F to induce a MPD *in vivo*.

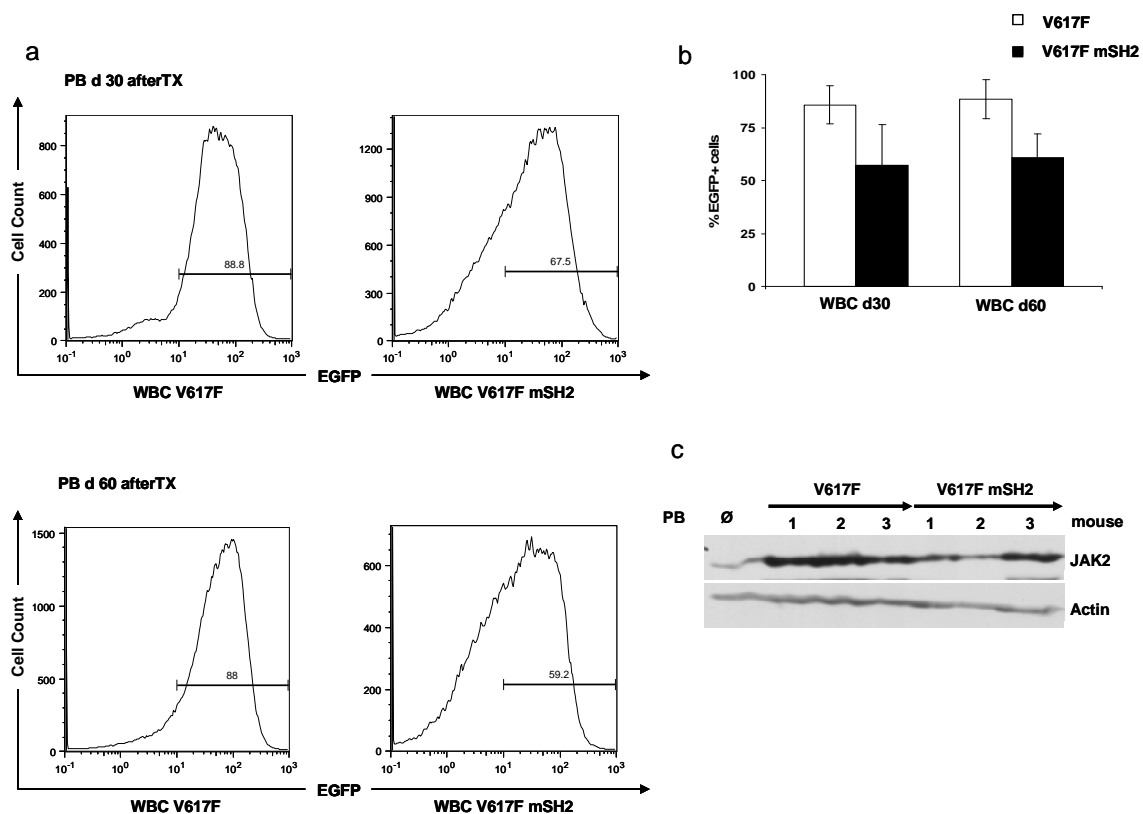


Figure 3.24: Expression of JAK2V617F and JAK2V617FmSH2 in a murine Bone Marrow Transplantation Experiment. Peripheral Blood (PB) was isolated from mice of different groups at 30 and 60 days after transplantation. After isolating WBC, cells were measured for EGFP-positivity by FACS-Analysis confirming persistent expression of JAK2V617F and JAK2V617FmSH2 after 30 days and 60 days (a). Quantification of 3 mice per group from the 2nd transplantation is shown in (b). (c) Immunoblotting of WBC isolated from PB (2nd TX) confirmed sustained JAK2V617F and JAK2V617FmSH2 expression. Expression levels of introduced JAK2 mutants were about 3-4 times higher than background wt JAK2.

On microscopy, these spleens showed a normal cellularity indistinguishable from control mice. (Figure 3.25 a, left and right panel). Analysis of the bone marrow from JAK2V617F mice revealed an increased and left shifted myelopoiesis reminiscent of a human MPN, whereas the BM of JAK2V617F mSH2 mice was normal and virtually identical to the BM of mock mice (Figure 3.25 a, upper panel). In addition, JAK2V617F induced a marked increase of collagen fibers resembling secondary myelofibrosis (Figure 3.25 b, lower panel). In contrast, myelofibrosis was absent in control and JAK2V617F mSH2 transplanted animals. Therefore, in murine hematopoietic cells with physiologic cytokine expression deficiency of the SH2 function in JAK2V617F is associated with the complete loss of its oncogenic potential. Thus, a functional SH2 domain is indispensable for JAK2V617F to induce both a MPN and myelofibrosis *in vivo*.

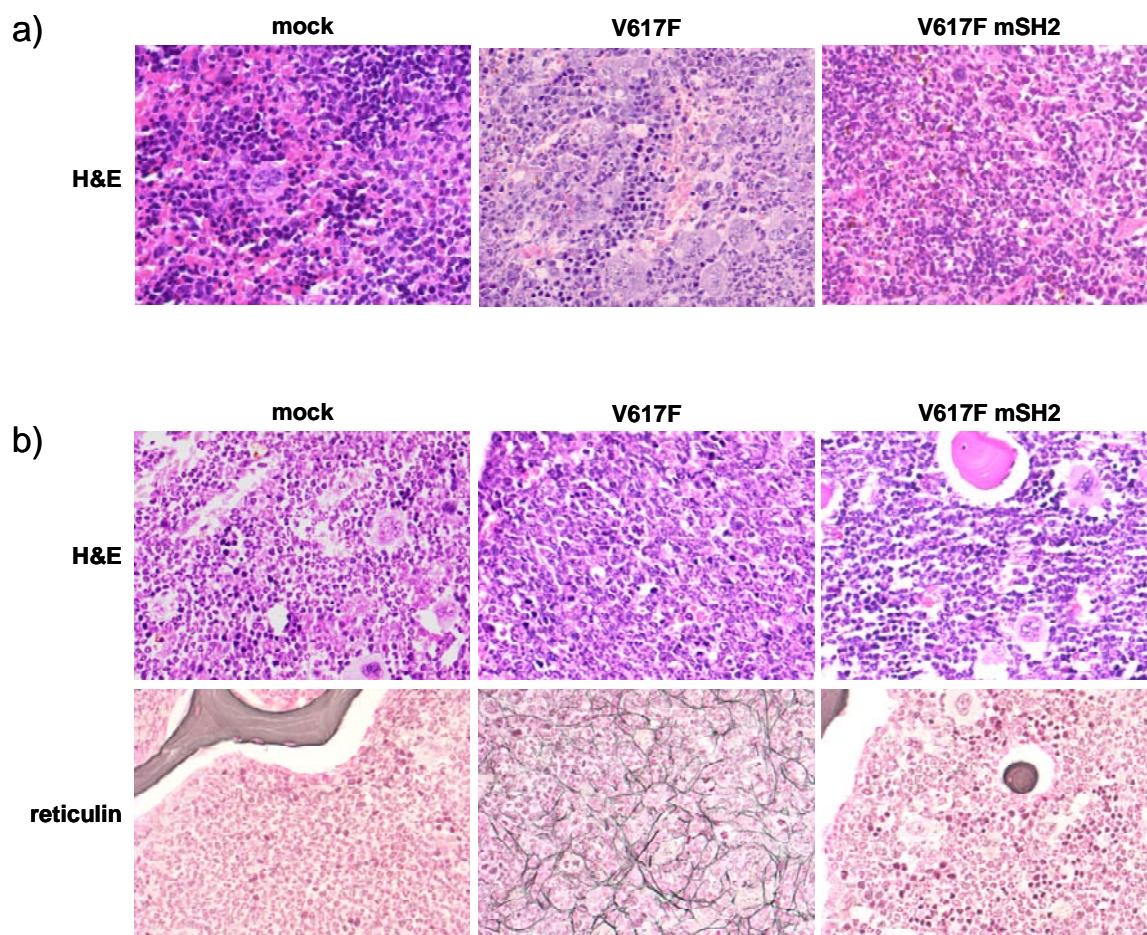


Figure.3.25: JAK2V617F transplanted mice shows typical features of MPN phenotype and myelofibrosis: The histopathologic analysis revealed hyperplastic, left shifted myelopoiesis and clusters of megakaryocytes in the spleens of JAK2V617F mice, whereas spleens of mock and JAK2V617F mSH2 mice showed normal cellularity (a). H&E and reticulin stainings as labeled of representative tissue samples are shown (x400): Left (mock) a normal cellular bone marrow is shown. Note, that all haematopoietic cell lines are present and the amount of bone marrow fibers is normal. In the middle, bone marrow from a JAK2V617F (V617F) mouse is shown, displaying a left shifted increase of myeloid cells and a marked presence of collagen fibers, similar to the increase of reticulin fibers in human myeloproliferative disorders. BM obtained from JAK2V617 mSH2 (V617F mSH2) mice shows cellularity and fiber distribution nearly identical to the mock mice shown on the left (b).

3.2. The concentration of imatinib determines the frequency and type of FP resistance mutations

With imatinib, growth of wild-type-FP (FP/wt) expressing Ba/F3 cells was suppressed with an IC₅₀ value in the range of 2 to 2.5 nM. Thus, we chose 7.5 nM (3 x IC₅₀), 15 nM (6 x), 30 nM (12 x), and 60 nM (24 x) for screening without ethylnitrosourea ENU pretreatment. The highest number of resistant clones occurred at imatinib 7.5 nM with a

frequency of 0.093 per 10^6 cells, and decreased with increasing concentrations of imatinib to 0.013 at 60 nM (Figure 3.26 a). Although the proportion of PDGFRA kinase domain mutated clones increased with escalating drug concentrations, the yield of mutant clones for all drug concentrations was only eight (Table 3.2 A). To increase the yield of mutant clones, we decided to pretreat cells with a chemical mutagen, ethylnitrosourea (ENU) ^{150,151}. Mutagenized Ba/F3 FP/wt cells were then exposed to graded concentrations of imatinib (100, 200, 500 and 4000 nM). The highest concentration approximates to plasma concentrations achievable in imatinib treated patients ¹⁵⁷. Despite higher imatinib concentrations, the frequency of resistant clones increased to 0.34 per 10^6 cells at 4000 nM to 1.56 at 100 nM (Figure 3.26 a). Also, the proportion of mutant clones increased to 72 percent at 100 nM and 100 percent at 4000 nM. With imatinib, mutations were distributed over the entire PDGFRA kinase domain (Table 3.2b, Figure 3.27). Of note, the F604S exchange located in the nucleotide-binding loop (P-loop) was predominant at low imatinib concentrations from 7.5 to 100 nM, and occurred mostly as compound exchange in combination with exchanges either in TK1 (V658, N659) or within the activation-loop in TK2 (A-loop; D842, Y849, V850). Interestingly, when we increased the imatinib concentration used for screening, we noted that a T674I exchange emerged in 73 percent of the clones at 200 nM, and constituted 100 percent of the exchanges identified at 500 and 4000 nM (Table 3.2 b). This exchange corresponds to the gatekeeper exchange T315I in Abl and is the only one isolated in clinical samples of FP positive myeloproliferation with clinical resistance to imatinib to date ^{103,146-148}. Notably, some of the clones derived from imatinib at 200 nM in contrast to clones from 500 and 2000 nM, displayed the gatekeeper exchange T674I in combination with exchanges of the kinase insert (L694V, N728D, and P744S). Over all these data indicate that our assay faithfully reproduced T674I and identified additional PDGFRA exchanges in imatinib resistant Ba/F3 cell clones.

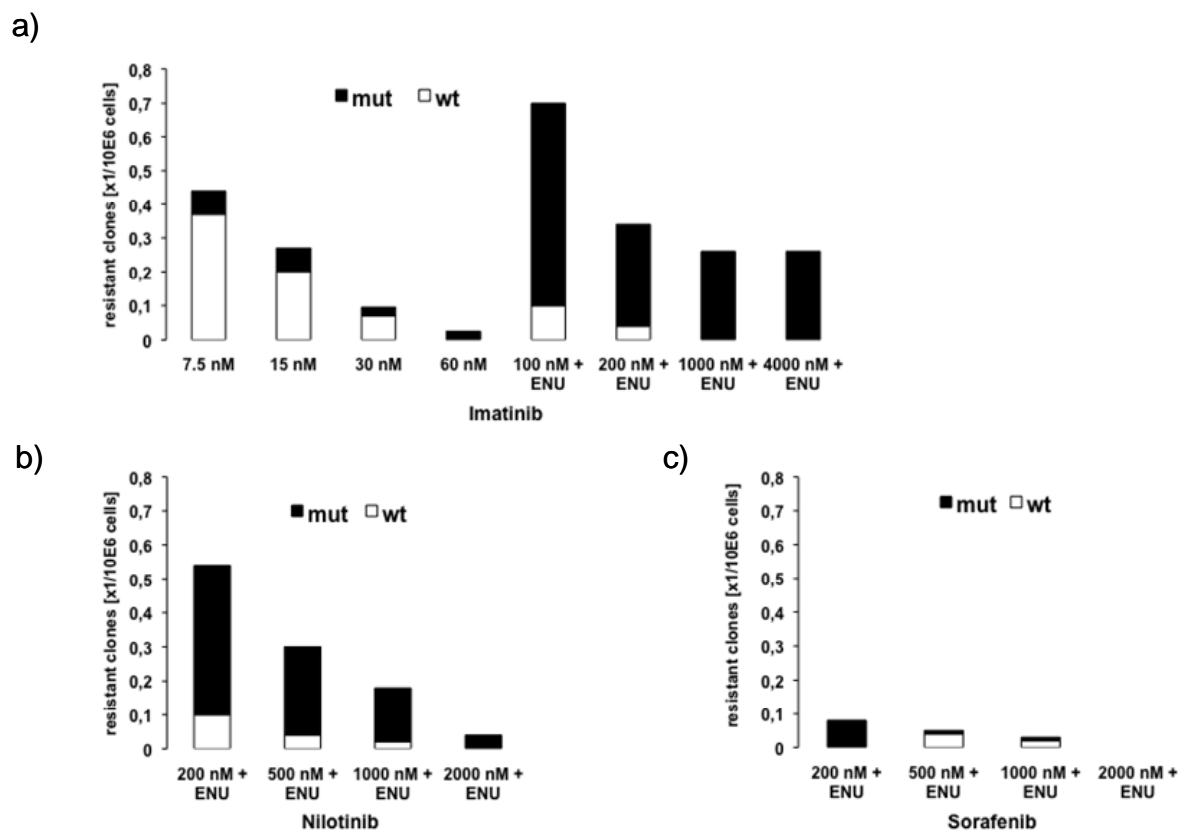


Figure 3.26: Frequency of resistant clones is determined by inhibitor, drug concentration and the presence of ENU. Single clones of Ba/F3 cells growing in 96-well plates in the presence of imatinib (a), nilotinib (b) or sorafenib (c) were picked and analyzed for the presence of FP kinase domain mutations. Shown is the frequency of resistant clones per million cells input. Wild-type (wt, open bars) and mutant (mut, filled bars) clones are shown separately. ENU pretreatment increased the clone frequency with imatinib. Therefore, screening with nilotinib and sorafenib was performed after ENU pretreatment only. Note that with imatinib, increasing drug concentration from 500 to 4000 nM did not further decrease the clone frequency (a), whereas with nilotinib (b) and sorafenib (c), clone frequencies decreased in a concentration-dependent manner.

3.2.1 With nilotinib, the profile of resistance mutations narrows to FP/D842V at clinically achievable concentrations

It has been demonstrated that nilotinib is active against FP¹⁵⁸. In contrast to imatinib, nilotinib has residual activity against FP/T674I¹⁵⁹. Given a cellular IC₅₀ value of 5 nM and serum trough levels around 2000 nM in treated patients¹⁶⁰, we selected nilotinib resistant Ba/F3 FP cell clones at 200, 500, 1000, and 2000 nM. At 200 nM, the overall frequency of resistant clones was 1.04 with nilotinib as opposed to 0.884 per 10⁶ cells with imatinib (Figure 3.26 a, b).

Tab 3.2: Spectrum and relative frequency of FP kinase domain mutations recovered at different inhibitor concentrations. Shown is the distribution of individual mutations recovered after ENU pretreatment with imatinib at low concentrations (a), and after ENU treatment with higher concentrations of imatinib, nilotinib and sorafenib (b). The total number of mutant clones and the relative frequency of exchanges per condition are shown. Positions refer to human PDGFRA (NM_006206). TK1: W586 through N689; kinase insert: R690 through D789; TK2: N790 through N952.

a)

No ENU pretreatment	Frequency of exchanges (per cent of all clones)
Inhibitor concentration (nM)	Imatinib
7.5	F604S + D842H (66.66%) F604S + D842G (33.3%)
15	F604S + D842E (33.33%) F604S + Y849L + Del850 (33.33%) F604S (33.33%)
30	F604S (100%)
60	F604S + V658A (100%)

b)

ENU pretreatment	Frequency of exchanges (per cent of all clones)		
Inhibitor concentration (nM)	Imatinib	Nilotinib	Sorafenib
100	F604S + V658G (23.2%) F604S + N659Y (9.3%) F604S + V658A (13.9%) F604S (41.86%) L694V (4.65%) S772Y (2.32%) M862I (4.65%)	ND	ND
200	T674I (73.3%) V658G (6.66%) G610R (6.66%) T674I + L694V (3.33%) T674I + N728D (3.33%) S618P (3.33%) T674I + P745S (3.33%)	T674I (6.66%) T674I + T874I (76.6%) R841G (3.33%) T874I(13.33%)	D842V (12.5%) N659Y (12.5%) K688R (12.5%) G610R (62.5%)
500	T674I (100%)	T674I + T874I (84.6%) P864S (3.84%) T799P (3.84%) T674I + L694V (7.6%)	A640G + N656Y (100%)
1000	ND	V850G (45.4%) D842V (54.6%)	S903C (100%)
2000	ND	D842V (100%)	No growth
4000	T674I (100%)	ND	ND

At higher concentrations, resistant clones steadily declined to 0.15 and 0.052 at 1000 and 2000 nM nilotinib, respectively. This was in contrast to imatinib, where the frequency of clones expressing T674I leveled off at 0.34 per 10^6 cells at 1000 and 4000 nM. With nilotinib, the T674I gatekeeper exchange alone or as a compound predominated at low and intermediate concentrations (Table 3.2 b). Notably, T674I in compound with T874I (TK2, c-terminal of the A-loop) constituted the most abundant finding at 200 and 500 nM, and exclusively emerged with nilotinib. However, in marked contrast to the imatinib screen, exchanges involving T674I disappeared in favor of the A-loop exchange D842V at higher nilotinib concentrations (1000 and 2000 nM; see Table 3.2 b). The frequency of D842V positive clones at 1000 and 2000 nM nilotinib was 0.078 and 0.052, respectively.

Together, at clinically achievable drug concentrations nilotinib produced D842V clones at a low frequency, in contrast to the more frequent finding of T674I with imatinib.

3.2.2 Sorafenib produces resistant FP cell clones at very low frequency

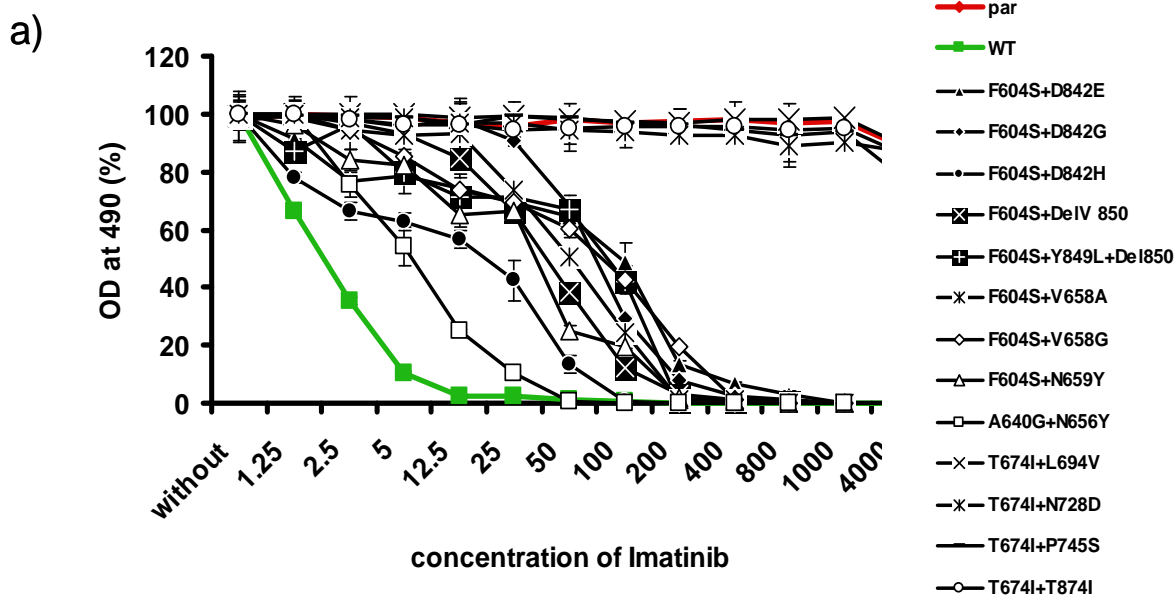
The bi-aryl urea sorafenib constitutes a compound structurally distinct from imatinib and nilotinib. Sorafenib was shown to suppress PDGFRA, FP and also FP/T674I^{161,162}. Sorafenib displays a cellular IC₅₀ of 0.25 nM with FP, and up to 4000 nM can be reached in plasma of treated patients¹⁶³. Screening with sorafenib at 200 nM produced drug resistant Ba/F3 clones at frequency of only 0.2 per 10⁶ cells input (Figure 3.26 c), further decreasing to 0.1 and 0.03 at 500 and 1000 nM. At 2000 nM, we were not able to obtain resistant clones, even though we performed screening after ENU pretreatment. The total number of resistant clones was only 16, and PDGFRA kinase domain mutations were identified in 10, including all clones derived from sorafenib at 200 nM, but only a proportion of clones at 500 and 1000 nM (20 and 33 percent respectively). This was in contrast to imatinib and nilotinib, where wt-clones disappeared in favor of mutant clones at higher inhibitor concentrations. In mutant clones, we identified seven different exchanges (Table. 3.2 b). The D842V exchange already had emerged with nilotinib at high concentrations. The N659Y (TK1) and G610R (TK1, P-loop) exchanges were both identified also with imatinib at low inhibitor concentrations. However, G610R made up five out of eight exchanges (63 %) at 200 nM sorafenib, but accounted only for 6 percent of exchanges at 200 nM imatinib. The remaining four exchanges exclusively came up with sorafenib, and included A640G, appearing as a compound exchange with N656Y (both TK1), K688R (TK1/kinase insert boundary), and S903C (c-terminal of activation loop). Also in contrast to imatinib and nilotinib, single and compound exchanges involving T674I, which made up the majority of exchanges with imatinib and nilotinib at 200 nM (83 percent each), did not emerge with sorafenib. Thus, sorafenib resistant FP Ba/F3 clones occurred at low and intermediate drug concentrations at a low frequency, but did not emerge at the clinically achievable concentration of 2000 nM. While D842V was identified, the gatekeeper mutation T674I did not come up with sorafenib.

PDGFRA	VIWKQKPRYE	IRWRVIESIS	PDGHEIY.V	DPMQLPYDSR	WEFPRDGLVL	595
PDGFRB	MLWQKKPRYE	IRWKVIESVS	SDGHEIY.V	DPMQLPYDST	WELPRDQLVL	602
c-Kit	YKYLQKPMYE	VQWKVVEEIN	..GNNYVY.I	DPTQLPYDHK	WEFPRNRLSF	591
c-Abl	...RNKPT..VYGV	SPH...YD.K	WEMERTDITM	244
PDGFRA	GRVLGSGAFG	KVVEGTAYGL	SRSQPVMKVA	VKMLKPTARS	SEKQALMSEL	645
PDGFRB	GRTLGSAGFG	QVVEATAHGL	SHSQATMKVA	VKMLKSTARS	SEKQALMSEL	652
c-Kit	GKTLGAGAFG	KVVEATAYGL	IKSDAAMTVA	VKMLKPSAHL	TEREALMSEL	641
c-Abl	KHKLGGGQYG	EVYEGV....	.WKKYSLTVA	VKTLKED..T	MEVEEFLKEA	287
PDGFRA	KINTHLGPHL	NIIVNLLGACT	KSGPIYIITE	YCFYGDLVNY	LHKNRDSFLS	695
PDGFRB	KINSHLGPHL	NVNVLLGACT	KGGPIYIITE	YCRYGDLDVY	LHRNKHTFLQ	702
c-Kit	KVLSYLGNHM	NIIVNLLGACT	IGGPTLVITE	YCCYGDLLNF	LRRKRDSFIC	691
c-Abl	AVMKEI.KHP	NLVQLLGVCT	REPPFYIITE	FMTYGNLLDY	LREC.....	330
PDGFRA	HHPEK...PK	KELDIFGLNP	ADESTRSYVI	LSFENMGDYM	DMKQADTTQY	742
PDGFRB	HHSDKRRPPS	AELYSNAL.P	VGLPLPSHVS	LTGESDGGYM	DMSKDESVDY	751
c-Kit	SKQEDH..AE	AALYKNLLH.SKES	SCSDSTNEYM	DMKPG..VSY	730
c-Abl	330
PDGFRA	VPMLERKEVS	KYSDIQRSLY	DRPASVKKK6	MLDSEVKNLL	SDDNSEGLTL	792
PDGFRB	VPMLDMKGDV	KYADIESSNY	MOPYDNYVPS	APERTCRATL	INE.SPVLVS	800
c-Kit	V.....VP	TKADKRRSV.RIGS	YIERDVTPTAI	MEDDELALDL	766
c-AblNRQEVNA	337
PDGFRA	LDLLSFYQV	ARGMEFLASK	NCVHRDLAAR	NVLLAQGKIV	KICDFGLARD	842
PDGFRB	MDLVGFSYQV	ANGMEFLASK	NCVHRDLAAR	NVLICEGKLV	KICDFGLARD	850
c-Kit	EDLLSFSYQV	AKGMAFLASK	NCIHRDLAAR	NILLTHGRIT	KICDFGLARD	816
c-Abl	VVLLYMATQI	SSAMEYLEKK	NFIHRDLAAR	NCLVGENHLV	KVADFGLSRL	387
PDGFRA	IMHDSNVSK	GSTFLPVKWM	APESIFDNLY	TTLSDVWSYG	ILLWEIFSLG	892
PDGFRB	IMRDSNYISK	GSTFLPLKWM	APESIFNSLY	TTLSDVWSFG	ILLWEIFTLG	900
c-Kit	IKNDSNVVVK	GNARLPVKWM	APESIFNCVY	TFESDVWSYG	IFLWELFSLG	866
c-Abl	.MTGDYTAH	AGAKFPKWT	APESLAYNKF	SIKSDVWAFG	VLLWEIATYG	436
PDGFRA	GTFYPGMNVD	STFYNKIKSG	YRMAKPDHAT	SEVYEINVKC	WNSEPEKRPS	942
PDGFRB	GTFYPELFMN	EQFYNAIKRG	YRMAQPAHAS	DEIYEIMQKC	WEEKFEIRPP	950
c-Kit	SSPYPGMPVD	SKFYKNIKEG	FRMLSPEHAP	ARMYDINKTC	WDADFLKRPT	916
c-Abl	HSPYPGIDL.	SQVYELLEKD	YRMERPEGCP	EKVYELMRAC	WQWNPSDRPS	485

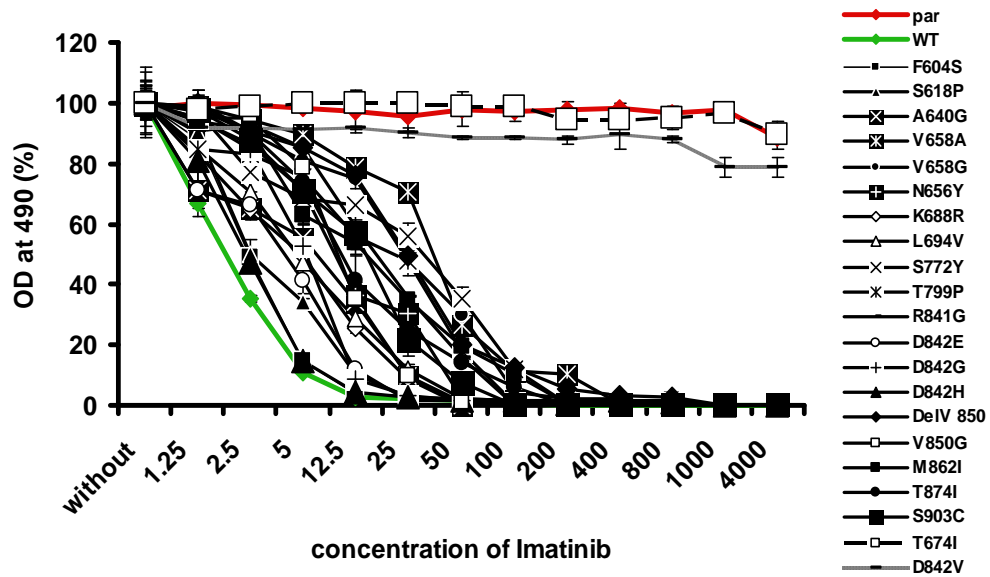
Figure.3.27: FIP1L1-PDGFR A resistance mutations and homologous positions in PDGFRB, c-Kit and c-Abl. Graphical representation of PDGFRA kinase domain (NM_006206) aligned with the kinase domains of PDGFRB (NM_002609), c-Kit (X06182) and c-Abl (NM_005157). Highlighted in red are positions of amino acid exchanges identified in resistant FP cell clones, and corresponding variants that were found in patients with GIST (c-Kit, PDGFRA) and CML (Bcr-Abl).

3.2.3 Limited cross resistance of identified FP exchanges favours nilotinib and sorafenib over imatinib

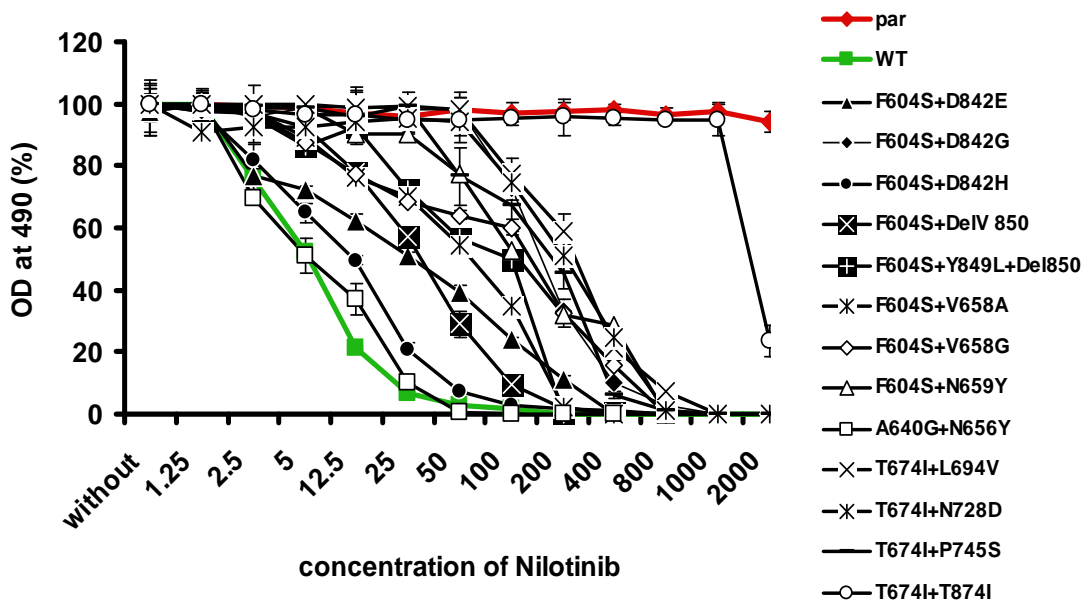
We next intended to determine the extent of cross-resistance of particular mutations. We therefore cloned all FP exchanges that were identified in the screens with imatinib, nilotinib and sorafenib using site-directed mutagenesis, including single constituents of compound exchanges. We transfected Ba/F3 cells and established stably expressing lines for all identified mutations, and examined growth suppression and phosphorylation of FP in individual cell lines in the presence of imatinib, nilotinib or sorafenib (Figure 3.28 a-f, Table 3.3). For FP/wt, cell growth assays indicated cellular IC₅₀ values of 2 nM, 5 nM, and 0.25 nM for imatinib, nilotinib, and sorafenib, respectively (Figure 3.29, Table 3.3), and these concentrations also lead to half maximal inhibition of FP autophosphorylation (Figure 3.30).

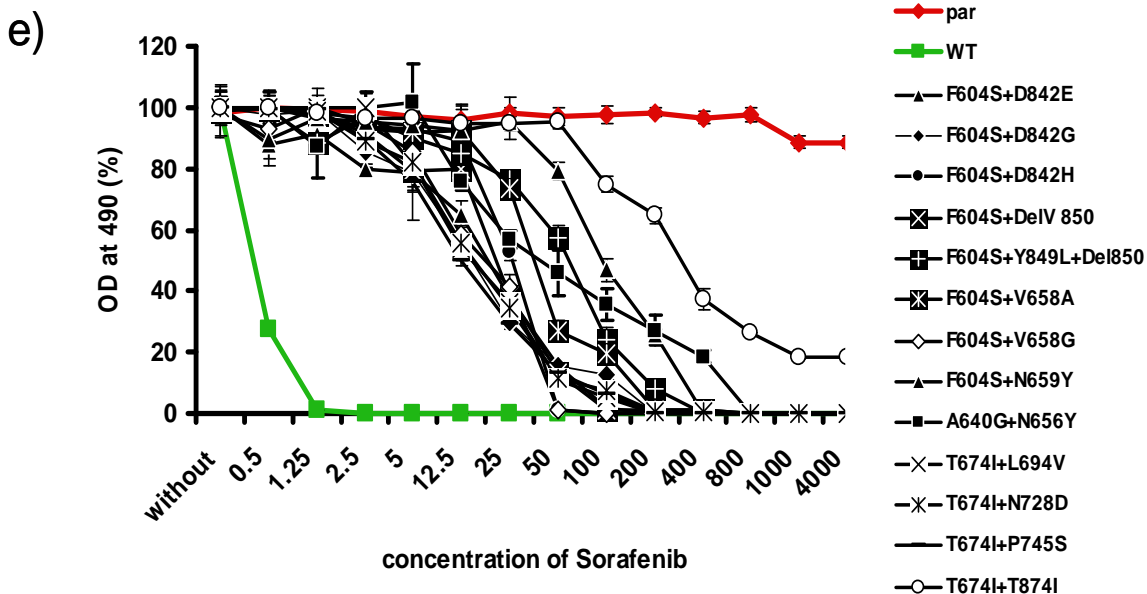
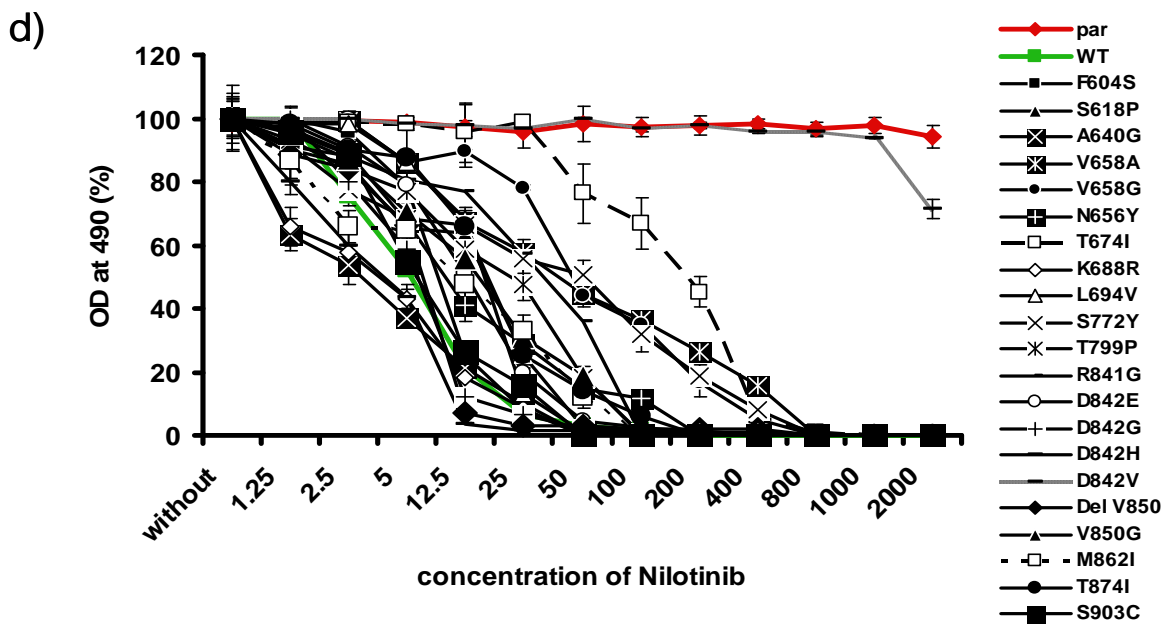


b)



c)





f)

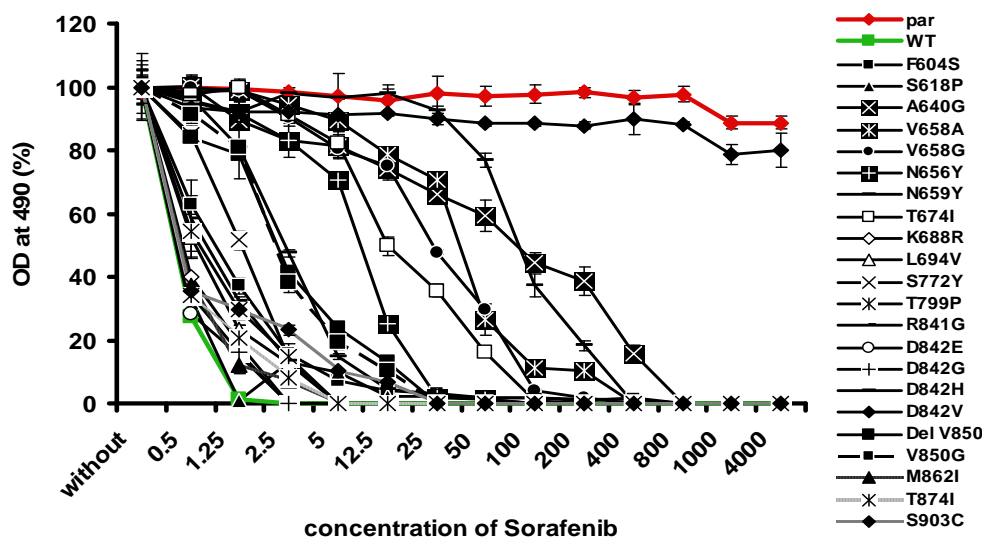


Figure. 3.28: FP/D842V is fully cross-resistant, whereas FP/T674I responds to nilotinib and sorafenib, but not to imatinib. FP point mutants that were identified with imatinib, nilotinib or sorafenib including single constituents of compound mutations were recreated in FP using site-directed mutagenesis. Constructs were stably expressed in Ba/F3 cells. Proliferation was measured using an MTS-based method after incubation for 24 and 48 hours without and in the presence of inhibitors. The clinically achievable plasma concentration was selected as maximum concentration for each compound (Imatinib 4000 nM¹⁵⁷; nilotinib 1700 nM¹⁶⁰; sorafenib 4000 nM¹⁶³). At least 2 independent experiments were performed for each construct. Shown are representative results of one experiment after 48 hours of incubation with imatinib (a and b), nilotinib (c and d), and sorafenib (e and f) for all exchanges. OD indicates optical density. Values are expressed as mean of triplicates. Bars: \pm SE.

Six out of the 27 exchanges that were identified in at least one of the screens displayed a complete imatinib resistance at 4000 nM, which corresponds to the concentration that can be reached in plasma of treated patients¹⁵⁷. In line with the imatinib screen (Table 3.2 b), where the relative abundance of the clinically reported gatekeeper exchange T674I increased in a concentration-dependent manner, five of these highly imatinib resistant exchanges involved T674I (Table 3.2).

Tab 3.3: Analysis of cellular resistance and cross-resistance of individual exchanges. FP point mutants that were identified with imatinib, nilotinib or sorafenib including single constituents of compound mutations were recreated and expressed in Ba/F3 cells. IC50 values (left) and fold increase compared to FP/wt (right) were calculated using results of the proliferation experiments shown in Figure 3.28. I/N/S/- denotes identified with imatinib (I) / nilotinib (N) /sorafenib (S) /not identified (-).

	Cellular IC50 (nM)			Cellular IC50 (fold wt)		
	Imatinib	Nilotinib	Sorafenib	Imatinib	Nilotinib	Sorafenib
wt	2	5	0,25	-	-	-
I F604S	2,5	9	0,6	1,25	1,8	3
- D842E	4	12,5	0,25	2	2,5	1
I F604S+D842E	94	25	18,5	47	5	74
- D842H	2,5	4	2	1,25	1	8
I F604S+D842H	18	12	25	9	2,4	100
- D842G	5	6,5	0,25	2,5	1,3	1
I F604S+D842G	73	158	14,5	36,5	31,6	58
- Del V850	24	7	2	12	1,4	8
- F604S+Del V 850	39	31	21	19,5	6,2	84
I F604S+Del V 850+Y849L	85	92	60	42,5	18,4	240
- V658A	35,5	38,5	36	17,75	7,7	144
I F604S+V658A	50	60	40	25	12	160
I V658G	47,5	45,5	21	23,75	9,1	84
I F604S+V658G	78	135	36	39	27	144
S N659Y	6,5	18,8	83	3,25	3,76	332
I F604S+N659Y	35	92	95	17,5	18,4	380
I/S G610R	N/A	N/A	N/A	-	-	-
I S618P	2,5	17	0,25	1,25	3,4	1
- A640G	6	3	78	3	1	312
- N656Y	9,5	9,5	18	4,75	1,9	72
S A640G+N656Y	6	5	93	3	1	361
I/N T674I	>4000	175	25	>2000	35	100
I L694V	4	16,5	0,5	2	3,3	2
I/N T674I+L694V	>4000	238	28	>2000	47,6	112
I T674I+N728D	>4000	200	28	>2000	40	112
I T674I+P744S	>4000	175	25	>2000	35	100
N T874I	10,2	17	0,5	5,1	3,4	2
N T674I+T874I	>4000	1500	300	>2000	300	1200
S K688R	4,8	4	0,25	2,4	1	1
I S772Y	31	50	4,3	15,5	10	17,2
I T799P	19	20,5	0,5	9,5	4,1	2
N R841G	17	35	0,5	8,5	7	2
N/S D842V	>4000	>2000	>4000	>2000	>400	>16000
N V850G	9,8	15	3,5	4,9	3	14
I M862I	12	10	0,25	6	2	1
S S903C	15	6	0,25	7,5	1,2	1

RESULTS

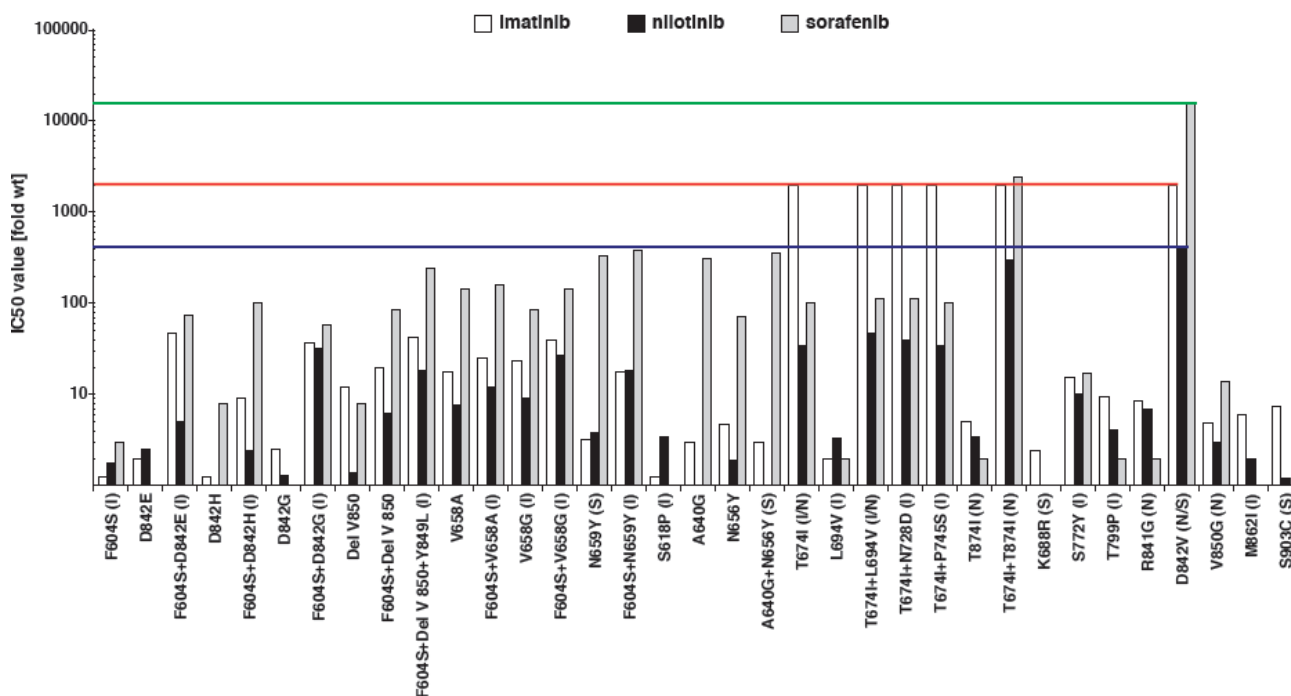
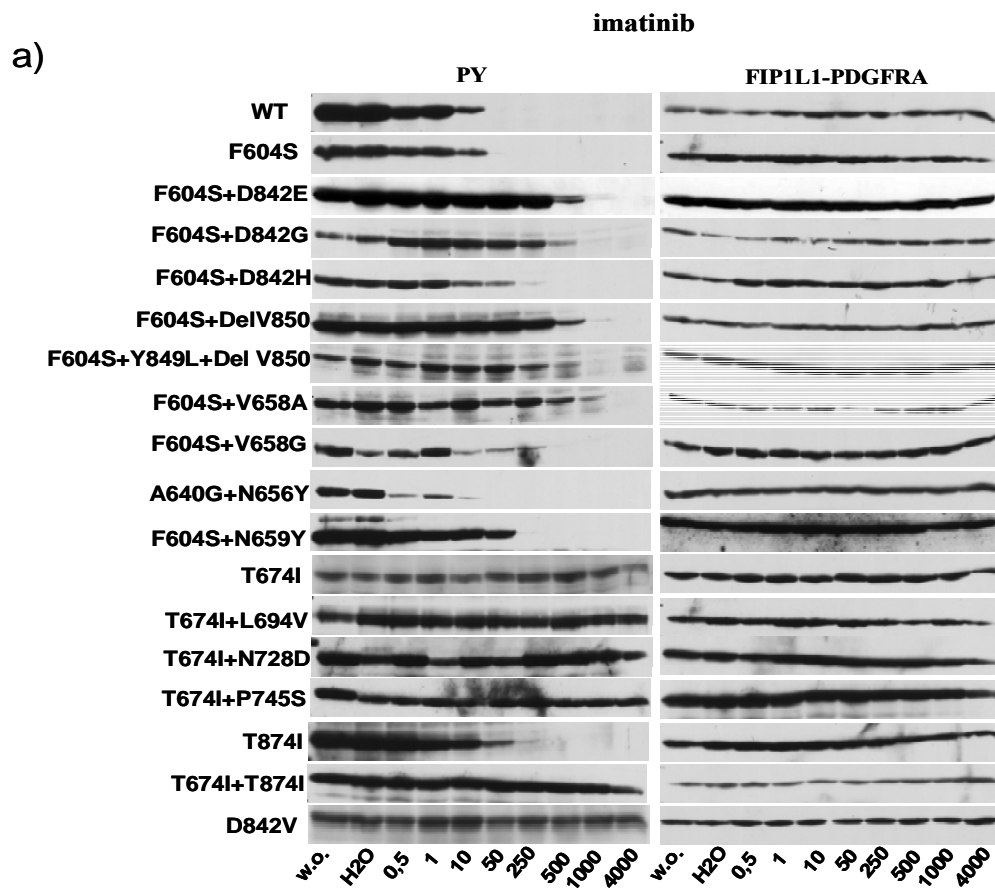
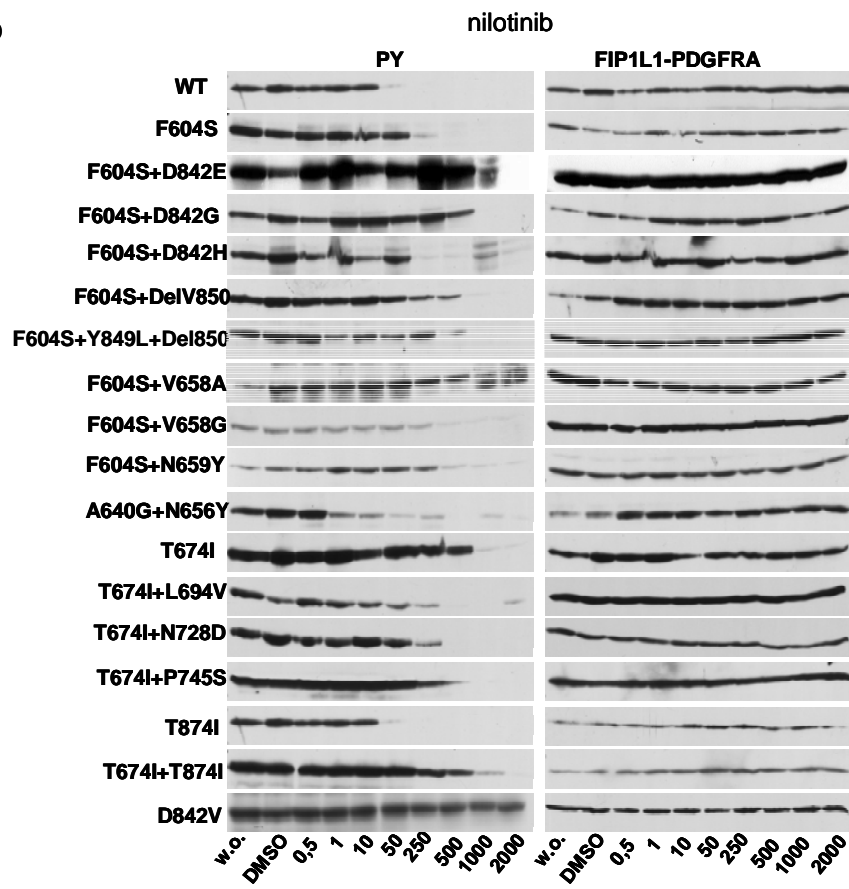


Figure. 3.29: Graphical representation of cellular IC50 fold increase as shown in table 3.3. Shown is the fold increase compared to cellular IC50 values of FP/wt for all exchanges with imatinib (IC50 2.5 nM), nilotinib (IC50 5 nM), and sorafenib (IC50 0.25 nM, see table 3.3). The cutoff values (dashed lines) correspond to fold inhibition of FP/wt at the clinically achievable plasma concentration, and are (4000 nM / 2 nM) 2000 for imatinib, (2000 nM / 5 nM) 400 for nilotinib, and (4000 nM / 0.25 nM) 16.000 for sorafenib, and thus indicate exchanges where a clinical benefit is not expected in the context of FP positive myeloproliferation harboring the respective exchange. I/N/S/- denotes: identified with imatinib/nilotinib/sorafenib/not identified.



b



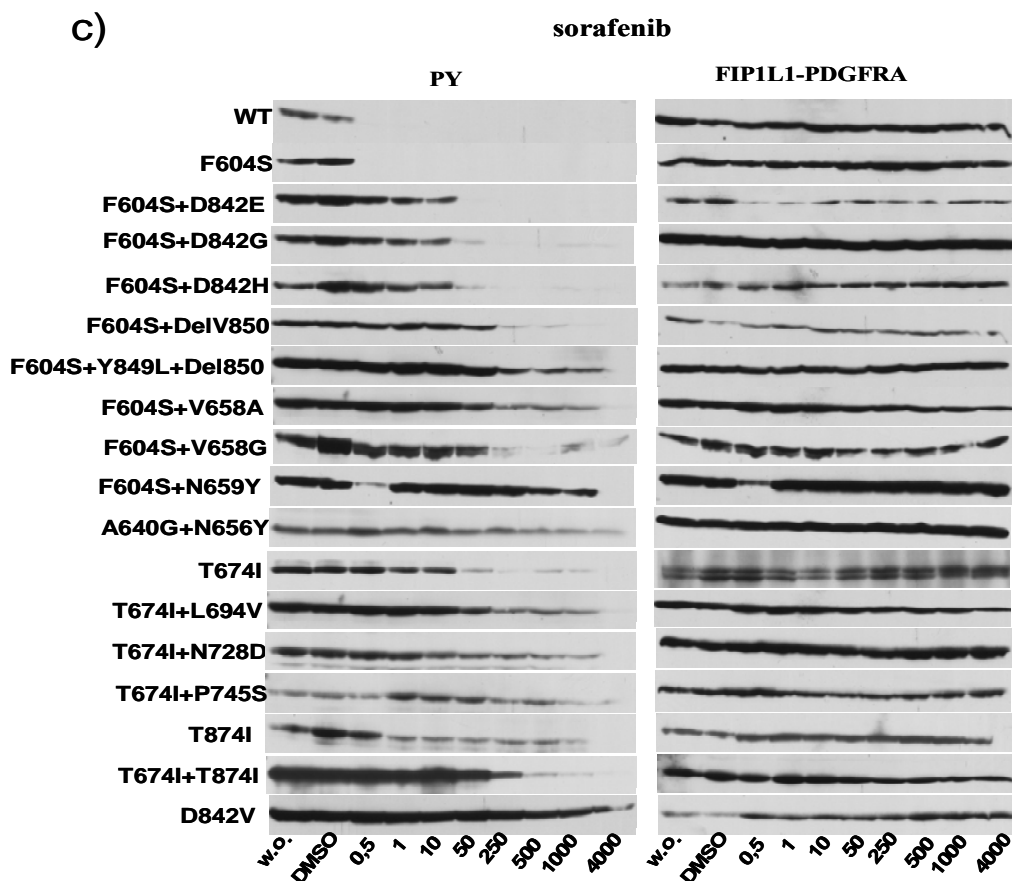


Figure. 3.30: Resistance mutations allow sustained FP autophosphorylation in the presence of inhibitor. Ba/F3 cells stably expressing wild-type (wt) or mutant FP were treated for 2.5 hours without and in the presence of imatinib (a), nilotinib (b), or sorafenib (c) at the indicated concentrations. Whole cell lysates were subjected to SDS-PAGE. Blots were probed for phosphotyrosine (left) and PDGFRA (right). Out of 27 exchanges identified, the 17 most abundant exchanges were selected for analysis.

Of these, four (T674I, T674I+L694V, T674I+N728D, and T674I+P744S; see Figure 3.28, 3.29 and Table 3.3) were fully suppressed by nilotinib and sorafenib at concentrations that can be reached in plasma of treated patients (1700 nM for nilotinib¹⁶⁰, and 4000 nM for sorafenib¹⁶³). The T674I+T874I exchange more profoundly altered nilotinib and sorafenib response (cellular IC₅₀ 1500 nM and 300 nM for nilotinib and sorafenib, respectively). However, whereas cell growth was not fully suppressed at 2000 nM nilotinib, 1000 nM sorafenib completely blocked cell growth (Figure 3.28 and 3.29). Also, FP/T674I+T874I autophosphorylation was inhibited at 2000nM nilotinib and 1000nM sorafenib (Figure 3.30 b, c). In accordance, T674I single exchange emerged in the nilotinib screen only at 200 nM, while T674I compound exchanges still came up with

500 nM, but not at higher nilotinib concentrations (Table 3.2 b). In line with its abundance in the nilotinib and sorafenib screens, D842V expectedly lead to a complete resistance to both nilotinib and sorafenib, but also imatinib (Figure 3.28, 3.29, Table 3.3). Dasatinib recently demonstrated activity against full-length PDGFRA/D842V (IC₅₀ 62 nM)¹⁶⁴. In FP/D842V however, dasatinib at therapeutic concentrations¹⁶⁵ lead to only marginal growth suppression and inhibition of autophosphorylation in Ba/F3 cells expressing FP/D842V, and also did not display activity against FP/T674I (Figure 3.31).

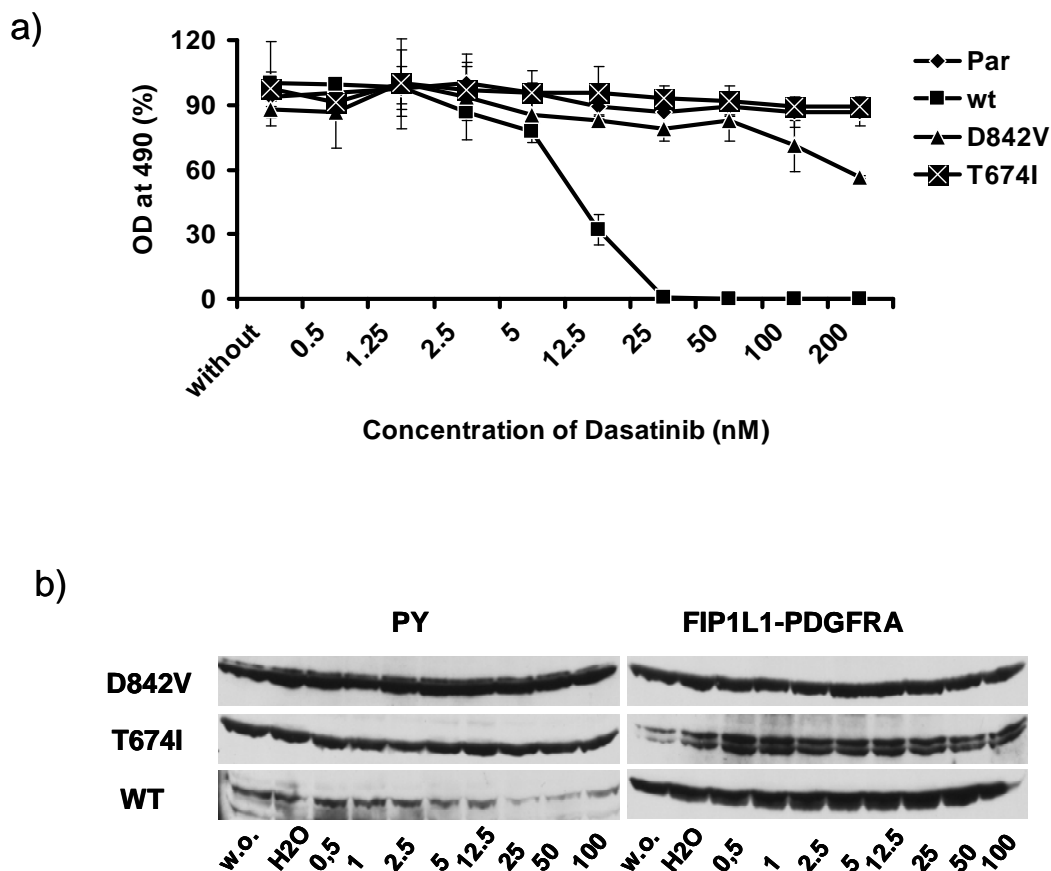


Figure 3.31: FP/T674I and FP/D842V do not respond to dasatinib. Parental Ba/F3 cells, and Ba/F3 cells stably expressing FP/wt, FP/T674I or FP/D842V were incubated for 24 and 48 hours without and in the presence of dasatinib at the indicated concentrations (a). The maximum concentration was selected according to plasma concentrations reported in treated patients¹⁶⁵. Proliferation was measured using an MTS-based method. Two independent experiments were performed. Shown are the representative results of one experiment after 48 hours of incubation. For western blot (b), cells were treated for 2.5 hours without and in the presence of dasatinib at the indicated concentrations. Whole cell lysates were subjected to SDS-PAGE. Blots were probed for phosphotyrosine (left) and PDGFRA (right).

In order to examine whether the presence of D842V in comparison to wild-type and other FP resistance mutations augments FP activation, we stably expressed wt, D842V, D842H, T674I, V658A, V658G and N659Y in Ba/F3 cells. All the FP variants showed similar transformation ability and similar levels of FP autophosphorylation and STAT5 activation (Figure 3.32 a and b). These results suggest that D842V or other FP variants which were identified at high frequency do not add oncogenic activity on the top of FP itself. Together, drug response analysis confirmed the results of our drug selection assay and suggests that in contrast to BCR-ABL, the armory of PDGFRA kinase mutations fit enough to escape inhibition by available PDGFR kinase inhibitors is limited to T674I, compound exchanges of T674I and D842V.

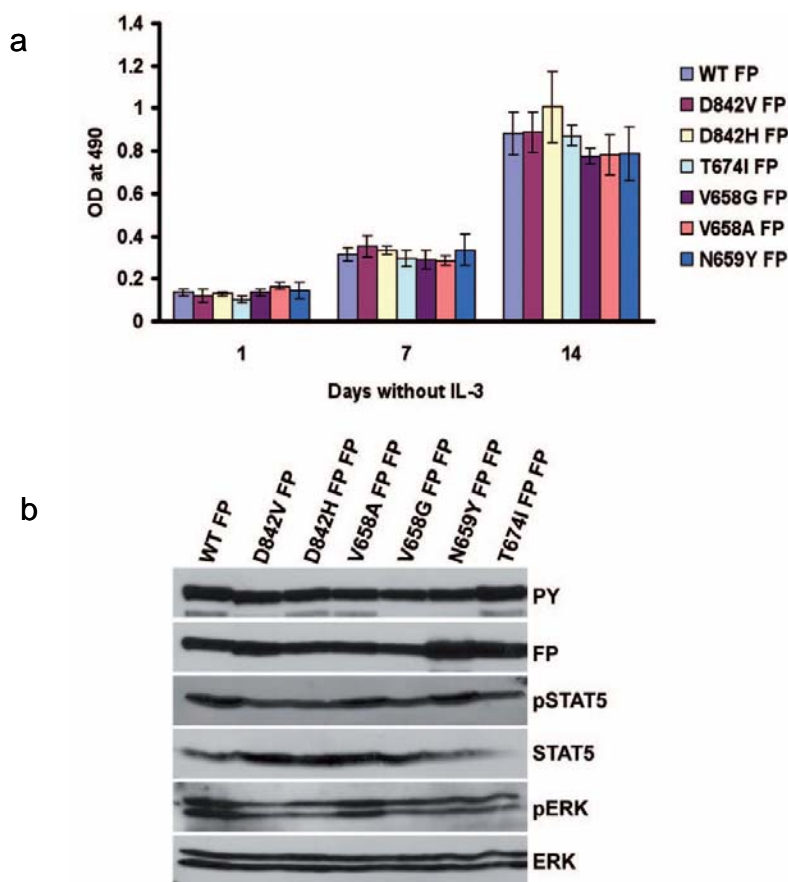


Figure 3.32: FP/D842V does not increase the transformation ability and kinase activity of FIP1L1-PDGFR. Ba/F3 cells stably expressing FP/wt, FP/D842V, FP/D842H, FP/T674I, FP/V658G, FP/V658A and FP/N659Y were grown in the absence of IL-3 for the indicated time periods (a). Cell proliferation was measured using an MTS-based method. The figures represent one out of three independent experiments. Values are expressed as mean of triplicates (\pm SEM). Whole cell lysates were subjected to SDS-PAGE (b). Blots were probed for phosphotyrosine, PDGFRA, pSTAT5, STAT5, pERK1/2 and ERK1/2.

All the exchanges from the imatinib, nilotinib and sorafenib screens except “strong” resistance mutations involving T674I or D842V were clearly responsive not only to imatinib, but also sorafenib and nilotinib at concentrations that are far below therapeutic drug levels (Figure 3.28, 3.29, Table 3.3). Eight exchanges involving F604S, which included seven compound exchanges, emerged in the low concentration screen with imatinib (Table 3.2 a), but not with nilotinib or sorafenib. However, both compounds were not tested at concentrations below 200 nM. In order to examine the contribution of F604S for resistance, we cloned single as well as double mutants. Single mutations did not affect (F604S, D842E, D842G, D842H) or only marginally interfered with imatinib response (delV850, V658A, V658G, N659Y): Mean cellular IC₅₀ values for single constituents for imatinib/nilotinib/sorafenib were 16/18/18 nM. In contrast, compound exchanges involving F604S increased mean cellular IC₅₀ values for imatinib/nilotinib/sorafenib to 62/82/41 nM (Table 3.3). In accordance, only the “stronger” single exchanges V658G (imatinib 200 nM screen; cellular IC₅₀ for imatinib/nilotinib/sorafenib 47.5/45.5/21 nM), and N659Y (sorafenib 200 nM screen; cellular IC₅₀ for imatinib/nilotinib/sorafenib 6.5/18.8/83 nM) emerged as single exchanges without F604S. These results indicate that weak TK1 or TK2 exchanges can be potentiated by F604S, which itself does not affect dose-response.

Exchanges that came up in the sorafenib screen only, such as N659Y and A640G+N656Y did not give rise to a significant cross-resistance to imatinib or nilotinib, but caused moderate sorafenib resistance (Figure 3.28, 3.29 and Table 3.3).

Thus, at therapeutic drug levels exchanges involving T674I were fully resistant to imatinib, but responsive to nilotinib, with exception of T674I+T874I, which remained sensitive to sorafenib. The only exchange displaying complete cross-resistance to all three inhibitors was D842V. For all remaining exchanges, resistance was overcome by switching the inhibitor or increasing concentrations to therapeutic drug levels.

3.2.4 FP G610R which was identified with imatinib and sorafenib lacks kinase activity and failed to transform Ba/F3 cells

The P-loop exchange G610R was the most abundant exchange identified with sorafenib at 200 nM and also emerged with imatinib at 200 nM. However, after transfection this exchange repeatedly failed to transform Ba/F3 cells upon IL-3 withdrawal (Figure 3.33 a

and b). Also, Ba/F3 cells expressing G610R did not show FP autophosphorylation or activation of STAT5 (Figure 3.33 c), indicating that G610R compromises kinase activity. This suggests that G610R positive cell clones emerging in the presence of imatinib or sorafenib might have grown out FP-independently.

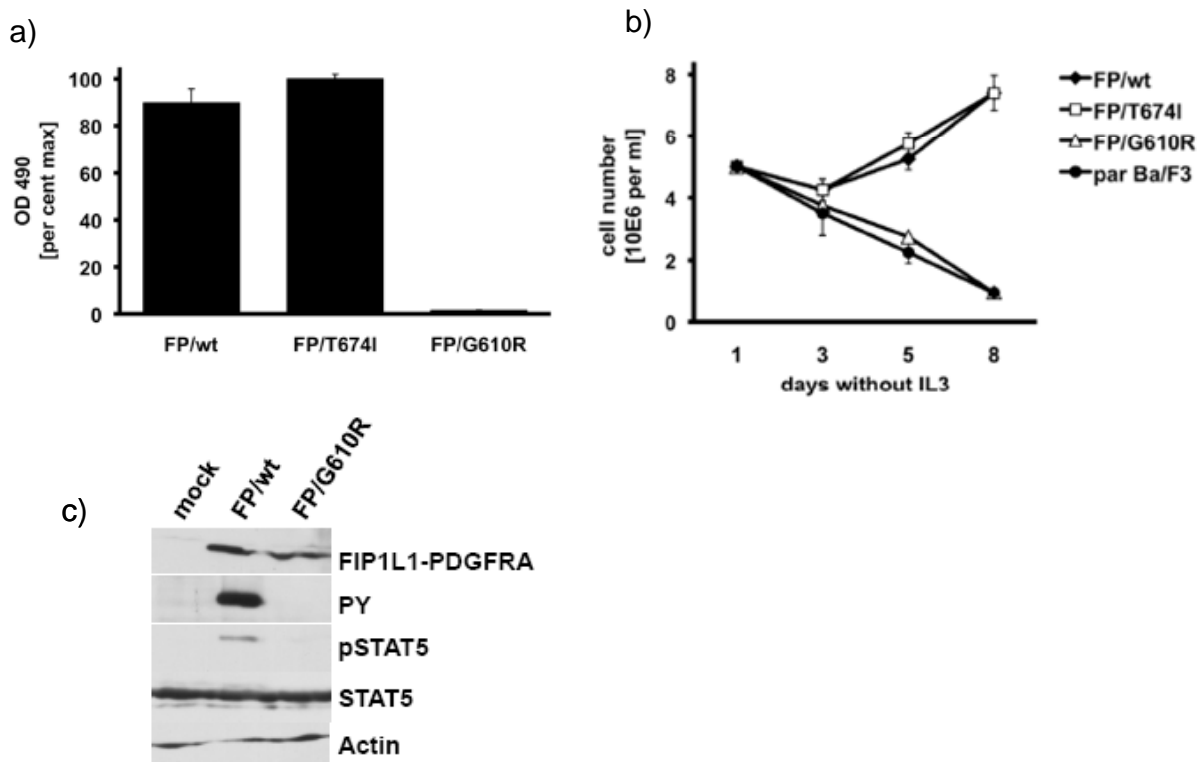


Figure 3.33: FP/G610R identified in imatinib and sorafenib screen lacks kinase activity and failed to transform Ba/F3 cells: FP/wt, T674I and G610R were stably expressed in Ba/F3 cells. Cell growth was determined after 48 hours using an MTS based method (a) and by cell counting with trypan blue exclusion (b). Whole cell lysates of Ba/F3 cells transfected with empty vector (mock), FP/wt and FP/G610R were subjected to SDS-PAGE. Blots were probed for, PDGFRA, phosphotyrosine, phospho STAT5, STAT5, and actin. Ba/F3 cells expressing FP/G610R failed to autophosphorylate FP and to activate STAT5 (c).

3.2.5 Structure analysis and discussion

The evolutionary pressure associated with drug treatment can lead to drug resistance by mutations that convert the drug target to a conformation that does not bind drug, either directly or by shifting equilibrium of conformational forms. If the mechanism weakens

drug binding, higher concentrations of drug might combat resistance. Otherwise, alternate drugs may be required. Thus, understanding and diagnostic of the resistance mechanisms are essential for choosing appropriate second line therapies and ultimately designing first line treatment to minimize the appearance of resistance.

The drug resistant forms described in this study show two different qualitative behaviours; for one set the mutants retains distinctly different sensitivities to the three inhibitors, as the wild type FP does, whereas the mutants of the other set acquire similar sensitivities to all three inhibitors (Figure 3.28 and Table 3.3). Retention of a selectivity profile, especially the higher sensitivity to sorafenib, provides evidence that the action of drug remains similar in the mutated cell. The loss of selectivity points toward drug action that involves loss of its specific high affinity binding interactions. This distinction provides clues for an analysis of the resistance mechanism of the variants.

Figure 3.34 shows the chemical structure and schematically highlights the key interactions with their target structures. All three are "type 2" inhibitors, that is, are anchored to the kinase hinge (Figure 3.35, sky blue) and bind additionally in a pocket that exists when the activation loop is in the "DFG out" conformation. All three inhibitors bind via aromatic-aromatic interactions with the Phe of the DFG motif, and bridge the main chain of the DFG motif (Figure 3.35, dark blue) to a conserved glutamic acid side chain from helix C (Figure 3.35, orange). Sorafenib uniquely has two hydrogen bonds to the kinase hinge, and three in the bridging interaction, whereas imatinib and nilotinib both have single hydrogen bonds to the hinge and two hydrogen bonds in the bridging interaction. On the other hand, only imatinib and nilotinib have direct hydrogen bonds to the gatekeeper threonine.

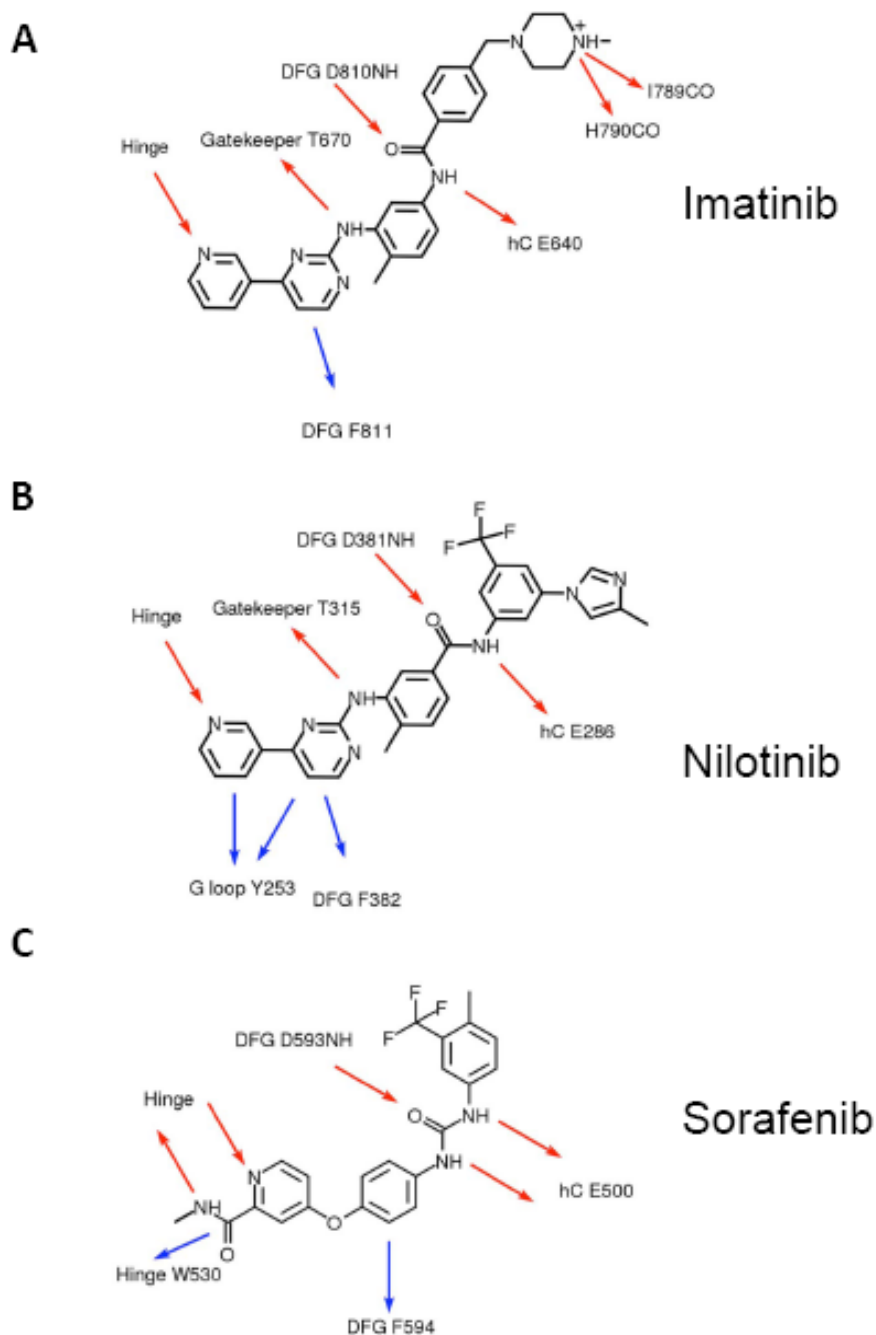


Figure 3.34: Structures of inhibitors used in this study and their key protein target interactions. Imatinib in cKIT, pdb code 1T45 (A). Nilotinib in ABL, pdb code 3CSB (B). Sorafenib in bRAF, pdb code 1UVH (C). Red arrows show denote hydrogen bonding donor to acceptor interactions, while blue arrows denote significant pi-pi interactions. The residue numbers show the numbering of the respective proteins of the crystal structure. All inhibitors share at least one hydrogen bond with the kinase hinge, pi-pi interactions with the Phe of the DFG motif at the onset of the activation loop, and hydrogen bonds bridging the Asp main chain of the DFG motif in the inactive conformation and the conserved catalytically important Glu of helix C. Because of the ability of the glycine rich (or “P”) loop to refold in ABL, nilotinib in ABL has additional pi-pi interactions relative to imatinib in cKIT and sorafenib in bRAF. Sorafenib has uniquely two hydrogen bonds to the hinge and three hydrogen bonds in the DFG Asp—helix C Glu bridge. In addition, sorafenib in bRAF has a significant pi-pi interaction with the hinge Trp530 of bRAF.

3.2.5.1 Position D842V (E,G,H): DFGLARDI

Mutations at this position are known to cause kinase activation and, in some cases, resistance to inhibitors in KIT (D816)¹⁶⁶, BRAF (V600)¹⁶⁷, EGFR (L861)¹⁶⁸, ABL (L387)¹⁶⁹, FLT3 (D835)¹⁷⁰, and MET (D1246)¹⁷¹, despite considerable diversity of the sequence after the conserved DFG motif. In PDGFR family kinases, the sequence is conserved as DFGLARDI, and point mutants D835E, Y, V, N, H in FLT3 are all constitutively activated¹⁷⁰. Thus, this position is a key element of a tyrosine or tyrosine like kinase activity modulation mechanism which also can control inhibitor efficacy, with important implications for targeted inhibitor therapies¹⁷². The degree of transformation depends both on the mutation and on the kinase. For example, among the PDGFR family kinases the D->V mutation is most strongly transforming, while the opposite mutation, V->D, is transforming for BRAF¹⁷³.

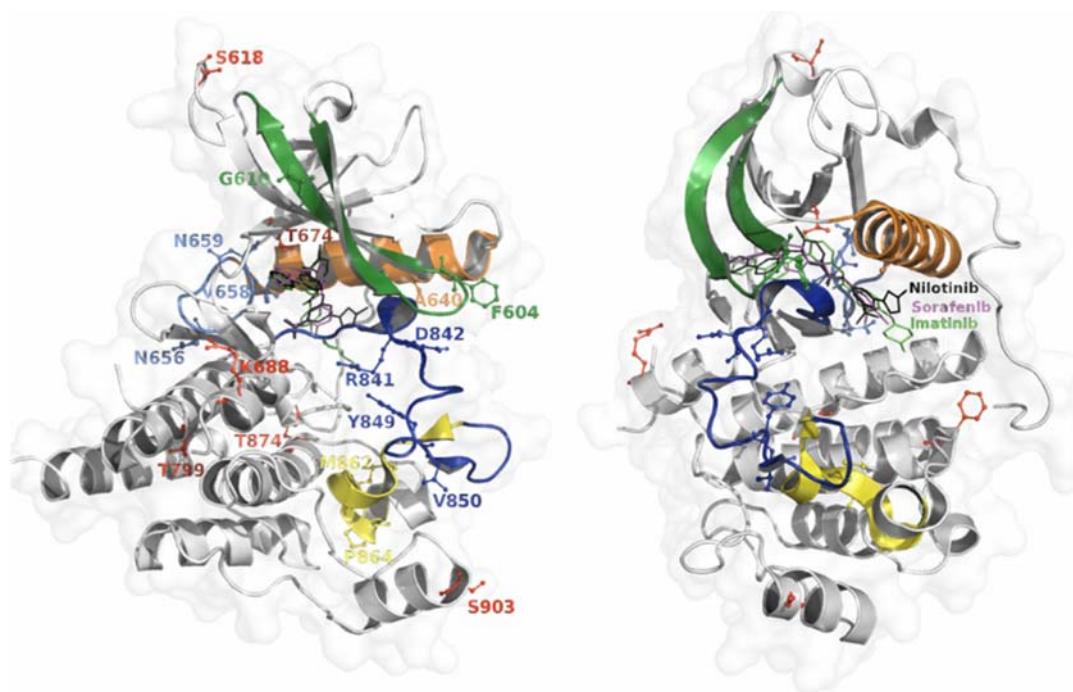


Figure. 3.35: Stereo views of the PDGFRA mutation sites relative to the schematic fold of inactive KIT. KIT residues are labelled according to PDGFRA mutations and numbering, from pdb code 1T46. Green shows the glycine rich (or "P") loop and the F604 (KIT: F600) mutation site, orange shows the alpha C helix, dark blue shows the activation loop and the key D842 (KIT: D816) mutation site, light blue shows the "molecular brake" HxN motif loop (α C- β 4 loop), and yellow highlights the P+1 loop and mutations. The remaining mutation positions are shown in red. The inhibitors of this study were modelled into the binding site by superposition of the KIT-imatinib complex (1T46) with kinase domains from ABL (nilotinib, PDB code 3cs9) and B-raf (PDB codes 1uwj, 1uwk).

Figure 3.28 highlights how the mutation D842V causes the greatest change from wt FP and also generates the highest level of drug resistance for all three inhibitors. The selectivity advantage of sorafenib has been lost entirely. The mechanism of drug resistance for mutations at this key position is generally described as the destabilization of the inactive conformation. This conclusion relies on structures of kinase domains that do not possess defective juxtamembrane domain autoinhibition mechanisms (e.g. as in FLT3-ITD, FIP1L1-PDGFR α , or cKIT mutations); however, type II inhibitor-tyrosine kinase domain structures such as imatinib in cKIT (PDB code 1T46) do show that inhibitor binding is accompanied by the loss of autoinhibitory interactions. By these analyses, mutations that disrupt stabilizing interactions and/or favor the beta sheet fold of the active form over the helical turn conformation of the inactive form would be activating. Proposed mechanisms include the removal of a helix stabilizing charge (D->V in the PDGFR kinases), or loss of the charge that determines the overall orientation of the segment in the inactive form ¹⁷⁴.

The structures do not show how the side chain of D842 is required for stability, or why this position is most critical. However, the fact that mutants D842E and D842G have relatively little effect on resistance demonstrates that identity of the mutation is more critical than the loss of the aspartate side chain. This then likely pertains more to its role in the active conformation (Figure 3.35 AB). The corresponding mutants in cKIT have a faster rate of autoactivation than wild type, but are virtually indistinguishable from WT after activation ¹⁷⁵. Thus, the transforming properties of the mutation may arise from the protein-protein interactions of the pair of kinases during the trans autoactivation step, in addition to destabilization of the inactive state.

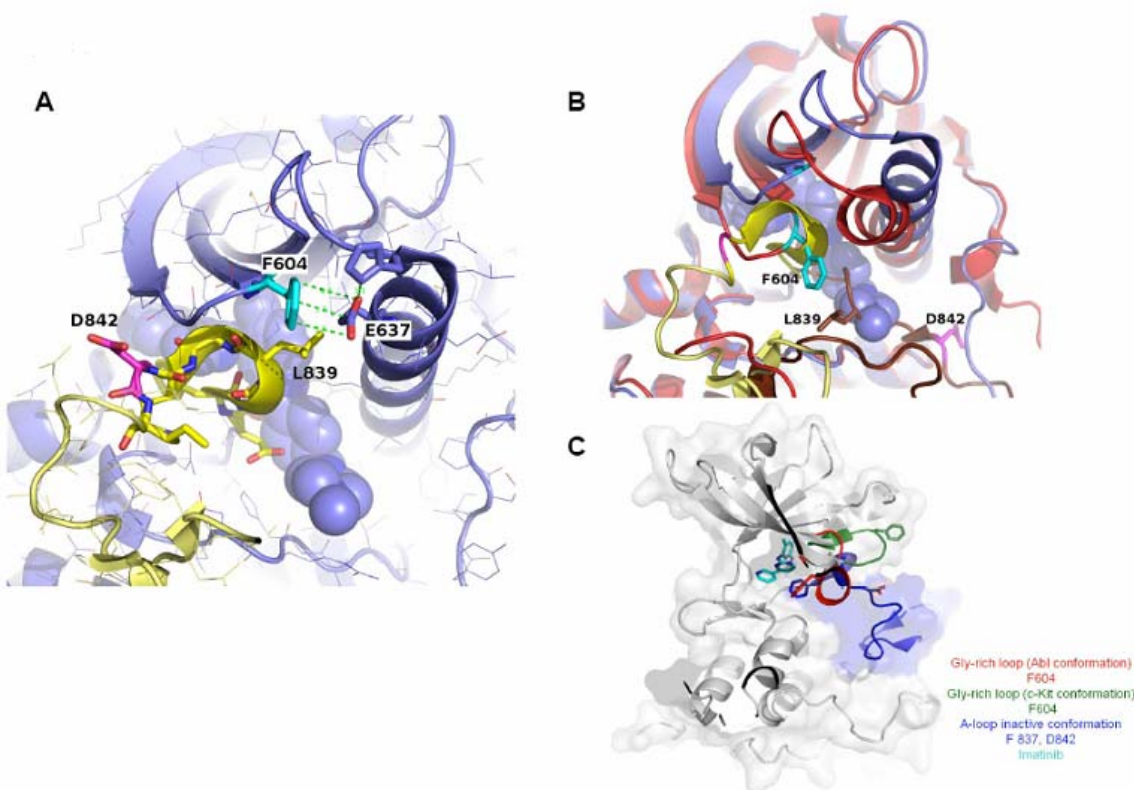


Figure. 3.36: Side chain positions of D842 and F604 in active, inactive, and inhibitor bound structures. (A) In the inactive form of imatinib (light blue spheres) bound cKIT (PDB code 1T46), the activation loop segment DFGLARDI (yellow) adopts a helical turn structure packed into a space between the C-helix, imatinib, and the beta turn of the glycine rich loop. The oncogenic mutation site D816 of cKIT (magenta, D842 in PDGFRA) is solvent exposed and is not obviously stabilizing in this geometry. Most stabilizing interactions seem to involve L813 (L839 in PDGFRA), including hydrophobic packing of the side chain and hydrogen bonding of the carbonyl group to main glycine loop atoms. There is a pi-pi interaction between F600 (F604 in PDGFRA) and E633 (E637 in PDGFRA) that contributes to the structure; this glutamate is conserved throughout the PDGFR and VEGFR kinases. (B) In the active form of cKIT (PDB code 1PKG), the activation loop segment DFGLARDI (brown) has refolded, and helix C (red) and the glycine rich loop (red) have moved to occupy the space previously filled by the DFGLARDI helical turn. In the active form, the oncogenic mutation site D816 of cKIT (D842 in PDGFRA, magenta) emerges from the back of the kinase domain. (C) Comparison of the glycine loop conformations in imatinib bound KIT (PDB code 1T46) and ABL (PDB code 1IEP). In ABL, imatinib binding is accompanied by a refolding of the glycine loop (red) to create a cluster of aromatic interactions between imatinib (cyan), the tyrosine at the position equivalent to F604 in PDGFRA, and the phenylalanine of the activation loop motif DFG in an inactive conformation (blue). In KIT, the glycine loop retains its beta hairpin turn conformation. An additional glycine in the glycine loop of ABL compared to KIT is a likely explanation (GGGQYG in ABL vs GAGAFG in KIT and GSGAFG in PDGFRA), although significant refolding of the glycine loop has been noted in other GxGxxG kinases, including Aurora A¹⁷⁶.

The fact that inhibitor selectivity is lost for the D842V, H mutations indicates that the inhibition mechanism of sorafenib is most significantly changed with respect to its inhibition in wt FP. It seems likely that the mutation changes the energies of DFGLARD structures and thereby weakens the DFG strand-helix C bridging interactions of the inhibitors (Figure 3.36 AB), disrupting especially sorafenib binding. Treatment of this

drug resistant form may preferentially involve inhibitors of the active conformation. However, this mutation is also resistant to midostaurin¹⁷⁷ at its available therapeutic levels.

3.2.5.2 Position F604S and combination mutants

The residue F604 of PDGFR (Figure 3.36 AB, cyan) is located at the beta hairpin turn between the beta strands 1 and 2 of the P-loop, G-loop, or glycine rich loop (from the consensus GxGxxG sequence). Although it is not essential for protein kinase activity, it is highly conserved as an aromatic across the protein kinases, usually as Phe, although Tyr is common and is found e.g. in ABL and the atypical PKC kinases. The aromatic is involved in inhibitor interactions that induce refolding of the glycine rich loop. Particularly notable is the refolding of the loop and inhibitor-Tyr interaction of imatinib bound ABL kinase (Figure 3.36 C), facilitated by the extra glycine in the ABL loop sequence GGGxYG. Mutations of the ABL tyrosine to histidine and phenylalanine are known to generate clinical resistance to imatinib^{115,178}.

Figure 3.35 A shows how the equivalent Phe in cKIT contributes to the stabilization of the imatinib bound inactive state. The phenyl group has an apparent stacking interaction with the delocalized carboxylate pi electrons of a conserved glutamic acid from helix C, which in turn is hydrogen bonded to a relatively conserved histidine. This interaction latches the glycine loop and helix C together and contributes thereby to the stabilization of the turn conformation of the DFGLARDI segment of the activation loop. Similar interactions are seen in BRAF¹⁶⁷ and EGFR¹⁷⁹. Activation of the kinase (as seen in cKIT PDB structure 1PKG) involves refolding of the activation loop whereby the Phe-Glu interaction is lost and both the glycine loop and helix C are shifted toward the catalytic site (Figure 3.36 B). This geometry lacks pi cloud interactions with the aromatic, although there is a hydrophobic contact to the leucine of DFGLARDI.

Although the mutation F604S alone has little effect on inhibitor resistance, it appears together with a wide variety of second mutations. Combinations with D842 mutations increase sorafenib resistance most, although all were generated by treatment with low concentrations of imatinib. As with the D842V mutation, the drug resistant combination

mutants mostly lose differential sensitivity to the drugs. As the concentration of imatinib increased, the combinations shifted from F604S and D842 mutant combinations to F604S and 658/659 mutant combinations. Thus, the resistance level remains correlated with the drug concentration; the mutations that appear are those that provide "just enough" resistance to overcome the inhibitor concentration. The most highly resistant mutations, T674I or D842V, appear at the highest concentrations, so they have a lower intrinsic probability or they are more disadvantageous in the absence of drug.

While some of the effects of these mutations may be rationalized by destabilization of the inactive state, other effects such as the increase of stability of FP due to the loss of SRC interactions likely play a role¹⁸⁰. A structural description of this phenomenon would require good models for the structure of a FP-SRC complex.

3.2.5.3 Position T674I: "the gatekeeper", and double mutants

The gatekeeper mutation T674I introduces resistance to all three inhibitors, with the strongest change for imatinib, and similar changes against nilotinib and sorafenib. Thus, because sorafenib has the strongest binding against wt PDGFRA, it remains the most effective inhibitor against these mutations as well. It also appears in combination with other mutants, but except for T674I + T874I these are not generally more resistant than the point mutation alone. Both nilotinib and imatinib generate the T674I mutation.

Retention of highest sensitivity to sorafenib binding is evidence that its binding mode is preserved for its mechanism of action. Figure 3.34 depicts how both imatinib and nilotinib are hydrogen bonded to the gatekeeper threonine (T674 in PDGFRA), whereas sorafenib avoids contact with the side chain (this remains true in three dimensions as well, see Figure 3.34). Both nilotinib and sorafenib share a trifluoromethylphenyl "anchor" in the type II inhibitor deep pocket. Assuming that this is well optimized for binding, one can rationalize the highest sensitivity of imatinib to the mutation. Further, assuming that the mutation also can shift an inactive-active conformation toward the active state, the binding strength of all three inhibitors would be weakened equivalently by this effect. This is consistent with analyses suggesting that the gatekeeper T->I mutation stabilizes the "hydrophobic spine" of the active kinase conformation¹⁸¹. The

combination of the two effects, directly on inhibitor binding, and indirectly via a shift toward the active conformation, reflects the sensitivities seen in our data.

3.2.5.4 Mutations in the α C- β 4 loop (N656Y, V658AG, N659Y)

The α C- β 4 loop (see Figure 3.35, light blue) forms part of the hinge mechanism of the protein kinase domain, linking the hinge segment, the C-lobe, and the C-terminus of helix C via multiple polar and hydrophobic nonbonded contacts. It contains the highly conserved "HxN" consensus¹⁸² and one of the "molecular brake" triad residues¹⁸³. Mutations in the loop have been linked to a wide range of maladies¹⁷², notably including GIST and imatinib resistance^{124,184,185}.

These mutations appear both as single point mutations and in combinations. The resultant IC50 sensitivities are roughly equivalent for all inhibitors, mutations, and combinations, whereby the N659Y is somewhat less resistant, except against sorafenib (Figure 3.28 e-f and Table 3.3).

Helix C (Figure 3.35, orange) spans the kinase domain, linking the α C- β 4 loop to the structures described above, including the glycine loop hairpin turn and helical turn of the DFGLARD activation loop segment. Although helix C is not completely rigid, disruption of the α C- β 4 loop structure and interactions with neighboring segments are associated with a rotation of the N-terminal lobe of the kinase and activation of the kinase domain¹⁸³. The α C- β 4 loop also shares hydrogen bonds with the hinge segment, and forms part of the inhibitor binding site.

The mutation N659Y disrupts the structuring interactions of the side chain with the loop, and also those with neighboring side chains^{183,185}. The mutations V658G, A would create a cavity at inhibitor binding site, and presumably induce local refolding and change the inhibitor binding mode. Eliminating the hydrogen bonding pattern bridging the DFG segment and helix C would eliminate a good part of the inhibitors' binding strengths, and particularly so for sorafenib. From the structure, it is not obvious that N656Y would similarly induce refolding, but the resistance data is consistent with this model.

3.2.5.5 Position Y849

This site is found mutated only once and under only one condition (15nM imatinib, no ENU pretreatment) and as a double nucleotide exchange in combination with F604S and Del850. What is notable here is its rarity, considering the frequency of resistant mutations generated by similar methods in FLT3¹⁸⁵. In FLT3, the high frequency of the equivalent Y842 mutations in vitro was explained with reference to the key role this residue plays in stabilizing an inactive conformation (PDB code 1RJB), although the structural effects of the internal tandem duplications on the inactive structure remain speculative. Because the mechanism of FIP1L1 transformation of PDGFRA involves a different type of disruption of JM autoinhibition¹¹², reasons for differences between FLT3 and PDGFRA are also speculative. However, the residues stabilizing the inactive conformation of cKIT are the aspartic acid of the HRD motif (nearly universally conserved in the kinome), the arginine five residues C-terminal to this (absolutely conserved in the receptor tyrosine kinases), and the aspartic acid C-terminal to the DFG motif (i.e. D842 in PDGFRA, conserved in the PDGFR family and some other tyrosine kinases). The conservation of these key residues is in contrast to the differences between PDGFRA and FLT3.

4. Discussion

4.1. Intact FERM is absolutely required for JAK2V617F mediated transformation

JAKs are necessary to activate signaling downstream of numerous cytokine receptors in hematopoietic progenitor cells. The identification of the V617F mutation within the pseudokinase domain of JAK2 in patients with MPNs elucidated a molecular mechanism for the pathogenesis of myeloproliferative disorders^{7-9,11,186,187}. Consequently, JAK inhibitors efficiently induced apoptosis in JAK2V617F-expressing Ba/F3 and HEL cells and marked attenuation of JAK2V617F-driven MPN in mice⁹⁵. Therefore, JAK2 inhibition might be an attractive pharmacological approach for the treatment of MPN patients, which led to the initiation of several phase I and II studies¹⁸⁸.

Although JAK2V617F is of major clinical interest, the mechanism leading to the constitutive activation of JAK2V617F is largely unclear. JAK2 is steadily bound to cytokine receptors through its amino-terminal FERM domain. Upon ligand binding, the activation of the JAK/STAT pathway occurs on the cytoplasmic tail of the cytokine receptor⁵³. Using the L40A/Y41A mutation, which impairs the FERM binding domain, we were able to demonstrate that an intact FERM domain is necessary for the transforming potential and constitutive activation of oncogenic JAK2V617F and its downstream target STAT5. Further analysis of this mutation revealed an absent membrane localization irrespectively of endogenous IL-3R or ectopic EpoR expression. In contrast to Huang and colleagues, we did not find a marked decrease in surface expression of the IL-3R or EpoR in cells expressing FERM domain mutated JAK2V617F. This discrepancy might be explained by the fact that Ba/F3 cells express endogenous levels of WT JAK2 possibly enabling proper receptor processing, whereas γ 2A cells are JAK2-negative⁴⁹. In fact, in our experiments using γ 2A cells we also observed decreased IL-3R expression in the absence of JAK2. Apart from absent receptor association, FERM domain-mutated, unbound JAK2 might also be inactive due to an auto-inhibitory interaction between the FERM and the kinase domain¹⁵⁶.

In accordance with our results, another group recently demonstrated that the FERM domain is required for the constitutive kinase activity of JAK2V617F suggesting that membrane localization is a prerequisite for JAK2V617F and subsequent STAT5 phosphorylation¹⁵⁴. In general, JAK2 is able to bind to numerous cytokine receptors, but

the receptor type required for the constitutive activation of JAK2V617F is still a matter of debate. Whereas some groups including ourselves showed transformation of IL-3R-positive Ba/F3 cells, Lu and co-workers found that a homodimeric type I cytokine receptor such as the EpoR is necessary for the oncogenic activation of JAK2V617F^{7,23,77}. As recently reported by the same group however, higher JAK2V617F expression levels circumvent the requirement of a homodimeric type I cytokine receptor for transformation⁷⁶. Moreover, in an earlier paper, Constantinescu et al. proposed that EpoR exists in an oligomerized state even in the absence of ligand¹⁸⁹. It is possible that oligomerized EpoR might facilitate the transphosphorylation of JAK2V617F in the absence of ligand stimulation, which might account for these discrepant findings.

Here we show that expression of JAK2V617F in γ 2A cells which contain the IL-3R alpha but not the beta chain does not lead to JAK2V617F activation. Expression of a functional cytokine receptor such as the IL-3R in these cells restored JAK2V617F activation in the absence of ligand. Thus, oncogenic JAK2V617F requires complex formation and expression of either heterodimeric (IL-3R) or homodimeric (EpoR) cytokine receptors.

4. 2. Intact SH2 domain is required for JAK2V617F-mediated myeloproliferative disease in mice.

Unlike the kinase, pseudokinase, and FERM domain, the function of the JAK2 SH2 domain in cytokine-induced and constitutive JAK2 activation is poorly understood. With our results we could provide evidence that the oncogenic and –to a lesser extent– cytokine-dependent JAK2 activation relies on a functional SH2 domain in the presence of the IL-3R. In accordance with previously published results, ectopic expression of JAK2V617F in parental Ba/F3 cells was able to induce IL-3-independent proliferation⁷. Notably, a point mutation within the SH2 domain (R426K) abrogated the transforming potential of JAK2V617F as efficiently as the FERM domain mutation. In accordance with these cell biological findings, both SH2- as well as FERM domain-mutated JAK2V617F lacked constitutive phosphorylation of JAK2 and STAT5. IP experiments showed that in contrast to FERM domain-mutated JAK2V617F, IL-3-induced phosphorylation, membrane and IL-3R association of SH2-mutated JAK2V617F in Ba/F3 cells was not impaired. In addition, protein stability as well as kinase activity was not affected by mutation of the SH2 domain. In γ 2A cells, IL-3-induced phosphorylation

of SH2-mutated JAK2 and STAT5 was intact but considerably reduced compared to WT-JAK2. These results indicate that both the FERM domain and the SH2 domain are necessary for JAK2V617F-induced transformation, although they seem to execute distinct molecular functions. The role of the SH2 domain in both WT-JAK2 and JAK2V617F has not been completely delineated yet. Mutation of arginine 426 in JAK2 did not seem to have a significant effect on interferon- γ signaling⁴⁶. Radtke et al. demonstrated that the corresponding SH2 mutation in JAK1 (R466K) did not impair JAK1 receptor binding but led to a downregulation of oncostatin M receptor surface expression⁴⁷. In our studies, IL-3R β and EpoR surface expression was unaffected by SH2-mutated JAK2V617F in different cell types, thus not explaining the profound loss of function of SH2 mutated JAK2V617F.

To further study the molecular mechanism regulated by the SH2 domain, we determined cytokine-independent growth and signaling in Ba/F3 cells expressing the various JAK2V617F mutants together with high and low levels of cytokine receptors. In contrast to Ba/F3 cells with endogenous IL-3R expression or Ba/F3 cells with low-level EpoR expression, SH2-mutated JAK2V617F induced proliferation in EpoR-Ba/F3 cells selected for high EpoR expression. These results show that the loss of the SH2 Domain in JAK2V617F can be compensated by high-density cytokine receptor expression. Since receptor density modulates constitutive activation and JAK2V617F is coupled to cytokine receptors independently from the SH2 domain, we reasoned that the supplementary function of the SH2 domain might be involved in crossphosphorylation and constitutive activation of JAK2V617F. Indeed oncogenic JAK2V617F coprecipitated with itself and underwent crossphosphorylation. Both coprecipitation and crossphosphorylation required an intact SH2 domain.

Reciprocal JAK phosphorylation is thought to occur as the first phosphorylation step upon ligand binding and receptor dimerization^{52,190}. It has been demonstrated that the phosphorylation of several tyrosine residues including Y1007 within the activation loop are essential for the regulation of JAK2 activity^{40,41,191}. However, structural requirements for JAK2 transphosphorylation –especially in the context of the V617F mutation- have not extensively been studied yet. Although cytokine-induced JAK2 phosphorylation was markedly reduced but still detectable in JAK2 harboring the SH2 mutation, the SH2 domain seems to be indispensable for constitutive JAK2V617F activation. An

explanation for this discrepancy might be due to the fact that the SH2 domain mediates transphosphorylation when oncogenic JAKV617F is associated with a cytokine receptor in the absence of ligands. In the presence of ligands leading to the annealing of the receptor chains, the SH2 domain seems to be important for full activation, but not absolutely required. The notion that close proximity of receptor chains might overcome the strict requirement for the SH2 domain is further supported by the fact that a high density of EpoR on the cell surface is able to rescue the SH2 mutation. The exact role of the JAK2 SH2 domain remains to be determined. We and others demonstrated that the JAK SH2 domain does not function as a classical phospho-tyrosine-binding SH2 domain⁴⁷. However, the SH2 domain seems to be required for self-aggregation and transphosphorylation of JAK2V617F. Funakoshi-Tago et al. found that JAK2V613E but not JAK2V617F requires ectopic expression of EpoR for constitutive activation¹⁵⁶. This phenotype is reminiscent of the JAK2V617F+R426K double mutant described in this study. The authors speculate that enhanced binding of the Y613E-mutated JH1 domain to the FERM domain might lead to increased self-inhibition. According to their model, ectopic expression of a homodimeric cytokine receptor could then result in enhanced FERM domain-receptor binding and a release of self-inhibition. Although this is an attractive model, we did not detect any difference in kinase activity between SH2-unmutated and -mutated JAK2V617F. Instead, we raised two hypotheses, which might explain our findings. First, JAK2V617F self-aggregation is dependent on the binding between the SH2 domain and a region within the JAK2 molecule, which has not been defined yet. Second, the SH2 domain is important for intrastuctural integrity of the JAK2V617F protein, which is a prerequisite for proper complex formation, transphosphorylation and signal transduction. To address these questions, the crystal structure of JAK2V617F would be of great interest.

Finally we wished to determine the functional importance of the SH2 domain for oncogenic activation of JAK2V617F under physiological cytokine receptor density in primary hematopoietic cells in an *in vivo* system. In accordance with other groups we found that retroviral infection of murine BM cells with JAK2V617F resulted in a MPN reminiscent of PV^{65,66}. Importantly, mice transplanted with BM cells expressing SH2-mutated JAK2V617F did not develop a MPN-like disease as determined by hematocrit, reticulocytes, leukocytes spleen weight and histopathology and showed a phenotype

indistinguishable from mock-infected control animals. In addition, myelofibrosis was only detectable in JAK2V617F and not in JAK2V617F mSH2 or control-infected mice. These results strongly indicate that JAK2V617F-induced MPN and myelofibrosis require an intact SH2 domain *in vivo*. Together with our *in vitro* data this results corroborate the critical role of the SH2 domain for JAK2V617F signaling under physiological cytokine receptor expression and underscores the need for careful interpretation of data using cell lines overexpressing cytokine receptors at high densities.

The need for proper localization and cytokine receptor expression distinguishes JAK2V617F from other oncogenes associated with MPNs such as BCR-ABL or FIP1L1-PDGFR. These oncogenic fusion proteins are activated in a very different way compared to their normal cellular counterparts. In contrast, JAK2V617F and endogenous ligand-activated JAK2 seem to have very similar requirements for activation. This similarity may make it difficult to develop JAK2V617F-specific inhibitors, which do not interfere with normal cytokine signaling.

4.3 In vitro resistance screening identifies nilotinib and sorafenib as candidates to overcome imatinib resistance in myeloproliferation with FIP1L1-PDGFR

The Abl, Kit and PDGFR small molecule kinase inhibitor imatinib mesylate (Gleevec) constitutes the current standard treatment for Bcr-Abl positive CML, and is active in gastrointestinal stromal tumor (GIST), were it suppresses constitutively activating mutations of c-kit or PDGFR. Both, in CML¹¹³⁻¹¹⁹ as well in GIST¹²⁰⁻¹²⁴, acquired resistance to imatinib is associated with the emergence of secondary kinase domain mutations that interfere with drug binding to the target kinase. Alternative kinase inhibitors are emerging as the most promising strategy to overcome drug resistance induced by kinase domain mutations. In CML, novel Abl kinase inhibitors display only partially overlapping profile of resistance mutations with imatinib¹²⁵⁻¹²⁷. Sequential treatment with imatinib and the approved, second-generation Abl kinase inhibitors nilotinib (Tasigna) and dasatinib (Sprycel) has already become reality¹²⁸, and selection of the appropriate inhibitor is based on the presence of specific Bcr-Abl resistance mutations. Imatinib has demonstrated clinical activity and induced complete remissions in the majority of cases with myeloproliferation positive for PDGFR-A abnormalities

DISCUSSION

including FP^{103,104,129-131}, and BCR-PDGFR¹³², but also in PDGFR-B abnormalities, including ETV6-PDGFRB^{133,134}, TEL-PDGFRB¹³³, and others¹³⁵⁻¹⁴³.

We here describe a cell-based screening system for the prediction of specific FP kinase domain mutations that cause resistance to the small molecule kinase inhibitors imatinib, nilotinib, and sorafenib. Our results suggest that in imatinib resistant patients with FP positive myeloproliferation, two resistance mutations will predominate: One is T674I, the other D842V. PDGFRA/T674I corresponds to exchanges identified in patients with imatinib resistant CML (Bcr-Abl/T315I) and GIST (cKit/T670I)^{113,120} (Fig.3.28). These “gatekeeper” exchanges confer absolute resistance to imatinib by interfering with drug binding¹⁹². Accordingly in our screen, while F604S compound exchanges predominated at low imatinib concentrations, increasing concentrations generated mostly T674I, which persisted at a high frequency of 0.34 per million cells input at clinically achievable imatinib concentrations. In contrast, in the nilotinib screen with increasing drug concentrations exchanges switched from T674I (200 nM) to compound exchanges involving T674I (500 nM) and finally to D842V at a frequency of 0.052 per million cells input at the highest concentration of 2000 nM nilotinib. Thus, at therapeutic drug levels, T674I probably would not come up with nilotinib. This is in accordance with our previous observation that nilotinib suppressed FP/T674I in vitro¹⁵⁹. In contrast, however nilotinib is not active against Bcr-Abl/T315I¹⁴⁵ and cKit/T670I¹⁹³. In our screen, T674I also did not emerge with sorafenib at any of the concentrations tested, in line with the cellular and biochemical IC50 value of approximately 25 nM, which is below the starting concentration in our screen (200 nM), and also far below achievable plasma levels in treated patients of 4000 nM. This is in accordance with a previous report showing that sorafenib has activity against FP/T674I in vitro¹⁶². In addition, the staurosporine derivative PKC412 was reported to be active against FP/T674I¹¹⁰. Moreover, we did not see activity of dasatinib in cells expressing FP/T674I at concentrations that are achieved in plasma of treated patients. Consequently, nilotinib, sorafenib, and PKC412 currently remain as appropriate second-line treatment options for T674I after imatinib failure. However, a T674I + T874I compound exchange, which emerged in 22 out of 26 clones in the nilotinib screen at 500 nM, shifted nilotinib dose-response to 1500 nM, and thus must

be regarded as fully nilotinib resistant. In that case, sorafenib might still be active at clinical concentrations, since it displayed a cellular IC₅₀ of 300 nM for this exchange. It is not known whether clinical resistance to imatinib in myeloid neoplasms associated with abnormalities of PDGFRA will occur in a frequency similar to that observed in CML. Our results suggest that the repertoire of possible PDGFRA kinase domain mutations leading to a shift of drug response sufficient to cause clinical resistance to available PDGFR inhibitors at therapeutic drug levels is limited. This may be explained on condition that FIP1L1-PDGFRA is 100-fold more sensitive to imatinib compared to Bcr-Abl. If this will translate into a low frequency of clinical resistance to therapeutic PDGFR inhibition in myeloproliferation remains to be shown. To date, seven cases of FP positive myeloproliferation and acquired imatinib resistance with a secondary mutation in the FP kinase domain have been reported. In five out of these cases, drug resistance occurred in the setting of blast crisis, with a preceding “chronic phase” reported in four cases^{103,148,194,195}. This is similar to CML, where imatinib resistance occurs more frequently and is more often associated with kinase domain mutations in advanced phase disease than in chronic phase¹⁹⁶. In accordance to our results, in six out of seven cases either FP/T674I or FP/D842V were identified^{103,146-148,195,197}, including one patient relapsing with FP/D842V receiving treatment with sorafenib¹⁹⁵. The remaining patient was found with a S601P + L629P double mutation¹⁹⁸, which we did not identify. This or similar approaches to identify resistance mutations in kinases have been utilized with Bcr-Abl and Abl kinase inhibitors where they demonstrated to cover most Bcr-Abl mutations known from imatinib resistant CML patients and moreover faithfully predicted most exchanges associated with resistance to nilotinib and dasatinib^{126-128,146,151,199,200}. Still, it can not be excluded that the method used failed to detect single exchanges in FIP1L1-PDGFRA that in the future might evolve in the clinic.

In some GIST patients, a D842V exchange in full-length PDGFRA can be identified²⁰¹, and the corresponding exchange D816V in cKit can be found in patients with mastocytosis²⁰² (Fig.3.28 and 3.29). Both act as activating mutations but at the same time give rise to imatinib resistance^{203,204}, probably by destabilizing the inactive conformational state of the kinase, to which imatinib binds²⁰⁵. The D842V exchange in full-length PDGFRA was shown to cause resistance to nilotinib²⁰⁶, while PKC412,

sorafenib and dasatinib had some residual activity, although at concentrations that might be above achievable plasma levels^{164,207,208}. In our screen, FP/D842V was recovered with nilotinib and sorafenib, but however was missed in the imatinib screen, although a total number of 133 imatinib resistant cell clones harbored mutations, including three other exchanges at the same position (D842E/G/H). We tested activity of dasatinib with FP/D842V and did not see inhibition at therapeutic drug levels. Thus, FP/D842V came out as fully cross-resistant and did not respond to imatinib, nilotinib, sorafenib and dasatinib at clinically achievable levels.

Other mutations that emerged from the FP screen only lead to low-grade resistance. Interestingly, some correspond to exchanges that were described in different oncogenic kinases (see Figure 3.27). For example, the moderately sorafenib resistant, but imatinib sensitive FP/N659Y finds its counterpart in an activating, imatinib responsive PDGFRA/N659K mutation identified in GIST^{184,209}, and complies with FLT3-ITD/N676K, which was identified in a patient with AML and resistance to PKC412²¹⁰. The weak A-loop mutation FP/Y849L matches FLT3/Y842, where an exchange to cysteine was identified as activating FLT3 mutation in AML²¹¹, and a mutation to histidine on FLT3-ITD background was associated with resistance to su5614 in vitro²¹². Also, an exchange of the corresponding Y823 in cKit to aspartic acid has been identified as activating mutation associated with imatinib resistance in GIST¹²⁴, and FP/V658A conforms to cKit/V654A, which also can be found in imatinib resistant GIST¹²².

At present time, it is not clear whether clinical resistance to imatinib in myeloproliferation with PDGFR-A and -B abnormalities will occur in a similar frequency as it is observed in CML and GIST patients. However, four cases of FP positive myeloproliferation and acquired imatinib resistance with a secondary mutation in the FP kinase domain have been reported, and in all cases FP/T674I was identified^{103,146-148}. FP positive acute myelogenous leukemia (AML) has been described. In all cases, a preceding “chronic phase” was reported^{103,146,148,213}, resembling the natural course of other myeloproliferative neoplasms such as CML. Thus, as more patients with myeloproliferation and PDGFR-A and -B abnormalities are treated with imatinib, it is probably a question of time that more secondary PDGFR resistance mutations will be reported, as it was the case with CML, where multiple BCR-ABL resistance mutations were reported shortly after T315I was identified for the first time. In that case, the

availability of alternative PDGFR inhibitors and specific resistance profiles for each compound will facilitate clinical decision making with regard to selection of the appropriate second- or third line agent, based on the presence of a specific resistance mutation in the PDGFRA or -B kinase domain.

Very recently, Lierman et al. reported a case of a patient with FIP1L1-PDGFR α -positive chronic eosinophilic leukemia (CEL) in blast crisis relapsing with FIP1L1-PDGFR α /T674I while receiving treatment with imatinib¹⁷⁷. After initially responding to sorafenib, the patient relapsed upon emergence of a FIP1L1-PDGFR α /D842V mutation under continued treatment with sorafenib, and later on did also not respond to nilotinib. This case supports our prediction of FP/D842V emerging as fully cross-resistant exchange after sequential inhibitor treatment of FIP1L1-PDGFR α -positive myeloproliferation.

4.4. Conclusion

The oncogenic JAK2V617F mutation is found in the majority of myeloproliferative diseases like polycythemia Vera (PV), essential thrombocythemia (ET) and primary myelofibrosis (PMF). However, the molecular mechanism leading to constitutive kinase activity is largely unclear. In this study we aim to dissect the role of SH2 and FERM domains in JAK2V617F mediated myeloproliferative disorders. Here we show that JAK2V617F requires an intact SH2 and FERM domains for constitutive activation. In a murine transplantation model we found that an intact SH2 domain in JAK2V617F was required for the induction of a MPD-like disease. Thus, our results points to an important role of the SH2 and FERM domains for the constitutive activation of JAK2V617F.

FIP1L1-PDGFR α (FP) is a constitutively activated protein kinase which was reported in chronic eosinophilic leukemia (CEL) and in cases of hypereosinophilic syndrome and mastocytosis with eosinophilia. Imatinib is clinically active against FIP1L1-PDGFR α positive disease. However, clinical resistance to imatinib has been observed in FIP1L1-PDGFR α positive leukemia and was shown to occur due to a secondary mutation (T674I) in the PDGFR α kinase domain. We therefore aimed to generate specific resistance profiles for available PDGFR kinase inhibitors. To this end, we generated clones of FP expressing Ba/F3 cells resistant to imatinib, nilotinib

DISCUSSION

(Tasigna), and BAY 43-9006 (sorafenib, Nexavar) and show that different PDGFRA kinase inhibitors indeed produce distinct profiles of resistance mutations in PDGFRA. Specific profiles of FP resistance mutations may help in guiding treatment for myeloproliferative diseases positive for activating PDGFR-A and -B rearrangements in the setting of acquired imatinib resistance.

5. Summary / Zusammenfassung

Aberrant activated tyrosine kinase signaling pathway plays a major role in several hematological malignancies. Understanding the molecular mechanism of constitutive activation of tyrosine kinases is essential in order to develop targeted therapy towards dysregulated tyrosine kinases. In this work we have focused on two constitutively activated tyrosine kinases JAK2V617F and FIP1L1-PDGFR α which are involved in myeloproliferative neoplasms.

The oncogenic JAK2V617F mutation is found in the majority of myeloproliferative diseases like polycythemia Vera (PV), essential thrombocythemia (ET) and primary myelofibrosis (PMF). However, the molecular mechanism leading to constitutive kinase activity is largely unclear. Here we show that JAK2V617F requires an intact SH2 domain and FERM domain for constitutive activation of downstream signaling pathways. In addition, there is a strict requirement of cytokine receptor expression for the activation of this oncogene. Further analysis showed that the SH2 domain mutation did not interfere with JAK2 membrane distribution. However, co-IP experiments revealed a role for the SH2 domain in the aggregation and crossphosphorylation of JAK2V617F at the cell membrane. In a murine transplantation model we found that an intact SH2 domain in JAK2V617F was required for the induction of a MPD-like disease. Thus, our results points to an indispensable role of the SH2 domain in JAK2V617F induced MPN.

FIP1L1-PDGFR α (FP) is a constitutively activated protein kinase which was reported in chronic eosinophilic leukemia (CEL) and in cases of hypereosinophilic syndrome and mastocytosis with eosinophilia. Imatinib is clinically active against FIP1L1-PDGFR α positive disease. However, clinical resistance to imatinib has been observed in FIP1L1-PDGFR α positive leukemia and was shown to occur due to a secondary mutation (T674I) in the PDGFR α kinase domain. We therefore aimed to generate specific resistance profiles for available PDGFR kinase inhibitors. To this end, we generated clones of FP expressing Ba/F3 cells resistant to imatinib, nilotinib (Tasigna), and BAY 43-9006 (sorafenib, Nexavar) and show that different PDGFR α kinase inhibitors indeed produce distinct profiles of resistance mutations in PDGFR α . Specific profiles of FP resistance mutations may help in guiding treatment for myeloproliferative diseases positive for activating PDGFR-A and -B rearrangements in the setting of acquired imatinib resistance.

Zahlreiche Erkrankungen des hämatopoetischen Systems sind durch eine Überaktivierung von Rezeptor-Tyrosin-Kinase Signalwegen gekennzeichnet, weshalb deren molekulares Verständnis bei der Bekämpfung dieser Erkrankungen eine entscheidende Rolle spielt. Ziel dieser Arbeit war es daher zwei konstitutiv aktive Tyrosinkinasen JAK2 V617F und FIP1L1-PDGFR α zu untersuchen, welche in myeloproliferativen Erkrankung (MPN) auftreten.

In den myeloproliferativen Erkrankungen Polyzythämie Vera (PV), Essentielle Thrombozythämie (ET) und die Primäre Myelofibrose (PMF) tritt unter anderem die onkogene JAK2V617F Mutation auf. Die molekularen Mechanismen, die zur konstitutiven Aktivierung der JAK2-Kinase führen sind weitestgehend ungeklärt. Eigene Untersuchungen zeigen, dass für die onkogene Funktion von JAK2V617F eine intakte SH2 und FERM Domäne für die konstitutive Aktivierung nachgeschalteter Signalkaskaden notwendig sind. Voraussetzung hierfür ist ein funktioneller Zytokinrezeptor der die Aktivierung von JAK2V617F stimuliert. Weitere Untersuchungen zeigen, dass die Bindung von JAK2V617F an die Zellmembran unabhängig von der SH2 Domäne ist, aber Aggregation und Transphosphorylierung von JAK2V617F werden durch deren SH2 Domäne vermittelt. Knochenmarkstransplantationen in Mäusen zeigen, dass die SH2 Domäne von JAK2V617F für die Entstehung einer MPN-ähnlichen Erkrankung mitverantwortlich ist, was auf eine unverzichtbare Funktion dieser Domäne hindeutet.

Die konstitutiv aktive FIP1L-PDGFR α Kinase wurde in der chronischen Eosinophilen Leukämie, dem Hypereosinophilen Syndrom und der Eosinophilie verbundenen Mastozytose beschrieben. FIP1L-PDGFR α assoziierte Erkrankungen in Patienten werden unter anderem mit dem Kinaseinhibitor Imatinib behandelt. Imatinib Resistenzen wurden bei Patienten mit einer zusätzlichen Mutation (T674I) in der PDGFR α Kinasedomäne beobachtet. Ziel der Arbeit war es daher ein Resistenzprofil verfügbarer PDGFR α Kinaseinhibitoren zu erstellen. Resistente Baf3-Zellklone gegen die Kinaseinhibitoren Imatinib, Nilotinib und Sorafenib wurden in Zellkultur generiert. Dabei zeigen aufgetretene Mutationen in FIP1L-PDGFR α unterschiedliche Sensitivitäten gegenüber verschiedenen PDGFR α Inhibitoren. Die dabei gemachten Erkenntnisse der Inhibitoreigenschaften gegenüber unterschiedlichen FIP1L-PDGFR α Mutationen stellen

eine Hilfe bei der Behandlung von myeloproliferativen Erkrankungen mit PDGFR-A sowie PDGFR-B Hintergrund dar.

6. References

1. Vardiman JW, Harris NL, Brunning RD. The World Health Organization (WHO) classification of the myeloid neoplasms. *Blood*. 2002;100:2292-2302.
2. Smith CA, Fan G. The saga of JAK2 mutations and translocations in hematologic disorders: pathogenesis, diagnostic and therapeutic prospects, and revised World Health Organization diagnostic criteria for myeloproliferative neoplasms. *Hum Pathol*. 2008;39:795-810.
3. Nowell PC, Hungerford DA. Chromosome studies on normal and leukemic human leukocytes. *J Natl Cancer Inst*. 1960;25:85-109.
4. Ward HP, Vautrin R, Kurnick J, Robinson WA. Presence of a myeloproliferative factor in patients with polycythemia vera and agnogenic myeloid metaplasia. I. Expansion of the erythropoietin-responsive stem cell compartment. *Proc Soc Exp Biol Med*. 1974;147:305-308.
5. Adamson JW, Fialkow PJ, Murphy S, Prchal JF, Steinmann L. Polycythemia vera: stem-cell and probable clonal origin of the disease. *N Engl J Med*. 1976;295:913-916.
6. Fialkow PJ, Jacobson RJ, Papayannopoulou T. Chronic myelocytic leukemia: clonal origin in a stem cell common to the granulocyte, erythrocyte, platelet and monocyte/macrophage. *Am J Med*. 1977;63:125-130.
7. James C, Ugo V, Le Couedic JP, et al. A unique clonal JAK2 mutation leading to constitutive signalling causes polycythaemia vera. *Nature*. 2005;434:1144-1148.
8. Levine RL, Wadleigh M, Cools J, et al. Activating mutation in the tyrosine kinase JAK2 in polycythemia vera, essential thrombocythemia, and myeloid metaplasia with myelofibrosis. *Cancer Cell*. 2005;7:387-397.
9. Baxter EJ, Scott LM, Campbell PJ, et al. Acquired mutation of the tyrosine kinase JAK2 in human myeloproliferative disorders. *Lancet*. 2005;365:1054-1061.
10. Kralovics R, Guan Y, Prchal JT. Acquired uniparental disomy of chromosome 9p is a frequent stem cell defect in polycythemia vera. *Exp Hematol*. 2002;30:229-236.
11. Kralovics R, Passamonti F, Buser AS, et al. A gain-of-function mutation of JAK2 in myeloproliferative disorders. *N Engl J Med*. 2005;352:1779-1790.
12. Steensma DP, Dewald GW, Lasho TL, et al. The JAK2 V617F activating tyrosine kinase mutation is an infrequent event in both "atypical" myeloproliferative disorders and myelodysplastic syndromes. *Blood*. 2005;106:1207-1209.
13. Levine RL, Loriaux M, Huntly BJ, et al. The JAK2V617F activating mutation occurs in chronic myelomonocytic leukemia and acute myeloid leukemia, but not in acute lymphoblastic leukemia or chronic lymphocytic leukemia. *Blood*. 2005;106:3377-3379.
14. Scott LM, Tong W, Levine RL, et al. JAK2 exon 12 mutations in polycythemia vera and idiopathic erythrocytosis. *N Engl J Med*. 2007;356:459-468.
15. Mercher T, Wernig G, Moore SA, et al. JAK2T875N is a novel activating mutation that results in myeloproliferative disease with features of megakaryoblastic leukemia in a murine bone marrow transplantation model. *Blood*. 2006;108:2770-2779.

REFERENCES

16. Malinge S, Ben-Abdelali R, Settegrana C, et al. Novel activating JAK2 mutation in a patient with Down syndrome and B-cell precursor acute lymphoblastic leukemia. *Blood*. 2007;109:2202-2204.
17. Lacronique V, Boureux A, Valle VD, et al. A TEL-JAK2 fusion protein with constitutive kinase activity in human leukemia. *Science*. 1997;278:1309-1312.
18. Heiss S, Erdel M, Gunsilius E, Nachbaur D, Tzankov A. Myelodysplastic/myeloproliferative disease with erythropoietic hyperplasia (erythroid preleukemia) and the unique translocation (8;9)(p23;p24): first description of a case. *Hum Pathol*. 2005;36:1148-1151.
19. Reiter A, Walz C, Watmore A, et al. The t(8;9)(p22;p24) is a recurrent abnormality in chronic and acute leukemia that fuses PCM1 to JAK2. *Cancer Res*. 2005;65:2662-2667.
20. Griesinger F, Hennig H, Hillmer F, et al. A BCR-JAK2 fusion gene as the result of a t(9;22)(p24;q11.2) translocation in a patient with a clinically typical chronic myeloid leukemia. *Genes Chromosomes Cancer*. 2005;44:329-333.
21. Campbell PJ, Scott LM, Buck G, et al. Definition of subtypes of essential thrombocythaemia and relation to polycythaemia vera based on JAK2 V617F mutation status: a prospective study. *Lancet*. 2005;366:1945-1953.
22. Moliterno AR, Hankins WD, Spivak JL. Impaired expression of the thrombopoietin receptor by platelets from patients with polycythemia vera. *N Engl J Med*. 1998;338:572-580.
23. Lu X, Levine R, Tong W, et al. Expression of a homodimeric type I cytokine receptor is required for JAK2V617F-mediated transformation. *Proc Natl Acad Sci U S A*. 2005;102:18962-18967.
24. Pikman Y, Lee BH, Mercher T, et al. MPLW515L is a novel somatic activating mutation in myelofibrosis with myeloid metaplasia. *PLoS Med*. 2006;3:e270.
25. Pardanani AD, Levine RL, Lasho T, et al. MPL515 mutations in myeloproliferative and other myeloid disorders: a study of 1182 patients. *Blood*. 2006;108:3472-3476.
26. Leonard WJ, O'Shea JJ. Jaks and STATs: biological implications. *Annu Rev Immunol*. 1998;16:293-322.
27. Darnell JE, Jr., Kerr IM, Stark GR. Jak-STAT pathways and transcriptional activation in response to IFNs and other extracellular signaling proteins. *Science*. 1994;264:1415-1421.
28. Bach EA, Aguet M, Schreiber RD. The IFN gamma receptor: a paradigm for cytokine receptor signaling. *Annu Rev Immunol*. 1997;15:563-591.
29. Horvath CM, Darnell JE. The state of the STATs: recent developments in the study of signal transduction to the nucleus. *Curr Opin Cell Biol*. 1997;9:233-239.
30. Ihle JN, Witthuhn BA, Quelle FW, Yamamoto K, Silvennoinen O. Signaling through the hematopoietic cytokine receptors. *Annu Rev Immunol*. 1995;13:369-398.

31. Krolewski JJ, Lee R, Eddy R, Shows TB, Dalla-Favera R. Identification and chromosomal mapping of new human tyrosine kinase genes. *Oncogene*. 1990;5:277-282.
32. Wilks AF, Harpur AG, Kurban RR, Ralph SJ, Zurcher G, Ziemiecki A. Two novel protein-tyrosine kinases, each with a second phosphotransferase-related catalytic domain, define a new class of protein kinase. *Mol Cell Biol*. 1991;11:2057-2065.
33. Harpur AG, Andres AC, Ziemiecki A, Aston RR, Wilks AF. JAK2, a third member of the JAK family of protein tyrosine kinases. *Oncogene*. 1992;7:1347-1353.
34. Rane SG, Reddy EP. JAK3: a novel JAK kinase associated with terminal differentiation of hematopoietic cells. *Oncogene*. 1994;9:2415-2423.
35. Takahashi T, Shirasawa T. Molecular cloning of rat JAK3, a novel member of the JAK family of protein tyrosine kinases. *FEBS Lett*. 1994;342:124-128.
36. Kawamura M, McVicar DW, Johnston JA, et al. Molecular cloning of L-JAK, a Janus family protein-tyrosine kinase expressed in natural killer cells and activated leukocytes. *Proc Natl Acad Sci U S A*. 1994;91:6374-6378.
37. Kono DH, Owens DG, Wechsler AR. Jak3 maps to chromosome 8. *Mamm Genome*. 1996;7:476-477.
38. Guschin D, Rogers N, Briscoe J, et al. A major role for the protein tyrosine kinase JAK1 in the JAK/STAT signal transduction pathway in response to interleukin-6. *Embo J*. 1995;14:1421-1429.
39. Briscoe J, Rogers NC, Witthuhn BA, et al. Kinase-negative mutants of JAK1 can sustain interferon-gamma-inducible gene expression but not an antiviral state. *Embo J*. 1996;15:799-809.
40. Feng J, Witthuhn BA, Matsuda T, Kohlhuber F, Kerr IM, Ihle JN. Activation of Jak2 catalytic activity requires phosphorylation of Y1007 in the kinase activation loop. *Mol Cell Biol*. 1997;17:2497-2501.
41. Yasukawa H, Misawa H, Sakamoto H, et al. The JAK-binding protein JAB inhibits Janus tyrosine kinase activity through binding in the activation loop. *Embo J*. 1999;18:1309-1320.
42. Lindauer K, Loerting T, Liedl KR, Kroemer RT. Prediction of the structure of human Janus kinase 2 (JAK2) comprising the two carboxy-terminal domains reveals a mechanism for autoregulation. *Protein Eng*. 2001;14:27-37.
43. Frank SJ, Gilliland G, Kraft AS, Arnold CS. Interaction of the growth hormone receptor cytoplasmic domain with the JAK2 tyrosine kinase. *Endocrinology*. 1994;135:2228-2239.
44. Saharinen P, Takaluoma K, Silvennoinen O. Regulation of the Jak2 tyrosine kinase by its pseudokinase domain. *Mol Cell Biol*. 2000;20:3387-3395.
45. Kampa D, Burnside J. Computational and functional analysis of the putative SH2 domain in Janus Kinases. *Biochem Biophys Res Commun*. 2000;278:175-182.
46. Kohlhuber F, Rogers NC, Watling D, et al. A JAK1/JAK2 chimera can sustain alpha and gamma interferon responses. *Mol Cell Biol*. 1997;17:695-706.

REFERENCES

47. Radtke S, Haan S, Jorissen A, et al. The Jak1 SH2 domain does not fulfill a classical SH2 function in Jak/STAT signaling but plays a structural role for receptor interaction and up-regulation of receptor surface expression. *J Biol Chem.* 2005;280:25760-25768.
48. Chen M, Cheng A, Chen YQ, et al. The amino terminus of JAK3 is necessary and sufficient for binding to the common gamma chain and confers the ability to transmit interleukin 2-mediated signals. *Proc Natl Acad Sci U S A.* 1997;94:6910-6915.
49. Huang LJ, Constantinescu SN, Lodish HF. The N-terminal domain of Janus kinase 2 is required for Golgi processing and cell surface expression of erythropoietin receptor. *Mol Cell.* 2001;8:1327-1338.
50. Vainchenker W, Dusa A, Constantinescu SN. JAKs in pathology: Role of Janus kinases in hematopoietic malignancies and immunodeficiencies. *Semin Cell Dev Biol.* 2008.
51. Lu X, Gross AW, Lodish HF. Active conformation of the erythropoietin receptor: random and cysteine-scanning mutagenesis of the extracellular juxtamembrane and transmembrane domains. *J Biol Chem.* 2006;281:7002-7011.
52. Yamaoka K, Saharinen P, Pesu M, Holt VE, 3rd, Silvennoinen O, O'Shea JJ. The Janus kinases (Jaks). *Genome Biol.* 2004;5:253.
53. Levy DE, Darnell JE, Jr. Stats: transcriptional control and biological impact. *Nat Rev Mol Cell Biol.* 2002;3:651-662.
54. Ihle JN. STATs: signal transducers and activators of transcription. *Cell.* 1996;84:331-334.
55. Parganas E, Wang D, Stravopodis D, et al. Jak2 is essential for signaling through a variety of cytokine receptors. *Cell.* 1998;93:385-395.
56. Neubauer H, Cumano A, Muller M, Wu H, Huffstadt U, Pfeffer K. Jak2 deficiency defines an essential developmental checkpoint in definitive hematopoiesis. *Cell.* 1998;93:397-409.
57. James C. The JAK2V617F mutation in polycythemia vera and other myeloproliferative disorders: one mutation for three diseases? *Hematology Am Soc Hematol Educ Program.* 2008:69-75.
58. Michiels JJ, De Raeve H, Hebeda K, et al. WHO bone marrow features and European clinical, molecular, and pathological (ECMP) criteria for the diagnosis of myeloproliferative disorders. *Leuk Res.* 2007;31:1031-1038.
59. Delhommeau F, Dupont S, Tonetti C, et al. Evidence that the JAK2 G1849T (V617F) mutation occurs in a lymphomyeloid progenitor in polycythemia vera and idiopathic myelofibrosis. *Blood.* 2007;109:71-77.
60. Ishii T, Bruno E, Hoffman R, Xu M. Involvement of various hematopoietic-cell lineages by the JAK2V617F mutation in polycythemia vera. *Blood.* 2006;108:3128-3134.
61. Dawson MA, Bannister AJ, Gottgens B, et al. JAK2 phosphorylates histone H3Y41 and excludes HP1alpha from chromatin. *Nature.* 2009;461:819-822.

62. James C, Mazurier F, Dupont S, et al. The hematopoietic stem cell compartment of JAK2V617F-positive myeloproliferative disorders is a reflection of disease heterogeneity. *Blood*. 2008;112:2429-2438.
63. Ishii T, Zhao Y, Sozer S, et al. Behavior of CD34+ cells isolated from patients with polycythemia vera in NOD/SCID mice. *Exp Hematol*. 2007;35:1633-1640.
64. Pardanani A, Fridley BL, Lasho TL, Gilliland DG, Tefferi A. Host genetic variation contributes to phenotypic diversity in myeloproliferative disorders. *Blood*. 2008;111:2785-2789.
65. Wernig G, Mercher T, Okabe R, Levine RL, Lee BH, Gilliland DG. Expression of Jak2V617F causes a polycythemia vera-like disease with associated myelofibrosis in a murine bone marrow transplant model. *Blood*. 2006;107:4274-4281.
66. Lacout C, Pisani DF, Tulliez M, Gachelin FM, Vainchenker W, Villeval JL. JAK2V617F expression in murine hematopoietic cells leads to MPD mimicking human PV with secondary myelofibrosis. *Blood*. 2006;108:1652-1660.
67. Zaleskas VM, Krause DS, Lazarides K, et al. Molecular pathogenesis and therapy of polycythemia induced in mice by JAK2 V617F. *PLoS ONE*. 2006;1:e18.
68. Bumm TG, Elsea C, Corbin AS, et al. Characterization of murine JAK2V617F-positive myeloproliferative disease. *Cancer Res*. 2006;66:11156-11165.
69. Tefferi A, Lasho TL, Schwager SM, et al. The clinical phenotype of wild-type, heterozygous, and homozygous JAK2V617F in polycythemia vera. *Cancer*. 2006;106:631-635.
70. Villeval JL, James C, Pisani DF, Casadevall N, Vainchenker W. New insights into the pathogenesis of JAK2 V617F-positive myeloproliferative disorders and consequences for the management of patients. *Semin Thromb Hemost*. 2006;32:341-351.
71. Tiedt R, Hao-Shen H, Sobas MA, et al. Ratio of mutant JAK2-V617F to wild-type Jak2 determines the MPD phenotypes in transgenic mice. *Blood*. 2008;111:3931-3940.
72. Dupont S, Masse A, James C, et al. The JAK2 617V>F mutation triggers erythropoietin hypersensitivity and terminal erythroid amplification in primary cells from patients with polycythemia vera. *Blood*. 2007;110:1013-1021.
73. Scott LM, Scott MA, Campbell PJ, Green AR. Progenitors homozygous for the V617F mutation occur in most patients with polycythemia vera, but not essential thrombocythemia. *Blood*. 2006;108:2435-2437.
74. Capello D, Deambrogi C, Rossi D, et al. Epigenetic inactivation of suppressors of cytokine signalling in Philadelphia-negative chronic myeloproliferative disorders. *Br J Haematol*. 2008;141:504-511.
75. Jost E, do ON, Dahl E, et al. Epigenetic alterations complement mutation of JAK2 tyrosine kinase in patients with BCR/ABL-negative myeloproliferative disorders. *Leukemia*. 2007;21:505-510.
76. Lu X, Huang LJ, Lodish HF. Dimerization by a cytokine receptor is necessary for constitutive activation of JAK2V617F. *J Biol Chem*. 2008;283:5258-5266.

REFERENCES

77. Staerk J, Kallin A, Demoulin JB, Vainchenker W, Constantinescu SN. JAK1 and Tyk2 activation by the homologous polycythemia vera JAK2 V617F mutation: cross-talk with IGF1 receptor. *J Biol Chem.* 2005;280:41893-41899.
78. Funakoshi-Tago M, Pelletier S, Matsuda T, Parganas E, Ihle JN. Receptor specific downregulation of cytokine signaling by autophosphorylation in the FERM domain of Jak2. *Embo J.* 2006;25:4763-4772.
79. Kralovics R, Teo SS, Li S, et al. Acquisition of the V617F mutation of JAK2 is a late genetic event in a subset of patients with myeloproliferative disorders. *Blood.* 2006;108:1377-1380.
80. Kiladjian JJ, Elkassar N, Cassinat B, et al. Essential thrombocythemias without V617F JAK2 mutation are clonal hematopoietic stem cell disorders. *Leukemia.* 2006;20:1181-1183.
81. Levine RL, Belisle C, Wadleigh M, et al. X-inactivation-based clonality analysis and quantitative JAK2V617F assessment reveal a strong association between clonality and JAK2V617F in PV but not ET/MMM, and identifies a subset of JAK2V617F-negative ET and MMM patients with clonal hematopoiesis. *Blood.* 2006;107:4139-4141.
82. Campbell PJ, Baxter EJ, Beer PA, et al. Mutation of JAK2 in the myeloproliferative disorders: timing, clonality studies, cytogenetic associations, and role in leukemic transformation. *Blood.* 2006;108:3548-3555.
83. Hussein K, Bock O, Seegers A, et al. Myelofibrosis evolving during imatinib treatment of a chronic myeloproliferative disease with coexisting BCR-ABL translocation and JAK2V617F mutation. *Blood.* 2007;109:4106-4107.
84. Li S, Kralovics R, De Libero G, Theocharides A, Gisslinger H, Skoda RC. Clonal heterogeneity in polycythemia vera patients with JAK2 exon12 and JAK2-V617F mutations. *Blood.* 2008;111:3863-3866.
85. Nussenzweig RH, Swierczek SI, Jelinek J, et al. Polycythemia vera is not initiated by JAK2V617F mutation. *Exp Hematol.* 2007;35:32-38.
86. Kralovics R, Stockton DW, Prchal JT. Clonal hematopoiesis in familial polycythemia vera suggests the involvement of multiple mutational events in the early pathogenesis of the disease. *Blood.* 2003;102:3793-3796.
87. Bellanne-Chantelot C, Chaumarel I, Labopin M, et al. Genetic and clinical implications of the Val617Phe JAK2 mutation in 72 families with myeloproliferative disorders. *Blood.* 2006;108:346-352.
88. Kilpivaara O, Mukherjee S, Schram AM, et al. A germline JAK2 SNP is associated with predisposition to the development of JAK2(V617F)-positive myeloproliferative neoplasms. *Nat Genet.* 2009;41:455-459.
89. Olcaydu D, Harutyunyan A, Jager R, et al. A common JAK2 haplotype confers susceptibility to myeloproliferative neoplasms. *Nat Genet.* 2009;41:450-454.
90. Jones AV, Chase A, Silver RT, et al. JAK2 haplotype is a major risk factor for the development of myeloproliferative neoplasms. *Nat Genet.* 2009;41:446-449.

91. Verstovsek S. Therapeutic potential of JAK2 inhibitors. *Hematology Am Soc Hematol Educ Program*. 2009:636-642.
92. Quintas-Cardama A, Vaddi K, Liu P, et al. Preclinical characterization of the selective JAK1/2 inhibitor INCB018424: therapeutic implications for the treatment of myeloproliferative neoplasms. *Blood*;115:3109-3117.
93. Mesa RA, Tefferi A. Emerging drugs for the therapy of primary and post essential thrombocythemia, post polycythemia vera myelofibrosis. *Expert Opin Emerg Drugs*. 2009;14:471-479.
94. Geron I, Abrahamsson AE, Barroga CF, et al. Selective inhibition of JAK2-driven erythroid differentiation of polycythemia vera progenitors. *Cancer Cell*. 2008;13:321-330.
95. Wernig G, Kharas MG, Okabe R, et al. Efficacy of TG101348, a selective JAK2 inhibitor, in treatment of a murine model of JAK2V617F-induced polycythemia vera. *Cancer Cell*. 2008;13:311-320.
96. Lasho TL, Tefferi A, Hood JD, Verstovsek S, Gilliland DG, Pardanani A. TG101348, a JAK2-selective antagonist, inhibits primary hematopoietic cells derived from myeloproliferative disorder patients with JAK2V617F, MPLW515K or JAK2 exon 12 mutations as well as mutation negative patients. *Leukemia*. 2008;22:1790-1792.
97. Hexner EO, Serdikoff C, Jan M, et al. Lestaurtinib (CEP701) is a JAK2 inhibitor that suppresses JAK2/STAT5 signaling and the proliferation of primary erythroid cells from patients with myeloproliferative disorders. *Blood*. 2008;111:5663-5671.
98. Chusid MJ, Dale DC, West BC, Wolff SM. The hypereosinophilic syndrome: analysis of fourteen cases with review of the literature. *Medicine (Baltimore)*. 1975;54:1-27.
99. Gotlib J, Cools J, Malone JM, 3rd, Schrier SL, Gilliland DG, Coutre SE. The FIP1L1-PDGFRalpha fusion tyrosine kinase in hypereosinophilic syndrome and chronic eosinophilic leukemia: implications for diagnosis, classification, and management. *Blood*. 2004;103:2879-2891.
100. Gotlib J, Cools J. Five years since the discovery of FIP1L1-PDGFRα: what we have learned about the fusion and other molecularly defined eosinophilias. *Leukemia*. 2008;22:1999-2010.
101. Gleich GJ, Leiferman KM, Pardanani A, Tefferi A, Butterfield JH. Treatment of hypereosinophilic syndrome with imatinib mesilate. *Lancet*. 2002;359:1577-1578.
102. Ault P, Cortes J, Koller C, Kaled ES, Kantarjian H. Response of idiopathic hypereosinophilic syndrome to treatment with imatinib mesylate. *Leuk Res*. 2002;26:881-884.
103. Cools J, DeAngelo DJ, Gotlib J, et al. A tyrosine kinase created by fusion of the PDGFRA and FIP1L1 genes as a therapeutic target of imatinib in idiopathic hypereosinophilic syndrome. *N Engl J Med*. 2003;348:1201-1214.
104. Pardanani A, Brockman SR, Paternoster SF, et al. FIP1L1-PDGFRα fusion: prevalence and clinicopathologic correlates in 89 consecutive patients with moderate to severe eosinophilia. *Blood*. 2004;104:3038-3045.

REFERENCES

105. Baccarani M, Cilloni D, Rondoni M, et al. The efficacy of imatinib mesylate in patients with FIP1L1-PDGFRalpha-positive hypereosinophilic syndrome. Results of a multicenter prospective study. *Haematologica*. 2007;92:1173-1179.
106. Pardanani A, Ketterling RP, Li CY, et al. FIP1L1-PDGFRalpha in eosinophilic disorders: prevalence in routine clinical practice, long-term experience with imatinib therapy, and a critical review of the literature. *Leuk Res*. 2006;30:965-970.
107. Klion AD, Noel P, Akin C, et al. Elevated serum tryptase levels identify a subset of patients with a myeloproliferative variant of idiopathic hypereosinophilic syndrome associated with tissue fibrosis, poor prognosis, and imatinib responsiveness. *Blood*. 2003;101:4660-4666.
108. Helmling S, Zhelkovsky A, Moore CL. Fip1 regulates the activity of Poly(A) polymerase through multiple interactions. *Mol Cell Biol*. 2001;21:2026-2037.
109. Buitenhuis M, Verhagen LP, Cools J, Coffey PJ. Molecular mechanisms underlying FIP1L1-PDGFRalpha-mediated myeloproliferation. *Cancer Res*. 2007;67:3759-3766.
110. Cools J, Stover EH, Boulton CL, et al. PKC412 overcomes resistance to imatinib in a murine model of FIP1L1-PDGFRalpha-induced myeloproliferative disease. *Cancer Cell*. 2003;3:459-469.
111. Yamada Y, Rothenberg ME, Lee AW, et al. The FIP1L1-PDGFRalpha fusion gene cooperates with IL-5 to induce murine hypereosinophilic syndrome (HES)/chronic eosinophilic leukemia (CEL)-like disease. *Blood*. 2006;107:4071-4079.
112. Stover EH, Chen J, Folens C, et al. Activation of FIP1L1-PDGFRalpha requires disruption of the juxtamembrane domain of PDGFRalpha and is FIP1L1-independent. *Proc Natl Acad Sci U S A*. 2006;103:8078-8083.
113. Gorre ME, Mohammed M, Ellwood K, et al. Clinical resistance to STI-571 cancer therapy caused by BCR-ABL gene mutation or amplification. *Science*. 2001;293:876-880.
114. Branford S, Rudzki Z, Walsh S, et al. High frequency of point mutations clustered within the adenosine triphosphate-binding region of BCR/ABL in patients with chronic myeloid leukemia or Ph-positive acute lymphoblastic leukemia who develop imatinib (STI571) resistance. *Blood*. 2002;99:3472-3475.
115. von Bubnoff N, Schneller F, Peschel C, Duyster J. BCR-ABL gene mutations in relation to clinical resistance of Philadelphia-chromosome-positive leukaemia to STI571: a prospective study. *Lancet*. 2002;359:487-491.
116. Hofmann WK, Jones LC, Lemp NA, et al. Ph(+) acute lymphoblastic leukemia resistant to the tyrosine kinase inhibitor STI571 has a unique BCR-ABL gene mutation. *Blood*. 2002;99:1860-1862.
117. Roche-Lestienne C, Soenen-Cornu V, Grardel-Duflos N, et al. Several types of mutations of the Abl gene can be found in chronic myeloid leukemia patients resistant to STI571, and they can pre-exist to the onset of treatment. *Blood*. 2002;100:1014-1018.

118. Shah NP, Nicoll JM, Nagar B, et al. Multiple BCR-ABL kinase domain mutations confer polyclonal resistance to the tyrosine kinase inhibitor imatinib (STI571) in chronic phase and blast crisis chronic myeloid leukemia. *Cancer Cell*. 2002;2:117-125.
119. Hochhaus A. Cytogenetic and molecular mechanisms of resistance to imatinib. *Semin Hematol*. 2003;40:69-79.
120. Tamborini E, Bonadiman L, Greco A, et al. A new mutation in the KIT ATP pocket causes acquired resistance to imatinib in a gastrointestinal stromal tumor patient. *Gastroenterology*. 2004;127:294-299.
121. Wakai T, Kanda T, Hirota S, Ohashi A, Shirai Y, Hatakeyama K. Late resistance to imatinib therapy in a metastatic gastrointestinal stromal tumour is associated with a second KIT mutation. *Br J Cancer*. 2004;90:2059-2061.
122. Antonescu CR, Besmer P, Guo T, et al. Acquired resistance to imatinib in gastrointestinal stromal tumor occurs through secondary gene mutation. *Clin Cancer Res*. 2005;11:4182-4190.
123. Wardelmann E, Thomas N, Merkelbach-Bruse S, et al. Acquired resistance to imatinib in gastrointestinal stromal tumours caused by multiple KIT mutations. *Lancet Oncol*. 2005;6:249-251.
124. Heinrich MC, Corless CL, Blanke CD, et al. Molecular correlates of imatinib resistance in gastrointestinal stromal tumors. *J Clin Oncol*. 2006;24:4764-4774.
125. Azam M, Latek RR, Daley GQ. Mechanisms of autoinhibition and STI-571/imatinib resistance revealed by mutagenesis of BCR-ABL. *Cell*. 2003;112:831-843.
126. von Bubnoff N, Manley PW, Mestan J, Sanger J, Peschel C, Duyster J. Bcr-Abl resistance screening predicts a limited spectrum of point mutations to be associated with clinical resistance to the Abl kinase inhibitor nilotinib (AMN107). *Blood*. 2006;108:1328-1333.
127. Burgess MR, Skaggs BJ, Shah NP, Lee FY, Sawyers CL. Comparative analysis of two clinically active BCR-ABL kinase inhibitors reveals the role of conformation-specific binding in resistance. *Proc Natl Acad Sci U S A*. 2005;102:3395-3400.
128. Cortes J, Jabbour E, Kantarjian H, et al. Dynamics of BCR-ABL kinase domain mutations in chronic myeloid leukemia after sequential treatment with multiple tyrosine kinase inhibitors. *Blood*. 2007;110:4005-4011.
129. Jovanovic JV, Score J, Waghorn K, et al. Low-dose imatinib mesylate leads to rapid induction of major molecular responses and achievement of complete molecular remission in FIP1L1-PDGFR α -positive chronic eosinophilic leukemia. *Blood*. 2007;109:4635-4640.
130. Klion AD, Robyn J, Akin C, et al. Molecular remission and reversal of myelofibrosis in response to imatinib mesylate treatment in patients with the myeloproliferative variant of hypereosinophilic syndrome. *Blood*. 2004;103:473-478.
131. Metzgeroth G, Walz C, Erben P, et al. Safety and efficacy of imatinib in chronic eosinophilic leukaemia and hypereosinophilic syndrome - a phase-II study. *Br J Haematol*. 2008.

REFERENCES

132. Trempat P, Villalba C, Laurent G, et al. Chronic myeloproliferative disorders with rearrangement of the platelet-derived growth factor alpha receptor: a new clinical target for STI571/Glivec. *Oncogene*. 2003;22:5702-5706.
133. Apperley JF, Gardembas M, Melo JV, et al. Response to imatinib mesylate in patients with chronic myeloproliferative diseases with rearrangements of the platelet-derived growth factor receptor beta. *N Engl J Med*. 2002;347:481-487.
134. Pitini V, Arrigo C, Teti D, Barresi G, Righi M, Alo G. Response to STI571 in chronic myelomonocytic leukemia with platelet derived growth factor beta receptor involvement: a new case report. *Haematologica*. 2003;88:ECR18.
135. Magnusson MK, Meade KE, Nakamura R, Barrett J, Dunbar CE. Activity of STI571 in chronic myelomonocytic leukemia with a platelet-derived growth factor beta receptor fusion oncogene. *Blood*. 2002;100:1088-1091.
136. Garcia JL, Font de Mora J, Hernandez JM, Queizan JA, Gutierrez NC, San Miguel JF. Imatinib mesylate elicits positive clinical response in atypical chronic myeloid leukemia involving the platelet-derived growth factor receptor beta. *Blood*. 2003;102:2699-2700.
137. Wilkinson K, Velloso ER, Lopes LF, et al. Cloning of the t(1;5)(q23;q33) in a myeloproliferative disorder associated with eosinophilia: involvement of PDGFRB and response to imatinib. *Blood*. 2003;102:4187-4190.
138. Walz C, Metzgeroth G, Haferlach C, et al. Characterization of three new imatinib-responsive fusion genes in chronic myeloproliferative disorders generated by disruption of the platelet-derived growth factor receptor beta gene. *Haematologica*. 2007;92:163-169.
139. Gallagher G, Horsman DE, Tsang P, Forrest DL. Fusion of PRKG2 and SPTBN1 to the platelet-derived growth factor receptor beta gene (PDGFRB) in imatinib-responsive atypical myeloproliferative disorders. *Cancer Genet Cytogenet*. 2008;181:46-51.
140. Cross NC, Reiter A. Fibroblast growth factor receptor and platelet-derived growth factor receptor abnormalities in eosinophilic myeloproliferative disorders. *Acta Haematol*. 2008;119:199-206.
141. Reiter A, Walz C, Cross NC. Tyrosine kinases as therapeutic targets in BCR-ABL negative chronic myeloproliferative disorders. *Curr Drug Targets*. 2007;8:205-216.
142. David M, Cross NC, Burgstaller S, et al. Durable responses to imatinib in patients with PDGFRB fusion gene-positive and BCR-ABL-negative chronic myeloproliferative disorders. *Blood*. 2007;109:61-64.
143. Walz C, Haferlach C, Hanel A, et al. Identification of a MYO18A-PDGFRB fusion gene in an eosinophilia-associated atypical myeloproliferative neoplasm with a t(5;17)(q33-34;q11.2). *Genes Chromosomes Cancer*. 2008.
144. Shah NP, Tran C, Lee FY, Chen P, Norris D, Sawyers CL. Overriding imatinib resistance with a novel ABL kinase inhibitor. *Science*. 2004;305:399-401.
145. Weisberg E, Manley PW, Breitenstein W, et al. Characterization of AMN107, a selective inhibitor of native and mutant Bcr-Abl. *Cancer Cell*. 2005;7:129-141.

146. von Bubnoff N, Veach DR, van der Kuip H, et al. A cell-based screen for resistance of Bcr-Abl-positive leukemia identifies the mutation pattern for PD166326, an alternative Abl kinase inhibitor. *Blood*. 2005;105:1652-1659.
147. Ohnishi H, Kandabashi K, Maeda Y, Kawamura M, Watanabe T. Chronic eosinophilic leukaemia with FIP1L1-PDGFR fusion and T674I mutation that evolved from Langerhans cell histiocytosis with eosinophilia after chemotherapy. *Br J Haematol*. 2006;134:547-549.
148. Gotlib J, Cools J. Five years since the discovery of FIP1L1-PDGFR: what we have learned about the fusion and other molecularly defined eosinophilias. *Leukemia*. 2008.
149. Wheeler TT, Broadhurst MK, Sadowski HB, Farr VC, Prosser CG. Stat5 phosphorylation status and DNA-binding activity in the bovine and murine mammary glands. *Mol Cell Endocrinol*. 2001;176:39-48.
150. Liu SX, Cao J, An H, Shun HM, Yang LJ, Liu Y. Analysis of spontaneous, gamma ray- and ethylnitrosourea-induced hprt mutants in HL-60 cells with multiplex PCR. *World J Gastroenterol*. 2003;9:578-583.
151. Bradeen HA, Eide CA, O'Hare T, et al. Comparison of imatinib mesylate, dasatinib (BMS-354825), and nilotinib (AMN107) in an N-ethyl-N-nitrosourea (ENU)-based mutagenesis screen: high efficacy of drug combinations. *Blood*. 2006;108:2332-2338.
152. Kleywegt GJ, Harris MR, Zou JY, Taylor TC, Wahlby A, Jones TA. The Uppsala Electron-Density Server. *Acta Crystallogr D Biol Crystallogr*. 2004;60:2240-2249.
153. Berman H, Henrick K, Nakamura H. Announcing the worldwide Protein Data Bank. *Nat Struct Biol*. 2003;10:980.
154. Wernig G, Gonneville JR, Crowley BJ, et al. The Jak2V617F oncogene associated with myeloproliferative diseases requires a functional FERM domain for transformation and for expression of the Myc and Pim proto-oncogenes. *Blood*. 2008;111:3751-3759.
155. Haan C, Is'harc H, Hermanns HM, et al. Mapping of a region within the N terminus of Jak1 involved in cytokine receptor interaction. *J Biol Chem*. 2001;276:37451-37458.
156. Funakoshi-Tago M, Pelletier S, Moritake H, Parganas E, Ihle JN. Jak2 FERM domain interaction with the erythropoietin receptor regulates Jak2 kinase activity. *Mol Cell Biol*. 2008;28:1792-1801.
157. Peng B, Hayes M, Resta D, et al. Pharmacokinetics and pharmacodynamics of imatinib in a phase I trial with chronic myeloid leukemia patients. *J Clin Oncol*. 2004;22:935-942.
158. Stover EH, Chen J, Lee BH, et al. The small molecule tyrosine kinase inhibitor AMN107 inhibits TEL-PDGFRbeta and FIP1L1-PDGFRalpha in vitro and in vivo. *Blood*. 2005;106:3206-3213.
159. von Bubnoff N, Gorantla SP, Thone S, Peschel C, Duyster J. The FIP1L1-PDGFR T674I mutation can be inhibited by the tyrosine kinase inhibitor AMN107 (nilotinib). *Blood*. 2006;107:4970-4971;

REFERENCES

160. Kantarjian H, Giles F, Wunderle L, et al. Nilotinib in imatinib-resistant CML and Philadelphia chromosome-positive ALL. *N Engl J Med*. 2006;354:2542-2551.
161. Wilhelm SM, Carter C, Tang L, et al. BAY 43-9006 exhibits broad spectrum oral antitumor activity and targets the RAF/MEK/ERK pathway and receptor tyrosine kinases involved in tumor progression and angiogenesis. *Cancer Res*. 2004;64:7099-7109.
162. Lierman E, Folens C, Stover EH, et al. Sorafenib is a potent inhibitor of FIP1L1-PDGFRalpha and the imatinib-resistant FIP1L1-PDGFRalpha T674I mutant. *Blood*. 2006;108:1374-1376.
163. Strumberg D, Richly H, Hilger RA, et al. Phase I clinical and pharmacokinetic study of the Novel Raf kinase and vascular endothelial growth factor receptor inhibitor BAY 43-9006 in patients with advanced refractory solid tumors. *J Clin Oncol*. 2005;23:965-972.
164. Dewaele B, Wasag B, Cools J, et al. Activity of dasatinib, a dual SRC/ABL kinase inhibitor, and IPI-504, a heat shock protein 90 inhibitor, against gastrointestinal stromal tumor-associated PDGFRAD842V mutation. *Clin Cancer Res*. 2008;14:5749-5758.
165. Sawyers CL, Kantarjian H, Shah NP, et al. Dasatinib (BMS-354825) in Patients with Chronic Myeloid Leukemia (CML) and Philadelphia-Chromosome Positive Acute Lymphoblastic Leukemia (Ph+ ALL) Who Are Resistant or Intolerant to Imatinib: Update of a Phase I Study. 2005 ASH Annual Meeting. Atlanta, GE: *Blood*; 2005:16a.
166. Furitsu T, Tsujimura T, Tono T, et al. Identification of mutations in the coding sequence of the proto-oncogene c-kit in a human mast cell leukemia cell line causing ligand-independent activation of c-kit product. *J Clin Invest*. 1993;92:1736-1744.
167. Wan PT, Garnett MJ, Roe SM, et al. Mechanism of activation of the RAF-ERK signaling pathway by oncogenic mutations of B-RAF. *Cell*. 2004;116:855-867.
168. Fu YN, Yeh CL, Cheng HH, et al. EGFR mutants found in non-small cell lung cancer show different levels of sensitivity to suppression of Src: implications in targeting therapy. *Oncogene*. 2008;27:957-965.
169. Corbin AS, La Rosee P, Stoffregen EP, Druker BJ, Deininger MW. Several Bcr-Abl kinase domain mutants associated with imatinib mesylate resistance remain sensitive to imatinib. *Blood*. 2003.
170. Yamamoto Y, Kiyoi H, Nakano Y, et al. Activating mutation of D835 within the activation loop of FLT3 in human hematologic malignancies. *Blood*. 2001;97:2434-2439.
171. Maritano D, Accornero P, Bonifaci N, Ponzetto C. Two mutations affecting conserved residues in the Met receptor operate via different mechanisms. *Oncogene*. 2000;19:1354-1361.
172. Torkamani A, Schork NJ. Prediction of cancer driver mutations in protein kinases. *Cancer Res*. 2008;68:1675-1682.
173. Dibb NJ, Dilworth SM, Mol CD. Switching on kinases: oncogenic activation of BRAF and the PDGFR family. *Nat Rev Cancer*. 2004;4:718-727.

174. Mol CD, Dougan DR, Schneider TR, et al. Structural basis for the autoinhibition and STI-571 inhibition of c-Kit tyrosine kinase. *J Biol Chem.* 2004;279:31655-31663.
175. Gajiwala KS, Wu JC, Christensen J, et al. KIT kinase mutants show unique mechanisms of drug resistance to imatinib and sunitinib in gastrointestinal stromal tumor patients. *Proc Natl Acad Sci U S A.* 2009;106:1542-1547.
176. Zhao B, Smallwood A, Yang J, et al. Modulation of kinase-inhibitor interactions by auxiliary protein binding: crystallography studies on Aurora A interactions with VX-680 and with TPX2. *Protein Sci.* 2008;17:1791-1797.
177. Lierman E, Michaux L, Beullens E, et al. FIP1L1-PDGFRalpha D842V, a novel panresistant mutant, emerging after treatment of FIP1L1-PDGFRalpha T674I eosinophilic leukemia with single agent sorafenib. *Leukemia.* 2009.
178. Roumiantsev S, Shah NP, Gorre ME, et al. Clinical resistance to the kinase inhibitor STI-571 in chronic myeloid leukemia by mutation of Tyr-253 in the Abl kinase domain P-loop. *Proc Natl Acad Sci U S A.* 2002;99:10700-10705.
179. Choi SH, Mendrola JM, Lemmon MA. EGF-independent activation of cell-surface EGF receptors harboring mutations found in gefitinib-sensitive lung cancer. *Oncogene.* 2007;26:1567-1576.
180. Gorantla SP, von Bubnoff N, Peschel C, Duyster J. Identification of a Novel Mode of Kinase Inhibitor Resistance: An F604S Exchange in FIP1L1-PDGFRalpha Modulates FIP1L1-PDGFRalpha Protein Stability in a SRC-Dependent Manner. 50th ASH Annual Meeting. San Francisco, CA: Blood; 2008:964-965a.
181. Azam M, Seeliger MA, Gray NS, Kuriyan J, Daley GQ. Activation of tyrosine kinases by mutation of the gatekeeper threonine. *Nat Struct Mol Biol.* 2008;15:1109-1118.
182. Kannan N, Neuwald AF. Did protein kinase regulatory mechanisms evolve through elaboration of a simple structural component? *J Mol Biol.* 2005;351:956-972.
183. Chen H, Ma J, Li W, et al. A molecular brake in the kinase hinge region regulates the activity of receptor tyrosine kinases. *Mol Cell.* 2007;27:717-730.
184. Corless CL, Schroeder A, Griffith D, et al. PDGFRA mutations in gastrointestinal stromal tumors: frequency, spectrum and in vitro sensitivity to imatinib. *J Clin Oncol.* 2005;23:5357-5364.
185. von Bubnoff N, Engh RA, Aberg E, Sanger J, Peschel C, Duyster J. FMS-like tyrosine kinase 3-internal tandem duplication tyrosine kinase inhibitors display a nonoverlapping profile of resistance mutations in vitro. *Cancer Res.* 2009;69:3032-3041.
186. Zhao R, Xing S, Li Z, et al. Identification of an acquired JAK2 mutation in polycythemia vera. *J Biol Chem.* 2005;280:22788-22792.
187. Jones AV, Kreil S, Zoi K, et al. Widespread occurrence of the JAK2 V617F mutation in chronic myeloproliferative disorders. *Blood.* 2005;106:2162-2168.

REFERENCES

188. Pardanani A. JAK2 inhibitor therapy in myeloproliferative disorders: rationale, preclinical studies and ongoing clinical trials. *Leukemia*. 2008;22:23-30.
189. Constantinescu SN, Keren T, Socolovsky M, Nam H, Henis YI, Lodish HF. Ligand-independent oligomerization of cell-surface erythropoietin receptor is mediated by the transmembrane domain. *Proc Natl Acad Sci U S A*. 2001;98:4379-4384.
190. Darnell JE, Jr. STATs and gene regulation. *Science*. 1997;277:1630-1635.
191. Argetsinger LS, Kouadio JL, Steen H, Stensballe A, Jensen ON, Carter-Su C. Autophosphorylation of JAK2 on tyrosines 221 and 570 regulates its activity. *Mol Cell Biol*. 2004;24:4955-4967.
192. Nagar B, Bornmann WG, Pellicena P, et al. Crystal structures of the kinase domain of c-Abl in complex with the small molecule inhibitors PD173955 and imatinib (STI-571). *Cancer Res*. 2002;62:4236-4243.
193. Guo T, Agaram NP, Wong GC, et al. Sorafenib inhibits the imatinib-resistant KITT670I gatekeeper mutation in gastrointestinal stromal tumor. *Clin Cancer Res*. 2007;13:4874-4881.
194. von Bubnoff N, Sandherr M, Schlimok G, Andreesen R, Peschel C, Duyster J. Myeloid blast crisis evolving during imatinib treatment of an FIP1L1-PDGFR alpha-positive chronic myeloproliferative disease with prominent eosinophilia. *Leukemia*. 2005;19:286-287.
195. Lierman E, Michaux L, Beullens E, et al. FIP1L1-PDGFRalpha D842V, a novel panresistant mutant, emerging after treatment of FIP1L1-PDGFRalpha T674I eosinophilic leukemia with single agent sorafenib. *Leukemia*. 2009;23:845-851.
196. Baccarani M, Cortes J, Pane F, et al. Chronic myeloid leukemia: an update of concepts and management recommendations of European LeukemiaNet. *J Clin Oncol*. 2009;27:6041-6051.
197. Score J, Walz C, Jovanovic JV, et al. Detection and molecular monitoring of FIP1L1-PDGFRalpha-positive disease by analysis of patient-specific genomic DNA fusion junctions. *Leukemia*. 2009;23:332-339.
198. Simon D, Salemi S, Yousefi S, Simon HU. Primary resistance to imatinib in Fip1-like 1-platelet-derived growth factor receptor alpha-positive eosinophilic leukemia. *J Allergy Clin Immunol*. 2008;121:1054-1056.
199. Hughes T, Saglio G, Branford S, et al. Impact of baseline BCR-ABL mutations on response to nilotinib in patients with chronic myeloid leukemia in chronic phase. *J Clin Oncol*. 2009;27:4204-4210.
200. Branford S, Melo JV, Hughes TP. Selecting optimal second-line tyrosine kinase inhibitor therapy for chronic myeloid leukemia patients after imatinib failure: does the BCR-ABL mutation status really matter? *Blood*. 2009;114:5426-5435.
201. Heinrich MC, Corless CL, Duensing A, et al. PDGFRA activating mutations in gastrointestinal stromal tumors. *Science*. 2003;299:708-710.
202. Nagata H, Worobec AS, Oh CK, et al. Identification of a point mutation in the catalytic domain of the protooncogene c-kit in peripheral blood mononuclear cells of patients who have

- mastocytosis with an associated hematologic disorder. *Proc Natl Acad Sci U S A*. 1995;92:10560-10564.
203. Hirota S, Ohashi A, Nishida T, et al. Gain-of-function mutations of platelet-derived growth factor receptor alpha gene in gastrointestinal stromal tumors. *Gastroenterology*. 2003;125:660-667.
204. Ma Y, Zeng S, Metcalfe DD, et al. The c-KIT mutation causing human mastocytosis is resistant to STI571 and other KIT kinase inhibitors; kinases with enzymatic site mutations show different inhibitor sensitivity profiles than wild-type kinases and those with regulatory-type mutations. *Blood*. 2002;99:1741-1744.
205. Torrent M, Rickert K, Pan BS, Sepp-Lorenzino L. Analysis of the activating mutations within the activation loop of leukemia targets Flt-3 and c-Kit based on protein homology modeling. *J Mol Graph Model*. 2004;23:153-165.
206. Weisberg E, Wright RD, Jiang J, et al. Effects of PKC412, nilotinib, and imatinib against GIST-associated PDGFRA mutants with differential imatinib sensitivity. *Gastroenterology*. 2006;131:1734-1742.
207. Debiec-Rychter M, Cools J, Dumez H, et al. Mechanisms of resistance to imatinib mesylate in gastrointestinal stromal tumors and activity of the PKC412 inhibitor against imatinib-resistant mutants. *Gastroenterology*. 2005;128:270-279.
208. Guida T, Anaganti S, Provitera L, et al. Sorafenib inhibits imatinib-resistant KIT and platelet-derived growth factor receptor beta gatekeeper mutants. *Clin Cancer Res*. 2007;13:3363-3369.
209. Medeiros F, Corless CL, Duensing A, et al. KIT-negative gastrointestinal stromal tumors: proof of concept and therapeutic implications. *Am J Surg Pathol*. 2004;28:889-894.
210. Heidel F, Solem FK, Breitenbuecher F, et al. Clinical resistance to the kinase inhibitor PKC412 in acute myeloid leukemia by mutation of Asn-676 in the FLT3 tyrosine kinase domain. *Blood*. 2006;107:293-300.
211. Kindler T, Breitenbuecher F, Kasper S, et al. Identification of a novel activating mutation (Y842C) within the activation loop of FLT3 in patients with acute myeloid leukemia (AML). *Blood*. 2005;105:335-340.
212. Bagrintseva K, Schwab R, Kohl TM, et al. Mutations in the tyrosine kinase domain of FLT3 define a new molecular mechanism of acquired drug resistance to PTK inhibitors in FLT3-ITD-transformed hematopoietic cells. *Blood*. 2004;103:2266-2275.
213. Metzgeroth G, Walz C, Score J, et al. Recurrent finding of the FIP1L1-PDGFR fusion gene in eosinophilia-associated acute myeloid leukemia and lymphoblastic T-cell lymphoma. *Leukemia*. 2007;21:1183-1188.

7. Publications

(1) Gorantla SP, Nikolas von Bubnoff, Christian Peschel, Justus Duyster. Identification of a novel mode of kinase inhibitor resistance: An F604S exchange in FIP1L1-PDGFR α modulates FIP1L1-PDGFR α protein stability in a SRC and SHP-2 dependent manner (In the process of submission).

(2) Gorantla SP, Tobias N. Dechow, Rebekka Grundler, Lena Illert, Christian Meyer zum Büschenfelde, Marcus Kremer, Christian Peschel and Justus Duyster. JAK2V617F requires an intact SH2 domain for constitutive activation and induction of a myeloproliferative disease (Blood 2010 in the press).

(3) Gorantla SP[§], Nikolas von Bubnoff[§], Silvia Thöne, Christian Peschel, Justus Duyster. In vitro resistance screening identifies nilotinib and sorafenib as candidates to overcome imatinib resistance in myeloproliferation with FIP1L1-PDGFR α (Oncogene 2010 in the press).

(4) Gorantla SP[§], Nikolas von Bubnoff[§], Thöne S, Peschel C, Duyster J. Blood. 2006 Jun 15; 107(12):4970-1 The FIP1L1-PDGFR α T674I mutation can be inhibited by the tyrosine kinase inhibitor AMN107 (nilotinib).

(5) Gorantla SP[§], Nikolas von Bubnoff[§], Kancha RK, Lordick F, Peschel C, Duyster J. Leukemia. 2005 Sep; 19(9):1670-1: The systemic mastocytosis-specific activating cKit mutation D816V can be inhibited by the tyrosine kinase inhibitor AMN107.

[§] In these authors equally contributed.

Selected presentations

(1) Sivahari P. Gorantla, Nikolas von Bubnoff, Ana Lena Illert, Nokolas Schneider, Christian Peschel, Justus Duyster. Identification of a novel mode of kinase inhibitor resistance: An F604S exchange in FIP1L1-PDGFR α modulates FIP1L1-PDGFR α protein stability in a SRC and SHP2 dependent manner. Young masters presentation in DGHO annual conference conducted in 2010.

PUBLICATIONS AND PRESENTATIONS

(2) Sivahari P. Gorantla, Nikolas von Bubnoff, Christian Peschel, Justus Duyster. Comparison of Imatinib and Nilotinib for FIP1L1-PDGFR secondary resistant mutations in a cell based screening method. Oral presentation in DGHO annual meeting 2007 in Basel.

(3) Sivahari P. Gorantla, Tobias N. Dechow, Rebekka Grundler, Christian Peschel and Justus Duyster JAK2V617F requires an intact SH2 domain for constitutive activation and induction of a myeloproliferative disease. Oral presentation in ASH annual meeting 2008 in Sanfrancisco.

(4) Sivahari P. Gorantla, Tobias N. Dechow, Rebekka Grundler, Christian Peschel and Justus Duyster JAK2V617F requires an intact SH2 domain for constitutive activation and induction of a myeloproliferative disease. Oral presentation in DGHO annual meeting 2008 in Vianna.

(5) Sivahari P. Gorantla, Nikolas von Bubnoff, Lena Illert, Nikolas Schneider, Christian Peschel, Justus Duyster. Identification of a novel mode of kinase inhibitor resistance: An F604S exchange in FIP1L1-PDGFR modulates FIP1L1-PDGFR protein stability in a SRC and SHP2 dependent manner. Oral presentation in AACR annual meeting 2010 in Washington D.C.

(6) Sivahari P. Gorantla, Nikolas von Bubnoff, Silvia Thöne, Christian Peschel, Justus Duyster. Identification of a novel mode of kinase inhibitor resistance: An F604S exchange in FIP1L1-PDGFR modulates FIP1L1-PDGFR protein stability in a SRC-dependent manner. Poster presentation in DGHO annual conference conducted in 2008.

(7) Sivahari P. Gorantla, Nikolas von Bubnoff, Silvia Thöne, Christian Peschel, Justus Duyster. Identification of a novel mode of kinase inhibitor resistance: An F604S exchange in FIP1L1-PDGFR modulates FIP1L1-PDGFR protein stability in a SRC-dependent manner. Poster presentation in ASH annual meeting (2008) in Sanfrancisco.

(8) Sivahari P. Gorantla, Tobias N. Dechow, Christian Peschel and Justus Duyster. JAK2V617F mediated transformation requires intact SH2 domain. Poster presentation in DGHO annual meeting 2006.

(9) Nikolas von Bubnoff, Sivahari P. Gorantla, Silvia Thöne, Jana Sanger, Christian Peschel, Justus Duyster. Generation of specific resistance profiles in FLT3-ITD and FIP1L1-PDGFRalpha towards specifically acting tyrosine kinase inhibitors. Poster presentation in ASH annual meeting 2006 in Orlando.

Lebenslauf

Persönliche Angaben

1. Nachname	Gorantla
2. Vorname	Sivahari Prasad
3. Geburtsdatum	25.07.1980
4. Staatsangehörigkeit	Indisch
5. Ausbildung	
ab 2005	Promotionsstudium. TU München
2003-2004	Wissenschaftlicher Mitarbeiter, Hyderabad Central University, Hyderabad, Indien
2001-2003	M.Sc. Biotechnology, University of Calicut, Kerala, Indien
1997-2000	B.Sc. Basic Science, Nagarjuna University, Guntur, Indien
1992-1994	Weiterführende Schulausbildung, Govt. Sr. Sec. School, Guntur, Indien
6. Title der dissertation	Studies on functional domains in oncogenic JAK2 and identification of drug resistant mutations in FIP1L1-PDGFR α
7. Betreuung	Prof. Dr. Justus Duyster

Acknowledgements

I wish to express my thanks to Prof. Dr. Bernhard Küster (Dept. of Proteomics and Bioanalytics, Technical University of Munich) my supervisor for his encouraging suggestions and for carefully reviewing the manuscript.

I wish to express my indebtedness and deep sense of gratitude to my project supervisor Prof. Dr. Justus Duyster, for his keen interest and encouragement throughout the course of this work Endeavour. His guidance and creative criticism enriched the quality of scientific component and I extend my sincere gratitude to him. He is clearly a master of his craft and I have benefited tremendously from observing him and conducting research with him. I wish to thank him for inspiring scientific discussions and motivations he offered.

I wish to express my thanks to Prof. Dr. Christian Peschel, Director of IIIrd Internal Medicine, for providing the facilities and infra structure that was needed to complete the project work. His vision and adept discussion technically and otherwise helped me to learn and understand the challenges.

The completion of my thesis work would not have been possible with out cooperation and friendly help by Dr. Nikolas von Bubnoff and Dr. Tobias Dechow. I thank them whole heartedly for their intellectual discussions and help during my thesis. I also thank to Richard Engh, Taiana De Oliveira and Epsen Aberg for structural discussion.

I wish to take this opportunity to express my special thanks to Rama Krishna Kancha for helping me through out my stay in Germany. I also wish to express my special thanks to Nicolas Schneider for helping me in the mice transplantations and discussions through out my thesis period.

I wish to express my thanks to Jana Saenger, Claudia Mugler, Astrid Froeschl, Sabine Woetzel, Melanie Sickinger, Christine von Klitzing, Anna Lena Illert, Rebekka Grundler, Wibke Leibig, Corinna Albers, Micheal Kulinski, Richard Huss, Catharin Moll,

Sebastian Kuhn, Susanne Raulefs, Anja Baumgart, Hannes Leischner for their affection and friendliness through out my stay in Germany. I wish to express my special thanks to Juliane Rhode, Benita Paraschoudis, and Petra Glaenzer for helping me in the bureaucracy stuff.

I take this opportunity to express my heart-felt gratefulness to Raja Ram Mohan Roy for his endless help and support. I also wish to express my special thanks to Kittu, Balaji, Indira, Prasad, Hema, Venu, Visu, Pravin, Damu and Puli for their help and support through out my life.

I would like to express my gratitude to Muneeth, Preethi, Rajeev, Bhavana, Bhaskar, Madhavi, Radha Damodar and Asshish for their support and encouragement.

Any appreciable word would be less to thank my revered parents for the blessings showered on me. My career would not have progressed in this direction and to this level without their help and encouragement. Their love and affection brought me to the level where I am today.

It has been a great joy and fun in my life and I cherish all the pleasant moments with my family members uncle, aunt, and sisters. My special thanks to my wife Bhargavi for sharing every emotion of mine and keeping me fit and fine through out my life.